Diana Oliveira da Silva

Bachelor degree in Biochemistry

Chemical synthesis of new histone deacetylase inhibitors and their evaluation as anticancer agents

Dissertation for the Master degree in Biochemistry for Health

Supervisor: Rita Ventura, PhD, ITQB-NOVA

Co-supervisor: Catarina Brito, PhD, IBET, ITQB-NOVA

November, 2016

Diana Oliveira da Silva

Bachelor degree in Biochemistry

Chemical synthesis of new histone deacetylase inhibitors and their evaluation as anticancer agents

Dissertation for the Master degree in Biochemistry for Health

Supervisor: Rita Ventura, PhD, ITQB-NOVA

Co-supervisor: Catarina Brito, PhD, IBET, ITQB-NOVA

Jury:

President: Doutor Pedro Manuel H. M. Matias, Investigador Principal ITQB-NOVA
Arguer: Doutor Hélder João Ferreira Vila Real, Investigador IBET
Vowels: Doutora Margarida Archer Franco Frazão, Investigadora Principal ITQB-NOVA
Doutora Maria Rita Mendes Bordalo Ventura, Investigadora Auxiliar ITQB-NOVA

Instituto de Tecnologia Química e Biológica António Xavier da Universidade Nova de Lisboa

November, 2016

Chemical synthesis of new histone deacetylase inhibitors and their evaluation as anticancer agents

(…). À parte isso, tenho em mim todos os sonhos do mundo.

Em Tabacaria. Álvaro de Campos, Heterónimo de Fernando Pessoa

Acknowledgements

I would like to acknowledge all the people directly or indirectly involved in this thesis.

To my supervisor, Dr. Rita Ventura, and my co-supervisor, Dr. Catarina Brito for the opportunity to work in such challenging project combining two very distinctive fields and for helping me to grow as a scientist in both areas.

To Dr. Rita Ventura for all the knowledge, guidance and for being so supportive since the beginning of this journey.

To Dr. Catarina Brito for all the scientific discussions and all guidance and knowledge provided. For all friendly conversations and motivation throughout this work.

To all colleagues in Bioorganic Chemistry and Organic Synthesis Units at ITQB-UNL, for the good working environment specially Vanessa Miranda, Filipa Almeida, Eva Lourenço, Saúl and Jessica Bevan.

To Osvaldo Ascenso, for all the guidance and help provided throughout the chemical synthesis.

To Animal Cell Technology Unit at IBET, ITQB-UNL colleagues for the good working environment and including me in the group with such joy. To 3D Advanced cell models group specially Sofia Abreu, Daniel Simão, Tatiana Martins, Francisca Arez, Ana Paula and Catarina Pinto, for all scientific discussions and knowledge provided. For all patience to teach me and answer all my questions.

To Marta Estrada, for all the support and patience to teach me all the techniques of animal cell culture. For all the advices and help throughout all year. For always being there.

A todos os meus colegas de mestrado que me apoiaram e ajudaram durante os últimos dois anos. Aprendi sempre algo mais com cada um de vocês.

Aos meus amigos, aqueles que acreditam em mim e nas minhas capacidades e por todos os bons momentos. Pela vossa amizade.

Ao Nuno, por toda a paciência e carinho.

Aos meus pais, irmão e avó, que sempre me apoiaram, acreditaram em mim e ajudaram em todos os momentos de forma a conseguir atingir os meus objetivos. Por serem um exemplo de força. Sem vocês não era possível. Obrigada

Abstract

Epigenetics and its key role in gene expression have become increasingly important in cancer research. Histone proteins play an important role in gene expression control through modifications like acetylation, phosphorylation and methylation. Histone deacetylases (HDAC) can regulate expression levels via acetylation of lysine residues of histone proteins.

Inhibitors of these HDAC have been associated with cancer and some are commercialized as anticancer drugs like SAHA (Vorinostat) and Belinostat (PXD101). These histone deacetylases inhibitors (HDACi) are known to have several effects in altered or malignant cells such as accumulation of acetylated proteins, proliferation arrest, cell cycle arrest, and induction of apoptosis.

The purpose of this work was to synthesize new HDACi with anticancer effects. For this, several analogues were synthesized inspired in the structures of SAHA and Belinostat where key aspects of the HDACi structures were altered. Breast cancer (MCF-7) and lung cancer (H460) cell lines were used in order to evaluate the newly synthesized compounds as antitumour agents.

Overall, 30 compounds were successfully synthesized and were used in further analysis in cancer cell lines.

Results showed that the synthesized compound N-hydroxy-N'-(4-iodophenyl)octanediamide (16c) is a putative new HDACi with anticancer effects, exhibiting an cytotoxic effect in both cancer cell lines tested and preliminary data suggested that it induced the same cell death mechanisms as the previously described for SAHA.

Keywords: HDACi; Chemical synthesis; Drug testing; Cancer cell lines; Anticancer agents

Resumo

A epigenética e o seu papel na regulação génica têm vindo a tornar-se muito importantes na investigação em oncologia. As histonas exercem uma função fundamental na regulação dos genes através de modificações como a acetilação, fosforilação e metilação. As deacetilases de histonas (HDAC) regulam os níveis de expressão através da acetilação de lisinas presentes em histonas.

Os inibidores destas enzimas têm sido usados na terapia do cancro e alguns são comercializados como fármacos anticancerígenos tais como o SAHA (Vorinostat) e o Belinostat (PXD101). Estes inibidores de deacetilases de histonas (HDACi) têm como efeitos conhecidos a acumulação de proteínas acetiladas, paragem da proliferação, paragem do ciclo celular e a indução da apoptose em células alteradas ou malignas.

O objetivo deste trabalho foi a síntese de novos HDACi com efeitos anticancerígenos. Para tal, vários compostos análogos foram sintetizados baseados nas estruturas dos fármacos SAHA e Belinostat onde aspetos importantes da estrutura foram alterados. Linhas celulares de cancro de mama (MCF-7) e de pulmão (H460) foram usadas para avaliar os compostos sintetizados como agentes anticancerígenos.

No total, foram sintetizados com sucesso e posteriormente testados em linhas celulares cancerígenas 30 compostos.

Os resultados obtidos mostraram que o composto sintetizado N-hidroxi-N'-(4-iodofenil)octanodiamida (16c), revelou um efeito anticancerígeno maior do que o provocado pelo SAHA em ambas as linhas celulares testadas e resultados preliminares sugerem que induz mecanismos de morte celular similares aos descritos previamente para o SAHA.

Palavras-chave: HDACi; Síntese Química; Ensaios farmacológicos; Agentes anticancerígenos; Linhas celulares cancerígenas

Contents

Figure Index

Table Index

Abbreviations and Symbols

^{13}C-NMR - Carbon-13 nuclear magnetic resonance

^{1}H-NMR - Proton nuclear magnetic resonance

APT - Attached proton test

Ar - Aromatics

ATR-FTIR - Attenuated Total Reflectance-Fourier Transform Infra-red Spectroscopy

$CDCl_3$ - Deuterated chloroform

COSY - Correlation Spectroscopy

d - Doublet

DMEM - Dulbecco's Modified Eagle Medium

DMF - Dimethylformamide

DMSO - Dimethyl sulfoxide

DMSO-d_6 - Deuterated dimethyl sulfoxide

DNA - Deoxyribonucleic acid

EDC - 1-Ethyl-3-(3-dimethylaminopropyl)carbodiimide

FBS - Fetal Bovine Serum

HAT - Histone acetyltransferase

HDAC - Histone deacetylase

HDACi - Histone deacetylase inhibitors

HDF - Human Dermal Fibroblasts

HMQC - Heteronuclear Multiple-Quantum Correlation

IC50 - Half maximal inhibitory concentration

IMDM - Iscove's Modified Dulbecco's Medium

IR - Infra-Red

m - Multiplet

MeOH - Methanol

NaOH - Sodium hydroxide

$NH_2OH.HCl$ - Hydroxylamine hydrochloride

PBS - Phosphate-buffered saline

PTM - post-translational modification

q - quartet

s - Singlet

SAHA - Suberoylanilide Hydroxamic acid or Vorinostat

SIRT - sirtuin

t - Triplet

THF - Tetrahydrofuran

TLC - Thin Layer Chromatography

UV - Ultraviolet

δ - Chemical shift

I. INTRODUCTION

I.1 Cancer and Epigenetics

Cancer is one of the leading causes of mortality worldwide, with approximately 8.2 million cancer related deaths in 2012. In the next 2 decades, the number of new cases is expected to increase by approximately 70%. The most common causes of cancer death are lung, liver, stomach, colorectal, breast and oesophageal cancer[1]. (Figure I.1).

Treatment options against cancer comprise surgery, chemotherapy and radiotherapy and an early detection, accurate diagnosis, and effective treatment are crucial for increasing cancer survival[1].

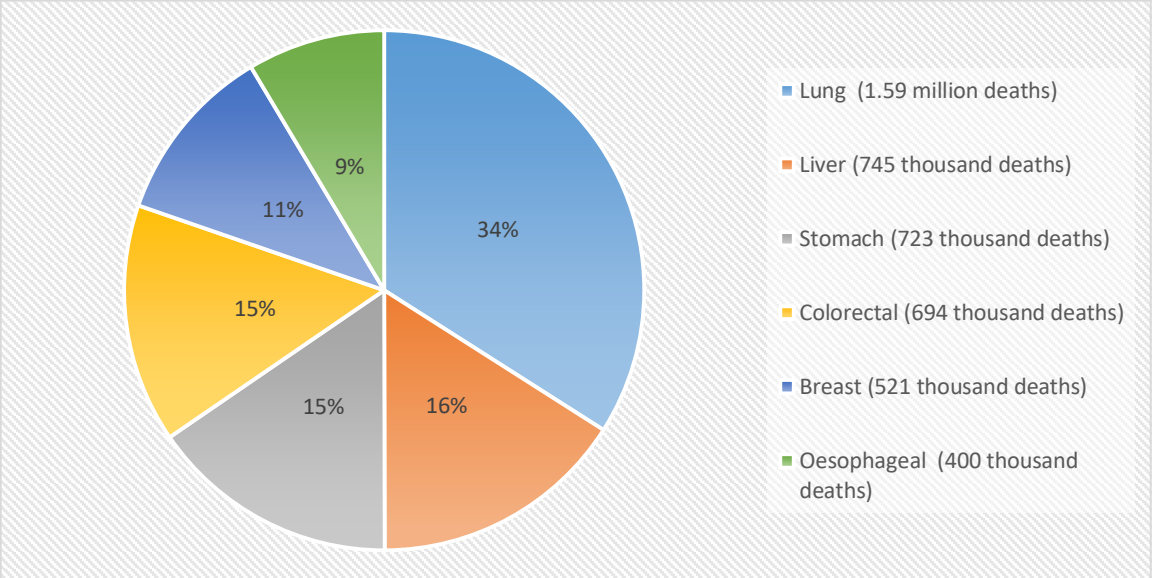

Figure I.1 - Most common causes of cancer death. Data obtained from the World Health Organization[1].

Cancer is characterized by cells with rapid and abnormal growth which are able to invade adjacent parts of the body and spread to other organs, a process called metastasizing. Cancerous cells are the result of genetic and genomic alterations such as point mutations, deletions and translocations[2]. Genetic alterations can ultimately lead to the activation of oncogenes and inactivation of tumor-suppressor genes. More recently, cancer development has been correlated not only with genetic alterations but also with epigenetic modifications that contribute to disease progression[3]. Genetics is concerned with the information transmitted on the basis of gene sequence whereas epigenetics studies the inheritance of information based on gene-expression levels that do not involve changes in the underlying DNA sequence[4].

In recent years, numerous studies described extensive reprogramming of epigenetic machinery components in cancer, including DNA methylation and histone modifications. A first indication that epigenetic modifications such as histone acetylation may be strongly involved in cancer onset and progression came from a study demonstrating a global loss of monoacetylation and trimethylation on histone H4 in cancer cells[5]. Other similar studies have shown that epigenetic enzymes are often dysregulated in human tumors[4].

Identification of these enzymes has driven the rapid development of small-molecule inhibitors that target the cancer epigenome. Within this purpose, histone deacetylases inhibitors (HDACi) were studied as potential antitumor agents. There are now several HDACi commercialized as anticancer medicines such as suberoylanilide hydroxamic acid (SAHA) and Belinostat (PXD101), approved for the treatment of specific types of cancer (see section I.4.2).

I.2 Histone Regulation and Acetylation

Eukaryotic organisms have their genetic information packaged inside the cell nucleus. This arrangement is mediated by histones which are small basic proteins rich in lysine and arginine residues that strongly adhere to negatively-charged DNA and form complexes called nucleosomes[6]. Nucleosomes are the basic units of chromatin and are formed by an octamer of the four core histones (H3, H4, H2A, H2B) around which DNA is wrapped [7].

The amino acid tails of core histones can be subjected to several post-translational modifications like acetylation, methylation and phosphorylation, and this facilitates processes including transcription, replication and repair[7,8]. While the base sequence of DNA provides the fundamental code for proteins, post-translational modifications (PTM´s) of histone proteins play a major role in the control of gene transcription [9]. These epigenetic modifications can lead to changes in function and/or regulation of several proteins including histones, without altering their primary sequences.

Histone acetylation is the modification most widely studied. In general, high levels of acetylation (hyperacetylation) are correlated with higher transcriptional activity and a more open chromatin conformation, whereas low levels of acetylation (hypoacetylation) cause chromatin condensation leading mainly to transcriptional suppression.

Histone acetylation levels are mediated by the opposing actions of two different enzymes: Histone acetyl-transferases (HATs) that are responsible for transferring acetyl groups to lysine residues in histones N-terminal tails and histone deacetylases (HDACs) that remove the acetyl group [7,10]. (Figure I.2)

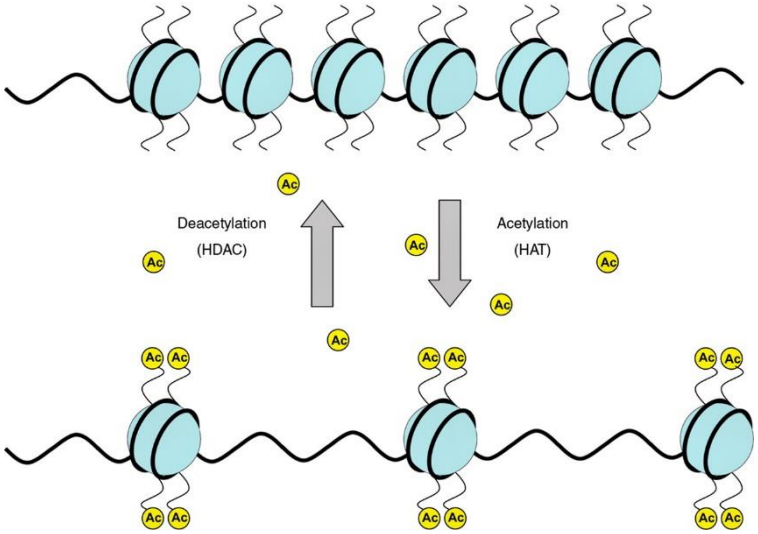

Figure I.2- Histone Acetylation - Acetylation of lysine residues (mediated by HATs) will neutralize the histone positive charge and weakening its interaction with DNA. Previously tightly wrapped DNA around the histone will be more loose and more accessible to several processes like transcription, replication, etc. By removing acetyl groups, HDACs will have the opposing action. Adapted from D.Pons et al[44].

I.3 Histone Deacetylase (HDAC)

To date, 18 mammalian HDAC enzymes have been identified and are classified based on their homology with yeast transcriptional regulators[11]. These enzymes are divided into four different classes: classes I, II and IV, from the Zinc-dependent family (also called classical), and class III, which is a NAD + (Nicotinamide adenine dinucleotide) dependent family (also called SIRT-sirtuins) [10]. Concerning the Zinc-dependent family of HDAC enzymes (Table I.1), class I contains HDAC1, 2, 3, and 8 and shares homology with the yeast transcriptional regulator RDP3. The class II enzymes share homology with the yeast HDAC1 and are subdivided into class IIa, consisting of HDAC4, 5, 7, and 9, and class IIb, containing HDAC6 and 10. Class IIb differs structurally by containing two catalytic sites. HDAC11 shares characteristics with both class I and class II HDACs, so it is included in class IV[12]. Concerning the NAD + dependent family (Table I.1), class III contains seven proteins (SIRT1 - 7) that differ in cellular localization, activity, and function[13].

Table I.1 - Classification of Zinc dependent family of HDAC enzymes.

CLASSES	HDAC ENZYME	LOCALIZATION
CLASS I	HDAC1	Nucleus
	HDAC2	Nucleus
	HDAC3	Nucleus
	HDAC8	Nucleus/Cytoplasm
CLASS IIa	HDAC4	Nucleus/Cytoplasm
	HDAC5	Nucleus/Cytoplasm
	HDAC7	Nucleus/Cytoplasm
	HDAC9	Nucleus/Cytoplasm
CLASS IIb	HDAC6	Cytoplasm
	HDAC10	Cytoplasm
CLASS III	SIRT1	Nucleus
	SIRT2	Cytoplasm
	SIRT3	Nucleus/Mitochondria
	SIRT4	Mitochondria
	SIRT5	Mitochondria
	SIRT6	Nucleus
	SIRT7	Nucleus
CLASS IV	HDAC11	Nucleus/Cytoplasm

HDAC enzymes are predominantly in the cell nucleus in order to exert their function. However, some HDAC can shuttle between the nucleus and the cytoplasm[11].

I.4 HDAC inhibitors (HDACi)

Over the years, many different types of HDAC inhibitors (HDACi) have been developed, ranging from simple structures like butyrate to more complex structures such as SAHA or romidepsin. HDACi can be categorised based on their structure: hydroxamic acids, cyclic peptides, benzamides, and short-chain fatty acids (Table I.2).

Table I.2 - HDAC inhibitors categories, structures and information about approval status as anticancer drugs.

	HDAC inhibitor	*Structure*	*Approval status as anticancer drug (commercial name/brand)*
Hydroxamic acids	Trichostatin A (TSA)	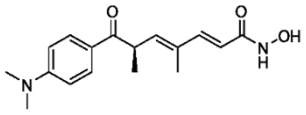	-
	SAHA (Vorinostat)	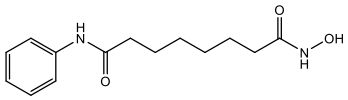	FDA Approved 2006 (Zolinza)
	Belinostat (PXD101)	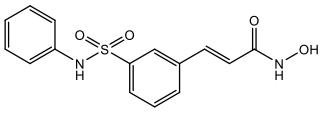	FDA Approved 2014 (BELEODAQ)
	Panobinostat (LBH589)	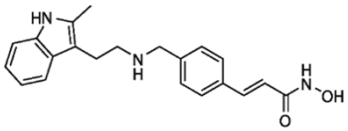	FDA Approved 2015 (FARYDAK)
	Givinostat (ITF2357)	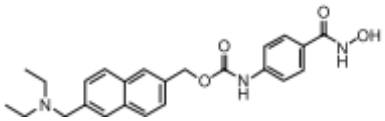	Undergoing clinical trials
Cyclic Peptide	Depsipeptide (romidepsin)	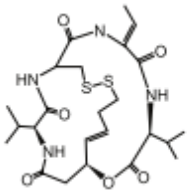	FDA Approved 2009 (ISTODAX)
Benzamides	Entinostat (MS-275)	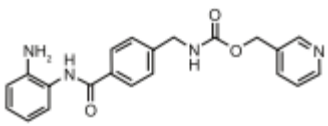	Undergoing clinical trials
	Mocetinostat (MGCD0103)	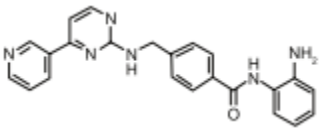	Undergoing clinical trials
Fatty acids	Sodium Butyrate	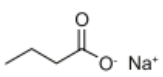	-
	Valproic acid (VPA)	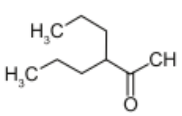	-

The first proposed HDACi were short chain fatty acids, like sodium butyrate, but these were shown to be less effective in comparison with inhibitors of the other categories. Trichostatin A was the first natural product discovered to inhibit HDACs. After that, several molecules with similar structure started to be produced and tested as HDACi, such as SAHA or Belinostat.

I.4.1 HDACi - multitargeted compounds

HDACi have been studied as potential drugs for different final goals. The action of these inhibitors leads to a more open chromatin conformation and DNA becomes more accessible to several processes. One of those processes can be transcription, so HDACi have been correlated with higher transcription activity. Therefore, these compounds and analogues have been studied as potential additives capable of enhancing the expression of recombinant proteins in mammalian cell cultures (SME, from Small Molecule Enhancers)[14]. Recently, SME are being studied also in plant cell cultures within the same purpose.

In the last decade, neurodegenerative diseases have also been proposed as targets for HDACi therapy. Brain disorders are often associated with imbalances in protein acetylation levels and transcriptional dysfunctions[15]. Treatment with various HDACi can potentially lead to the correction of these variations. In several animal models of neurodegenerative diseases (such as Parkinson´s disease and Alzheimer´s disease among others), treatments with HDACi revealed effectiveness against neuronal cell death and improved neurological outcome[16,17].

Cancer disease is another target of this type of compounds. HDACi have been studied as potential antitumor agents and there are now several approved as anti-cancer agents. Not only these compounds can act as radio-sensitizers in the treatment of cancer but also they show several effects against cancerous cells with an apparent selectivity, such as growth arrest, induction of apoptosis and cell cycle arrest. (See sections I.4.2 and I.4.3).

I.4.2 HDACi as anticancer agents

As mentioned before, the first evidences that epigenetics alterations, and especially histone acetylation could be involved in cancer came from studies showing different acetylation levels in cancerous and non-cancerous cells. *Fraga et al* showed global loss of monoacetylation and trimethylation of lysine residues in histone H4 in cancer cells[5]. In related studies, authors analyzed the expression of class I HDAC enzymes (HDAC1, 2, 3, and 8) in several cell lines and cancer tissues. Stomach, oesophagus, colon, prostate, breast, ovary, lung, pancreas and thyroid cancers were analysed and the results showed that over 75% of human cancer tissues and their corresponding non-cancerous epithelium showed high expression of these class I HDACs. Also, 5-40% of cancer tissues overexpressed class I HDACs, compared with corresponding normal epithelium[18].

Due to these and similar findings, inhibitors of HDAC enzymes emerged as a new class of targeted therapeutics for a variety of human cancers. Currently, there are several clinical trials of this type of drugs alone or in combination with drugs already used in cancer therapy. To date, four HDAC inhibitors were approved by the U.S Food and Drug Administration (FDA) for lymphoma and myeloma: Belinostat, Romidepsin, Panobinostat and SAHA (Table I.2).

Belinostat (BELEODAQ, Spectrum Pharmaceuticals, Inc.) was approved by the FDA in July, 2014, for the treatment of patients with relapsed or refractory peripheral T-cell lymphoma (PTCL)[19].

Romidepsin (ISTODAX, Gloucester Pharmaceuticals Inc.) was approved by the FDA in November, 2009, for the treatment of cutaneous T-cell lymphoma (CTCL) in patients that have received at least one prior systemic therapy[19].

Panobinostat (FARYDAK capsules, Novartis Pharmaceuticals) was approved by the FDA in February, 2015, in combination with bortezomib and dexamethasone for the treatment of patients with multiple myeloma[20].

SAHA or Vorinostat (Zolinza, Merck & Co., Inc.) acts as a strong chelator of Zinc ions and is an effective HDAC inhibitor. SAHA was approved by the FDA for the treatment of cutaneous T-cell lymphoma (CTCL) in October of 2006.[21,22] SAHA is capable of inhibiting all HDAC in classes I and II that are metal dependent (in nanomolar range)[23] so it is considered a pan-inhibitor of HDAC. However, like other HDACi, is not able of inhibiting class III HDAC.

Structurally, hydroxamic acids HDACi, such as SAHA, include three important domains: a capping group, a metal binding moiety and a linker. (Figure I.3)

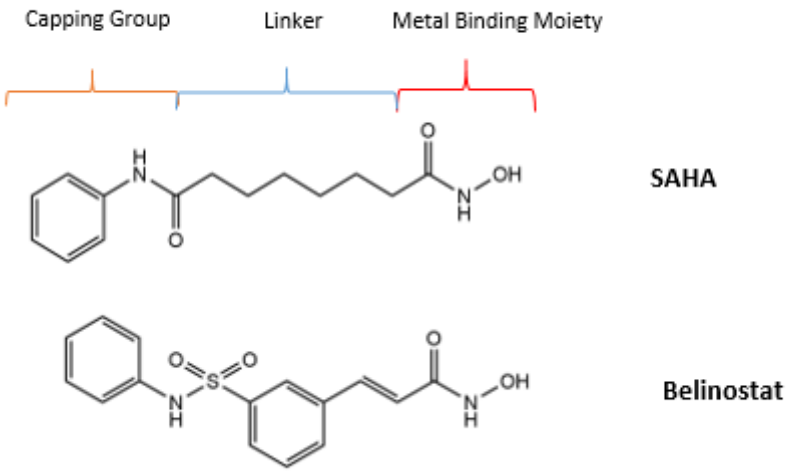

Figure I.3 - Structures of SAHA and Belinostat with their three important domains: capping group, linker and metal binding moiety.

The capping group is important in the interaction with the amino acid residues near the entrance of the active site. The metal binding moiety is crucial for the interaction with the zinc atom present in the catalytic pocket of HDAC enzyme (Figure I.4). The linker connects the two groups[10]. In case of SAHA, the linker is only a carbon chain with 8 carbons without double bonds, but in Belinostat the linker is much shorter with a double bond. Optimization of these key motifs is crucial for the discovery of a molecule better fitted to the catalytic pocket of the enzyme and consequently with higher potency, as HDAC inhibitor.

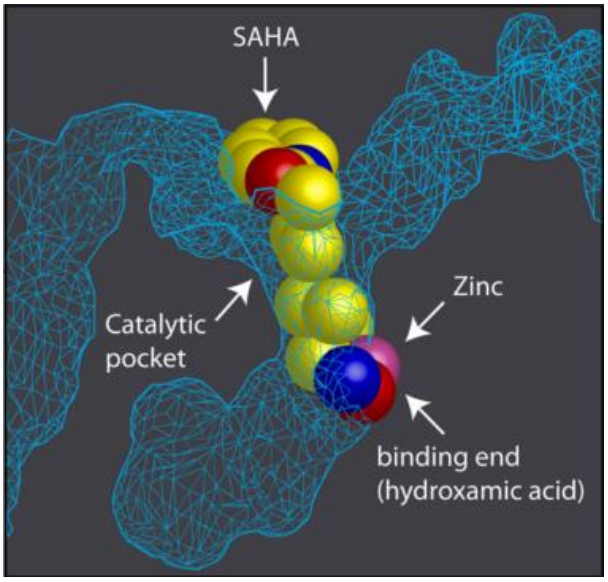

Figure I.4 – Representation of the catalytic pocket in the crystal structure of HDAC protein with SAHA. In the catalytic pocket of HDAC enzyme is a Zinc molecule (in pink) where the hydroxamic part of SAHA binds. Adapted from Marks, P. A. et al [45].

I.4.3 HDACi Action Mechanism

As previous mentioned in section I.1, cancer has been correlated in recent years with extensive reprogramming of epigenetic machinery components including DNA methylation and histone modifications. Treatment with HDACi can potentially lead to the correction of the epigenetic reprogramming found in cancer. HDACi have an important role in histone regulation, preventing the removal of acetyl groups from lysines by HDAC (see section I.2). Due to their effect in histone regulation, HDACi are responsible for an overall increase in acetylated histones causing altered gene transcription. HDACi can also act in other substrates leading to an increased acetylation level and altered gene transcription of non-histone proteins that are important regulators in several processes, resulting in numerous side effects that can also contribute to their anti-cancer action. Several studies have shown that HDACi can inhibit proliferation, stimulate apoptosis[24], and induce cell cycle arrest[25] in malignant cells[10]. (Figure I.5)

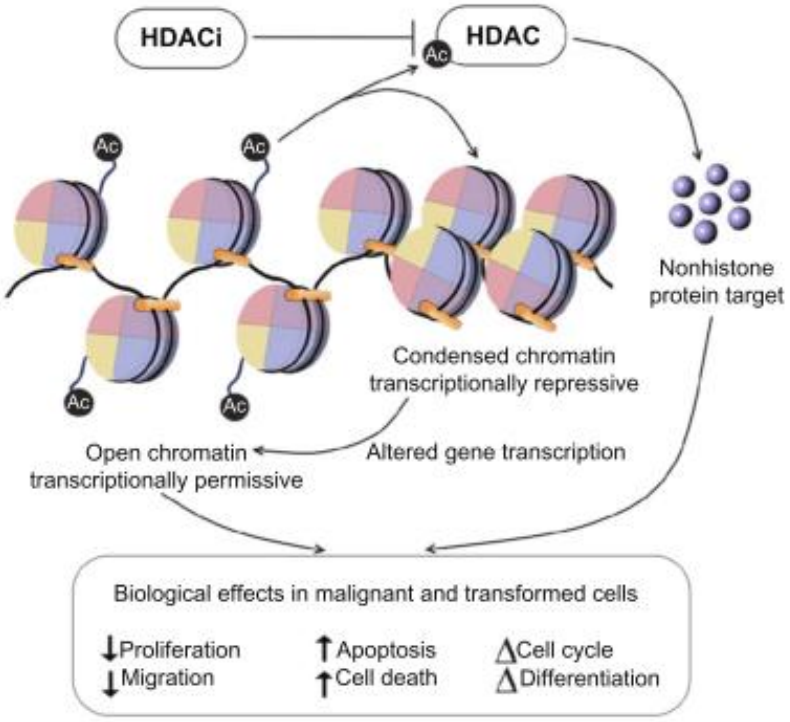

Figure I.5 - Biological effects of HDACi in malignant cells. Adapted from K.Ververis et al[10].

Moreover, the SAHA compound produces several effects in cancerous cells such as alteration in gene transcription, an increase of acetylated proteins, growth arrest *in vitro* and *in vivo*[26], induction of apoptosis[24] and cell cycle arrest[25] with little toxicity to normal cells[27]. The mechanisms behind these anticancer effects are not fully understood but several efforts have been made to correlate the increase of acetylation in histone and non-histone proteins with the effects in malignant cells.

Some mechanisms normally dysregulated in cancer are apoptosis/cell death and cell cycle progression, enabling cancer cells to growth in an abnormal and very rapid manner and enabling them to overcome checkpoints that usually lead to cell death. Therefore, these type of dysregulations are hallmarks for ongoing tumor progression and good targets for anticancer drugs.

Apoptosis is the process of programmed cell death and is mediated by intrinsic (mitochondrial) and extrinsic (death receptor) pathways. HDAC inhibitors induce apoptosis via both pathways by up-regulating pro-apoptotic and down-regulating anti-apoptotic proteins[28,29]. The p53 tumor suppressor gene encodes for a transcriptional factor whose activity is modulated by post-translational modifications including acetylation and protein stability. Studies showed that through acetylation of p53, HDACi were able to up-regulate pro-apoptotic proteins such as Bim, Bak, and Bax, which function as sensors of cellular stress and initiate the intrinsic pathway[29]. At a molecular level, apoptosis is caused by the activation of caspases[29].

Several HDAC inhibitors induce cell cycle arrest at G1 via induction of the cyclin-dependent kinase inhibitor $p21^{WAF/CIP1}$. HDAC inhibitors also induce G2/M arrest in normal and transformed cells, but the latter lack a functional G2 checkpoint and frequently undergo apoptosis[28].

As mentioned in section I.2, a higher acetylation of lysine residues of histones is correlated with a more open chromatin conformation. Therefore, DNA can be more accessible for DNA damage agents and reactive oxygen species (ROS) increasing the potential of causing DNA damage. Valproic acid has been reported to enhance the radiosensitivity of human tumour cells *in vivo* and *in vitro*. In mice, irradiation of brain tumour cells after treatment with valproic acid resulted in radiation-induced tumour growth delay[30]. Related studies with other HDACi showed similar results. Therefore, these compounds can act as radio-sensitizers, being helpful in combined therapies with radiotherapy for cancer treatment.

One additional characteristic that makes HDACi appealing as anticancer agents is the fact that these inhibitors are normally correlated with a normal cell resistance phenomenon. They have antitumor action in cancerous cells at concentrations at which normal cells show little toxicity. Normal cells are up to tenfold more resistant to SAHA-induced cell death than cancer cells [27]. The mechanism that leads to this selectivity of HDACi is not well understood and several studies tried to answer this question. One study suggests that thioredoxin, a small redox protein, has a key role in the response of normal and cancer cells to HDACi [27]. They show that higher levels of thioredoxin in normal cells could explain, in part, the relative resistance of normal cells to these compounds effects. Low levels of thioredoxin in transformed cells increased their sensitivity to HDACi-induced cell death[27].

Another study claims that HDACi are able to induce DNA damage in both cancerous and non-cancerous cells but only normal cells can repair this damage [31]. The authors demonstrated that SAHA is capable of inducing DNA double-strand breaks (DSB) in both normal (HFS-human

dermal fibroblasts) and cancer cells (LNCaP, A549). Using a marker of DNA DSB during continued culture with SAHA, the authors saw an increase in levels of that marker with time in cancer cells but a decrease in normal cells. Also, they found that SAHA was able to suppress DNA DSB repair proteins in cancer but not in normal cells[31].

I.4.4 HDACi Synthesis

Based on previously published synthesis for HDAC inhibitors and derivatives, the synthesis of hydroxamic or carboxylic derivatives can be achieved in two steps [32–34] (See scheme in figure I.6).

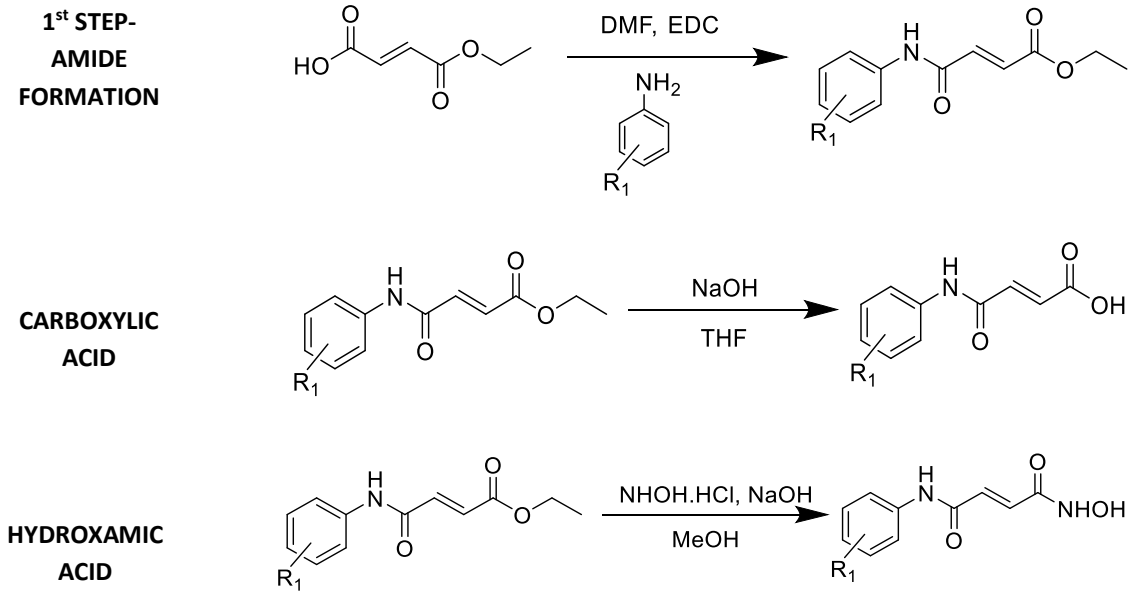

Figure I.6 - General scheme of HDAC inhibitors synthesis.

The first step consists on the formation of an amide under an inert atmosphere (argon), using an aniline derivative and a carboxylic acid with a coupling agent such as 1-Ethyl-3-(3-dimethylaminopropyl)carbodiimide (EDC) in dry dimethylformamide (DMF) . The obtained ester is then converted into its corresponding hydroxamic derivative by using hydroxylamine hydrochloride ($NH_2OH.HCl$) in dry methanol (MeOH) for 1-2h. The ester obtained in step 1 can also be transformed to its carboxylic derivate using sodium hydroxide (NaOH). The ester is dissolved in tetrahydrofuran (THF), NaOH added to the mixture and the reaction is stirred for 1-2h. (See scheme in figure 6).

Other reagents can be used as coupling agents such as N,N'-dicyclohexylcarbodiimide (DCC) and N,N'-Diisopropylcarbodiimide (DIC).

As mentioned before (See section I.4.2), HDACi such as SAHA and Belinostat structurally contain three important domains: a capping group, a metal binding moiety and a linker. Several analogues were synthesized where these key aspects were altered in order to assess which structures are more important to the effectiveness of these compounds.

Several analogues with different structures can be obtained changing the starting material and the aniline derivative used in the first step of synthesis. (See scheme in figure I.6). Different starting materials with different carbon lengths lead to analogues with different linkers. In this work, mono-ethyl fumarate, adipic acid monomethyl ester, suberic acid monomethyl ester and azelaic acid monomethyl ester were used as starting compounds. Also, different aniline derivatives used in the initial step (See scheme in figure I.6) will enable the synthesis of analogues containing different atoms in the benzenic ring, modifying the capping group.

Furthermore, a metal chelator moiety is crucial in the HDACi structure. Not only the hydroxamic acid moiety but also the carboxylic moiety are good chelators of metal, even though the carboxylic acid is less efficient in this role. Therefore, carboxylic acid analogues can also have activity as inhibitors of HDAC and were also synthesized and tested in cancer cell lines.

I.5 Thesis aim

The final goal of this work was to synthesize new HDAC inhibitors with anticancer effects. The first objective was to synthesize several compounds using the structures of SAHA and Belinostat as a starting point/model and evaluate them as anticancer agents in cancer cell lines. Within this purpose, the synthesized compounds were altered in key aspects of HDACi structure. All three important domains were changed: the capping group was altered with the addition of different atoms to the benzenic ring, the carbon length of linker was modified in different extents and both hydroxamic acid and carboxylic acid forms were synthesized. (Figure I.7).

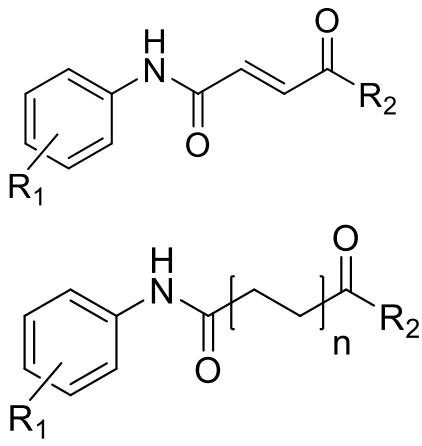

R_1 – F, I, Br, CF_3, OCH_3 at different positions

R_2 – OH, NHOH

n – 4,6, 7

Figure I.7 - General structure of HDACi.

These compounds were evaluated in cancer cell lines in parallel with SAHA as reference compound. The effect of the synthesized compounds on cell viability of a breast cancer cell line (MCF-7) and a lung cancer cell line (H460) was assessed in the presence and absence of the drugs to analyze which functional groups lead to a higher effect in cancer cells.

The second objective was to refine the compound structures taking to account the results obtained in the first round of drug testing by synthesizing new molecules combining the best groups in the same molecule, when possible.

The third objective was to evaluate these compounds in the same cancer cell lines and address the mechanisms of cell death of the compounds with higher impact on cancer cell viability.

II. MATERIALS AND METHODS

II.1 Synthesis of New HDACi

II.1.1 General conditions

All reactions were carried out under an inert atmosphere (argon), except when the solvents were not dried. The synthesized compounds were purified by recrystallization or silica flash-column chromatography. Reactions were followed by Analytical TLC (thin-layer chromatography). The characterization of compounds was done by ^{1}H-NMR, ^{13}C-NMR, ^{13}C-APT, 2D NMR techniques (COSY and HMQC), IR spectroscopy and melting point measurement. NMR peak assignments are supported by 2D correlation NMR studies and the peaks assigned when possible.

Analytical TLC was performed on aluminium-backed Merck 60 F254 silica gel plates. The spots corresponding to the products were identified by UV radiation (254 nm) and then immersed on a 5% phosphomolybdic acid solution in ethanol to be revealed. Compounds with the hydroxamic acid moiety were revealed using a solution containing 1-5% iron chloride (III) and 0.5 M HCl. After immersion in this solution, hydroxamic acids appear red instantly.

Silica flash-column chromatography in Silica gel Merck 60 was used, when applicable.

^{1}H-NMR spectra were recorded on a Bruker 400 spectrometer and obtained at 400 MHz in $CDCl_3$ (deuterated chloroform) or DMSO-d_6 (deuterated dimethyl sulfoxide). Chemical shifts are given in ppm, downfield from tetramethylsilane, for solutions in $CDCl_3$. ^{1}H-NMR spectra were analyzed using BRUKER TOPSIN 2.1.

^{13}C-NMR spectra were recorded on a Bruker 400 spectrometer at 100.61 MHz in $CDCl_3$ or DMSO-d_6. ^{13}C-NMR spectra were analyzed using Bruker Topsin 2.1 software.

IR spectra were measured on a Nicolet 6700 ATR-FTIR spectrometer with a diamond crystal. IR spectra were analyzed using Omnic software.

Melting Points were measured twice for each compound using a BUCHI 530 apparatus that contains a paraffin bath.

Solvent and Reagent Purification

All the used solvents were previously distilled in the laboratory.

Aniline – distilled under reduced pressure.

Dry DMF: to previously distilled DMF, calcium hydride (drying agent) was added and the mixture was left overnight, followed by decantation from the drying agent and distillation under reduced pressure.

Dry THF: to previously distilled THF, sodium wire and benzophenone were added, and the mixture was refluxed under argon for several hours until the solvent turned deep blue in colour. Then the mixture was kept at low reflux, being only distilled before its utilization.

Dry Methanol: to 50-70 mL of previously distilled methanol, 5g of magnesium turnings and iodine (0.5 g) were added. The mixture was refluxed until all the magnesium had been consumed. More methanol (1L) was added and the reflux was maintained for 2h before distillation.

II.1.2 General methods

Experiment A - General methods for the 1st Step synthesis – Amide formation

The experimental procedure to obtain the amides started by dissolving the starting material (mono-ethyl fumarate (Aldrich), adipic acid monomethyl ester (Aldrich), suberic acid monomethyl ester (Carbosynth) or azelaic acid monomethyl ester (Aldrich)) in dry DMF. The respective aniline was added (1.5 equivalents) and EDC (Fluka), a coupling agent was added (1.5 equivalents) stepwise. Reactions were maintained overnight under argon at room temperature. TLC (5:5 hexane: ethyl acetate) confirmed that the initial product was totally consumed. Reactions were stopped with the addition of water followed by organic phase extraction using ethyl acetate. Later, ethyl acetate and also DMF were evaporated, the last step using high vacuum. After the work-up procedure, purifications of the compounds were done by recrystallization using hexane and ethyl acetate or by silica flash column chromatography.

Experiment B - General methods for carboxylic acid synthesis

Compounds previously synthesized in the amide formation step were dissolved in THF and then NaOH 1M (1 equivalent) solution was added to the mixture. Reactions were stirred between 1h and 2h with strong agitation at room temperature. TLC (5:5 hexane: ethyl acetate) was performed to monitor the reactions. The reactions were stopped when the starting material was totally consumed with the addition of water followed by a washing step using ethyl ether. Subsequently, the aqueous phase was acidified using a solution of HCl 10% until it reached a pH

3-4. Precipitation of product occurred and was followed by organic phase extraction using ethyl acetate. Then, ethyl acetate was evaporated. After the work-up procedure, the purification of the compounds was done by recrystallization using hexane and ethyl acetate.

Experiment C - General methods for hydroxamic acid synthesis

Compounds previously synthesized in the amide formation step were dissolved in dry MeOH and then $NH_2OH.HCl$ (Merck) was added (0.8 equivalents) to the mixture. The reactions were then placed on an ice bath (0ºC) and NaOH 4M (8 equivalents) was also added to the flask. The reactions were maintained for 1-2h under argon at 0ºC. TLC (5:5 hexane:ethyl acetate) was performed to monitor the reactions and the reactions were stopped when the starting material was totally consumed, by adding water followed by a washing step using ethyl ether. Next, the aqueous phase was acidified using an aqueous solution of HCl 10% until pH 3-4. Precipitation of the product occurred and was followed by organic phase extraction using ethyl acetate. A washing step using sodium bicarbonate ($NaHCO_3$) was then performed and ethyl acetate phase was evaporated. After the work-up procedure, purification of the compounds was done by recrystallization using hexane and ethyl acetate.

II.1.3 Experimental Procedures

<u>Experiment 1:</u> Synthesis of ethyl (2E)-3-(phenylcarbamoyl)prop-2-enoate (1a)

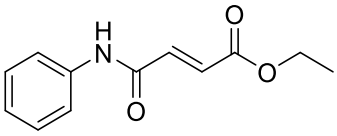

The procedure in experiment A was applied to the starting material mono-ethyl fumarate (0.5 g, 3.5 mmol). Previously distilled aniline (5.2 mmol) was used in this experiment. Purification of the reaction crude performed by recrystallization afforded compound **1a** (0.555 g, 73%) as a white solid. This reaction was repeated and compound **1a** was also obtained (0.463 g, 61%).

^{1}H-NMR ($CDCl_3$): δ 7.86 (1H, broad s, NH), 7.61 (2H, d, J= 7.8 Hz, Ar), 7.35 (2H, t, J=8.0 Hz, Ar), 7.18 – 7.14 (1H, m, Ar), 7.12 (1H, d. J= 15.2 Hz, C<u>H</u>=CH), 6.96 (1H, d, J=15.3 Hz, CH=C<u>H</u>) ,4.28 (2H, q, J=7.3 Hz, O<u>C</u>$H_2$$CH_3$), 1.33 (3H, t. J= 7.2 Hz, OCH_2<u>CH_3</u>)

^{13}C-NMR ($CDCl_3$): δ 165.7 (C=O), 161.5 (C=O), 137.3 (Ar, quaternary C), 136.8 (<u>C</u>=C), 131.4 (C=<u>C</u>), 129.1 (Ar), 125.0 (Ar), 120.0 (Ar), 61.4 (<u>C</u>$H_2$$CH_3$), 14.1 ($CH_2$<u>$CH_3$</u>)

Melting Point – 105 °C

FT-IR (ATR): 3348 (N-H), 1703 (C=O), 1677 (C=O) **(ν_{max}/cm^{-1})**

<u>Experiment 2:</u> Synthesis of (2E) -3-(phenylcarbamoyl) prop-2-enoic acid (1b)

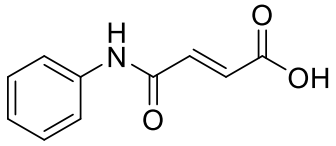

The procedure in experiment B was applied to compound **1a** (0.3 g, 1.4 mmol). Purification of the reaction crude performed by recrystallization afforded compound **1b** (69 mg, 26 %) as a white solid.

^{1}H-NMR (DMSO-d_6): δ 12.90 (1H, broad s, OH), 10.49 (1H, s, NH), 7.68 (2H, d, J= 7.7 Hz, Ar), 7.35 (2H, t, J= 7.8 Hz, Ar), 7.15 (1H, d, J=15.3 Hz, Ar), 7.10 (1H, d, J= 7.4 Hz, C<u>H</u>=CH), 6.66 (1H, d, J= 15.3 Hz, (CH=C<u>H</u>).

^{13}C-NMR (DMSO-d_6): δ 166.8 (C=O), 162.1 (C=O), 139.0 (Ar, quaternary C), 137.6 (<u>C</u>=C), 131.3 (C=<u>C</u>), 129.4 (Ar), 124.5 (Ar), 119.8 (Ar).

Melting Point – 228 °C

FT-IR (ATR): 3305 (O-H), 1659 (C=O), 1644 (C=O) **(v_{max}/cm^{-1})**

<u>Experiment 3:</u> Synthesis of (2E)-N-hydroxy-N'-phenylbut-2-enediamide (1c)

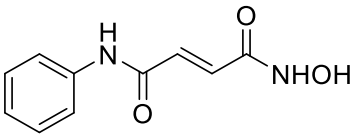

The procedure in experiment C was applied to compound **1a** (0.5 g, 2.3 mmol). Purification of the reaction crude performed by recrystallization afforded compound **1c** (203 mg, 43 %) as a white solid.

^{1}H-NMR (DMSO-d_6): δ 11.12 (1H, broad s, OH), 10.41 (1H, s, NH), 9.20 (1H, broad s, N<u>H</u>-OH), 7.67 (2H, d, J= 7.8 Hz, Ar), 7.34 (2H, t, J= 7.8 Hz, Ar), 7.10 (1H, s, Ar), 7.08 (1H, d, J= 15.2 Hz, CH=CH), 6.82 (1H, d, J= 15.2 Hz, CH=C<u>H</u>).

^{13}C-NMR (DMSO-d_6): δ 166.7 (C=O), 161.6 (C=O), 139.2 (Ar, quaternary C), 131.6 (<u>C</u>=C), 134.5 (C=<u>C</u>), 129.3 (Ar), 124.3 (Ar), 119.8 (Ar).

Melting Point – 197 °C

FT-IR (ATR): 3250 (O-H), 1687 (C=O), 1649 (C=O) **(v_{max}/cm^{-1})**

Experiment 4: Synthesis of ethyl (2E)-3-[(4-fluorophenyl)carbamoyl]prop-2-enoate (2a)

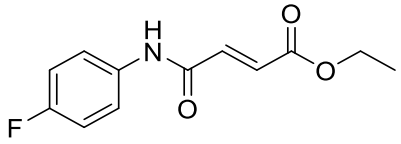

The procedure in experiment A was applied to mono-ethyl fumarate (0.8 g, 5.55 mmol). 2-Fluoroaniline (8.3 mmol) was used in this experiment. Purification of the reaction crude performed by recrystallization afforded compound **2a** (0.974 g, 74 %) as a white solid.

^{1}H-NMR ($CDCl_3$): δ 7.86 (1H, broad s, NH), 7.59 – 7.56 (2H, m, Ar), 7.09 (1H, d, J= 15.3 Hz, C<u>H</u>=CH), 7.07 – 7.02 (2H, m, Ar), 6.95 (1H, d, J= 15.24 Hz, CH=C<u>H</u>), 4.27 (2H, q, J=7.2 Hz, O<u>C</u>H_2CH_3), 1.33 (3H, t. J= 7.2 Hz, OCH_2<u>C</u>H_3)

^{13}C-NMR ($CDCl_3$): δ 165.6 (C=O), 161.5 (C=O), 160.1 (quaternary C, F-<u>C</u>), 136.4 (<u>C</u>=C), 133.4 (Ar, quaternary C), 131.5 (C=<u>C</u>), 121.9 (Ar), 121.8 (Ar), 115.9 (Ar), 115.7 (Ar), 61.5 (<u>C</u>H_2CH_3), 14.1 (CH_2<u>C</u>H_3)

Melting Point – 149 °C

FT-IR (ATR): 3302 (N-H), 1716 (C=O), 1670 (C=O) **(ν_{max}/cm^{-1})**

Experiment 5: Synthesis of (2E)-2-[(4-fluorophenyl)carbamoyl]prop-2-enoic acid (2b)

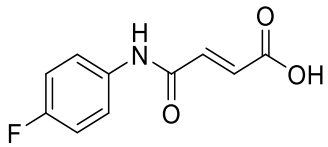

The procedure in experiment B was applied to compound **2a** (0.3 g, 1.3 mmol). Purification of the reaction crude performed by recrystallization afforded compound **2b** (70 mg, 27 %) as a white solid.

^{1}H-NMR (DMSO-d_6): δ 13.01 (1H, broad s, OH), 10.55 (1H, broad s, NH), 7.72 – 7.68 (2H, m, Ar), 7.19 (2H, t, J= 8.8 Hz, Ar), 7.10 (1H, d, J= 15.4 Hz, C<u>H</u>=CH), 6.66 (1H, d, J= 15.4 Hz, CH=C<u>H</u>)

^{13}C-NMR (DMSO-d_6): δ 166.7 (C=O), 162.0 (C=O), 160.1 (quaternary C, F-<u>C</u>), 137.3 (<u>C</u>=C), 135.4 (Ar, quaternary C), 131.4 (C=<u>C</u>), 121.7 (Ar), 121.6 (Ar), 116.1 (Ar), 115.9 (Ar)

Melting Point – 235 °C

FT-IR (ATR): 3306 (O-H), 1658 (C=O), 1643 (C=O) **(ν_{max}/cm^{-1})**

Experiment 6: Synthesis of (2E)-N'-(4-fluorophenyl)-N-hydroxybut-2-enediamide (2c)

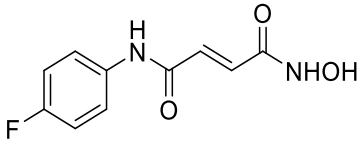

The procedure in experiment C was applied to compound **2a** (0.4 g, 1.7 mmol). Purification of the reaction crude performed by recrystallization afforded compound **2c** (147 mg, 39 %) as a white solid.

^{1}H-NMR (DMSO-d_6): δ 11.10 (1H, broad s, OH), 10.49 (1H, s, NH), 9.32 (1H, broad s, NH-OH), 7.71 – 7.66 (2H, m, Ar), 7.21 – 7.15 (2H, m, Ar), 7.06 (1H, d, J= 15.1 Hz, CH=CH), 6.82 (1H, d, J= 15.1 Hz, CH=CH)

^{13}C-NMR (DMSO-d_6): δ 162.5 (C=O), 159.9 (C=O), 157.6 (quaternary C, F-C), 135.6 (Ar, quaternary C), 131.6 (C=C), 121.6 (Ar), 121.5 (Ar), 116.0 (Ar), 115.8 (Ar)

Melting Point – 216 °C

FT-IR (ATR): 3257 (O-H), 1687 (C=O), 1647 (C=O) **(ν_{max}/cm^{-1})**

Experiment 7: Synthesis of ethyl (2E)-3-[(2-bromophenyl)carbamoyl]prop-2-enoate (3a)

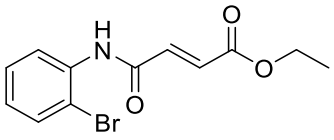

The procedure in experiment A was applied to mono-ethyl fumarate (0.8 g, 5.55 mmol). 2-Bromoaniline (8.3 mmol) was used in this experiment. Purification of the reaction crude performed by recrystallization afforded compound **3a** (0.671 g, 41 %) as a brown solid.

^{1}H-NMR ($CDCl_3$): δ 8.45 (1H, d, J= 8.1 Hz, Ar), 7.89 (1H, broad s, NH), 7.57 (1H, d, J=8.0 HZ, Ar), 7.35 (1H, t, J= 8.0 Hz, Ar), 7.09 (1H, d, J=15.3 Hz, CH=CH), 7.03 (1H, t, J= 8.0 Hz, Ar), 6.95 (1H, d, J= 15.3 Hz, CH=CH), 4.29 (2H, q, J=7.2, OCH_2CH_3), 1.35 (3H, t. J= 7.12 Hz, OCH_2CH_3)

^{13}C-NMR ($CDCl_3$): δ 166.7 (C=O), 161.5 (C=O), 136.1 (Ar, quaternary C), 135.7 (C=C), 131.8 (Ar), 127.9 (Ar), 127.5 (C=C), 125.5 (Ar), 117.5 (quaternary C, Br-C), 61.4 (CH_2CH_3), 14.4 (CH_2CH_3)

Melting Point – 115 °C

FT-IR (ATR): 3282 (N-H), 1712 (C=O), 1688 (C=O) **(ν_{max}/cm^{-1})**

Experiment 8: **Synthesis of (2E)-3-[(2-bromophenyl)carbamoyl]prop-2-enoic acid (3b)**

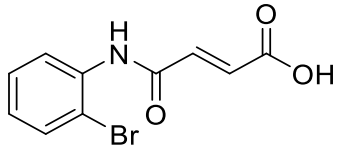

The procedure in experiment B was applied to compound **3a** (0.3 g, 1 mmol). Purification of the reaction crude performed by recrystallization afforded compound **3b** (133 mg, 49 %) as a brown solid.

^{1}H-NMR (DMSO-d_6): δ 13.02 (1H, broad s, OH), 10.08 (1H, s, NH), 7.70 - 7.65 (2H, m, Ar), 7.41 (1H, t, J= 7.8 Hz), 7.29 (1H. d, J= 15.4 Hz, CH=CH), 7.19 (1H, t, J= 7.9 Hz), 6.67 (1H, d, J= 15.4 Hz, CH=CH)

^{13}C-NMR (DMSO-d_6): δ 166.7 (C=O), 162.6 (C=O), 136.9 (C=C), 136.1 (Ar, quaternary C), 133.3 (Ar), 131.9 (C=C), 128.5 (Ar), 128.1 (Ar), 127.8 (Ar), 118.5 (quaternary C, Br-C)

Melting Point – 213 °C

FT-IR (ATR): 3271 (O-H), 1696 (C=O), 1662 (C=O) **(v_{max}/cm^{-1})**

Experiment 9: **Synthesis of (2E)-N'-(2-bromophenyl)-N-hydroxybut-2-enediamide (3c)**

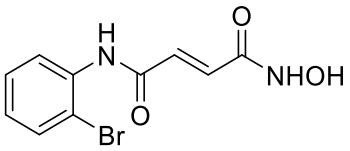

The procedure in experiment C was applied to compound **3a** (0.3 g, 1 mmol). Purification of the reaction crude performed by recrystallization afforded compound **3c** (146 mg, 51 %) as a white solid.

^{1}H-NMR (DMSO-d_6): δ 11.11 (1H, s, OH), 10.01 (1H, s, NH), 9.32 (1H, broad s, NH-OH), 7.70 – 7.65 (2H, m, Ar), 7.41 (1H, t, J= 7.4 Hz, Ar), 7.24 (1H, J= 15.2 Hz, CH=CH), 7.18 (2H, t, J= 7.4 Hz, Ar), 6.84 (1H, d, J= 15.2 Hz, CH=CH)

^{13}C-NMR (DMSO-d_6): δ 166.7 (C=O), 161.6 (C=O), 136.2 (Ar, quaternary C), 133.2 (C=C), 132.2 (Ar), 128.5 (C=C), 128.0 (Ar), 127.8 (Ar), 117.5 (quaternary C, Br-C)

Melting Point – 207 °C

FT-IR (ATR): 3255 (O-H), 1672 (C=O), 1623 (C=O) **(v_{max}/cm^{-1})**

Experiment 10: Synthesis of ethyl (2E)-3-[(4-bromophenyl)carbamoyl]prop-2-enoate (4a)

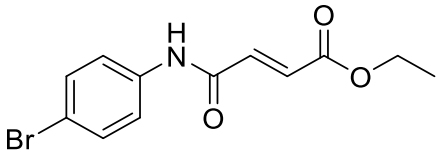

The procedure in experiment A was applied to mono-ethyl fumarate (0.8 g, 5.55 mmol). 4-Bromoaniline (8.4 mmol) was used in this experiment. Purification of the reaction crude performed by recrystallization afforded compound **4a** (1.484 g, 90 %) as a white solid.

^{1}H-NMR ($CDCl_3$): δ 7.82 (1H, broad s, NH), 7.52 (2H, d, J=8.8 Hz, Ar), 7.46 (2H, d, J= 8.8 Hz, Ar), 7.07 (1H, d, J=15.3 Hz, C<u>H</u>=CH), 6.95 (1H, d, J= 15.3 Hz, CH=C<u>H</u>), 4.28 (2H, q, J=7.2 Hz, O<u>C</u>H_2CH_3), 1.33 (3H, t. J= 7.2 Hz, OCH_2<u>C</u>H_3)

^{13}C-NMR ($CDCl_3$): δ 165.5 (C=O), 161.5 (C=O), 136.5 (Ar, quaternary C), 136.2 (<u>C</u>=C), 132.1 (Ar), 131.8 (C=<u>C</u>), 121.5 (Ar), 117.8 (quaternary C, Br-<u>C</u>), 61.5 (<u>C</u>H_2CH_3), 14.1 (CH_2<u>C</u>H_3)

Melting Point – 159 °C

FT-IR (ATR): 3295 (N-H), 1712 (C=O), 1669 (C=O) **(ν_{max}/cm^{-1})**

Experiment 11: Synthesis of (2E)-3-[(4-bromophenyl)carbamoyl]prop-2-enoic acid (4b)

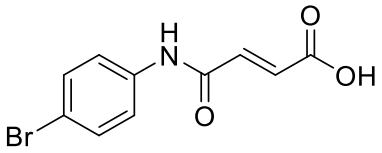

The procedure in experiment B was applied to compound **4a** (0.3 g, 1 mmol). Purification of the reaction crude performed by recrystallization afforded compound **4b** (202 mg, 74 %) as a white solid.

^{1}H-NMR (DMSO-d_6): δ 13.03 (1H, broad s, OH), 10.62 (1H, s, NH), 7.64 (2H, d, J= 8.9 Hz, Ar), 7.53 (2H, d, J=8.8 Hz, Ar), 7.11 (1H, d, J=15.4 Hz, C<u>H</u>=CH), 6.66 (1H, d, J= 15.4 Hz, CH=C<u>H</u>)

^{13}C-NMR (DMSO-d_6): δ 166.7 (C=O), 162.2 (C=O), 138.4 (Ar, quaternary C), 137.3 (<u>C</u>=C), 132.2 (Ar), 131.5 (C=<u>C</u>), 121.8 (Ar), 116.2 (quaternary C, Br-<u>C</u>)

Melting Point – >250 °C

FT-IR (ATR): 3296 (O-H), 1656 (C=O), 1647 (C=O) **(ν_{max}/cm^{-1})**

Experiment 12: Synthesis of (2E)-N'-(4-bromophenyl)-N-hydroxybut-2-enediamide (4c)

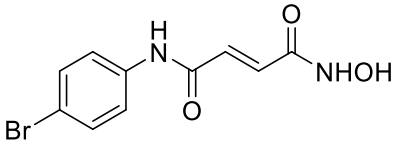

The procedure in experiment C was applied to compound **4a** (0.4 g, 1.3 mmol). Purification of the reaction crude performed by recrystallization afforded compound **4c** (110 mg, 29 %) as a yellowish solid.

^{1}H-NMR (DMSO-d_6): δ 11.15 (1H, broad s, OH), 10.59 (1H, s, NH), 9.36 (1H, broad s, NH-OH), 7.65 (2H, d, J=8.8 Hz, Ar), 7.53 (2H, d, J= 8.8 Hz, Ar), 7.07 (1H, d, J=15.3 Hz, CH=CH), 6.83 (1H, d, J= 15.3 Hz, CH=CH)

^{13}C-NMR (DMSO-d_6): δ 164.5 (C=O), 162.8 (C=O), 138.6 (Ar, quaternary C), 132.2 (Ar), 131.9 (C=C), 121.7 (Ar), 115.9 (quaternary C, Br-C).

Melting Point – 247 °C

FT-IR (ATR): 3207 (O-H), 1648 (C=O), 1621 (C=O) **(ν_{max}/cm^{-1})**

Experiment 13: Synthesis of ethyl (2E)-3-[(2-fluorophenyl)carbamoyl]prop-2-enoate (5a)

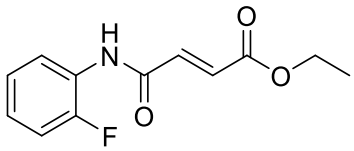

The procedure in experiment A was applied to mono-ethyl fumarate (0.8 g, 5.55 mmol). 2-Fluoroaniline (8.4 mmol) was used in this experiment. Purification of the reaction crude performed by recrystallization afforded compound **5a** (0.671 g, 52 %) as a white solid.

^{1}H-NMR ($CDCl_3$): δ 8.41 (1H, t, J=8.1 Hz, Ar), 7.66 (1H, broad s, NH), 7.19 – 7.12 (3H, m, Ar), 7.07 (1H, d, J=15.3 Hz, CH=CH), 6.95 (1H, d, J= 15.3 Hz, CH=CH), 4.29 (2H, q, J=7.2 Hz, OCH_2CH_3), 1.34 (3H, t, J= 7.2 Hz, OCH_2CH_3)

^{13}C-NMR ($CDCl_3$): δ 165.2 (C=O), 161.4 (C=O), 158.3 (F-C, quaternary C), 144.1 (Ar, quaternary C), 135.8(C=C), 132.1 (C=C), 125.2 (Ar), 124.7 (Ar), 121.8 (Ar), 114.9 (Ar), 61.4 (CH_2CH_3), 14.2 (CH_2CH_3)

Melting Point – 96 °C

FT-IR (ATR): 3355 (N-H), 1710 (C=O), 1678 (C=O) **(ν_{max}/cm^{-1})**

Experiment 14: Synthesis of (2E)-3-[(2-fluorophenyl)carbamoyl]prop-2-enoic acid (5b)

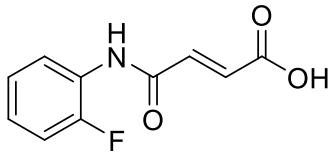

The procedure in experiment B was applied to compound **5a** (0.3 g, 1.3 mmol). Purification of the reaction crude performed by recrystallization afforded compound **5b** (195 mg, 74 %) as a white solid.

^{1}H-NMR (DMSO-d_6): δ 13.01 (1H, s, OH), 10.32 (1H, s, NH), 8.03 – 7.99 (1H, m, Ar), 7.33 (2H. d, J= 15.4 Hz, CH=CH), 7.30 – 7.26 (1H, m, Ar), 7.23 – 7.18 (2H, m, Ar), 6.68 (1H, d, J= 15.4 Hz, CH=CH)

^{13}C-NMR (DMSO-d_6): δ 166.7 (C=O), 162.6 (C=O), 155.3 (F-C, quaternary C), 152.8 (Ar, quaternary C), 136.9 (C=C), 131.8 (C=C), 126.4 (Ar), 124.9 (Ar), 124.5 (Ar), 115.9 (Ar)

Melting Point – 215 °C

FT-IR (ATR): 3290 (O-H), 1693 (C=O), 1665 (C=O) **(v_{max}/cm^{-1})**

Experiment 15: Synthesis of (2E)-N'-(2-fluorophenyl)-N-hydroxybut-2-enediamide (5c)

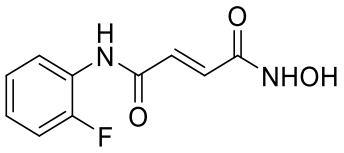

The procedure in experiment C was applied to compound **5a** (0.282 g, 1.2 mmol). Purification of the reaction crude performed by recrystallization afforded compound **5c** (98 mg, 37 %) as a white solid.

^{1}H-NMR (DMSO-d_6): δ 11.10 (1H, broad s, OH), 10.23 (1H, s, NH), 9.33 (1H, broad s, NH-OH), 8.01 – 7.96 (1H, m, Ar), 7.31 – 7.17 (4H, m, Ar and CH=CH), 6.84 (1H, d, J= 15.16 Hz, CH=CH).

^{13}C-NMR (DMSO-d_6): δ 166.7 (C=O), 163.1 (C=O), 155.3 (F-C, quaternary C), 132.2 (C=C), 126.3 (C=C), 126.2 (Ar, quaternary C), 124.9 (Ar), 124.6 (Ar), 116.1 (Ar), 115.9 (Ar)

Melting Point – 212 °C

FT-IR (ATR): 3067 (O-H), 1681 (C=O), 1614 (C=O) **(v_{max}/cm^{-1})**

Experiment 16: Synthesis of ethyl (2E)-3-[(2-chlorophenyl)carbamoyl]prop-2-enoate (6a)

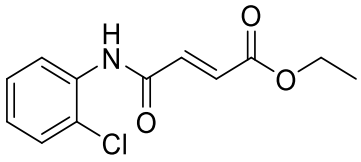

The procedure in experiment A was applied to mono-ethyl fumarate (0.8 g, 5.55 mmol). 2-chloroaniline (8.3 mmol) was used in this experiment. Purification of the reaction crude performed by recrystallization afforded compound **6a** (0.758 g, 54 %) as a white solid.

^{1}H-NMR ($CDCl_3$): δ 8.52 (1H, t, J=8.1 Hz, Ar), 7.91 (1H, broad s, NH), 7.42 (1H, d, J= 8.1 Hz, Ar), 7.31 (1H, t, J=8.0 Hz, Ar) 7.12 – 7.07 (2H, m. Ar and C<u>H</u>=CH), 6.95 (1H, d, J= 15.3 Hz, CH=C<u>H</u>), 4.29 (2H, q, J=7.2 Hz, O<u>C</u>H_2CH_3), 1.35 (3H, t, J= 7.2 Hz, OCH_2<u>C</u>H_3)

^{13}C-NMR ($CDCl_3$): δ 165.2 (C=O), 160.6 (C=O), 134.1 (Ar, quaternary C), 136.1(<u>C</u>=C), 132.1 (C=<u>C</u>), 129.1 (Ar),128.2 (Cl-<u>C</u>, quaternary C), 127.9 (Ar), 125.4 (Ar), 121.8 (Ar), 121.6 (Ar), 61.4 (<u>C</u>H_2CH_3), 14.2 (CH_2<u>C</u>H_3)

Melting Point – 100 °C

FT-IR (ATR): 3282 (N-H), 1712 (C=O), 1667 (C=O) **(ν_{max}/cm^{-1})**

Experiment 17: Synthesis of (2E)-3-[(2-chlorophenyl)carbamoyl]prop-2-enoic acid (6b)

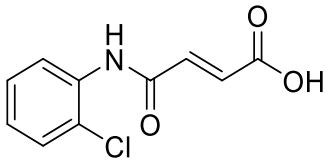

The procedure in experiment B was applied to compound **6a** (0.3 g, 1.1 mmol). Purification of the reaction crude performed by recrystallization afforded compound **6b** (233 mg, 88 %) as a white solid.

^{1}H-NMR (DMSO-d_6): δ 12.96 (1H, broad s, OH), 10.13 (1H, s, NH), 7.79 (1H, d, J=7.9 Hz, Ar), 7.53 (1H, d, J= 7.9 Hz, Ar), 7.39 – 7.32 (2H, m, Ar and C<u>H</u>=CH), 7.25 (1H, t, J=7.8 Hz, Ar), 6.68 (1H, d, J= 15.4 Hz, CH=C<u>H</u>)

^{13}C-NMR (DMSO-d_6): δ 166.8 (C=O), 162.6 (C=O), 137.0 (<u>C</u>=C), 134.7 (Ar, quaternary C), 131.8 (C=<u>C</u>), 130.1 (Ar), 127.9 (Ar), 127.4 (Ar), 127.1 (quaternary C, Cl-<u>C</u>), 126.8 (Ar)

Melting Point – 220 °C

FT-IR (ATR): 3275 (O-H), 1694 (C=O), 1663 (C=O) **(ν_{max}/cm^{-1})**

Experiment 18: Synthesis of (2E)-N'-(2-chlorophenyl)-N-hydroxybut-2-enediamide (6c)

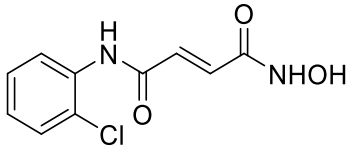

The procedure in experiment C was applied to compound **6a** (0.3 g, 1.1 mmol). Purification of the reaction crude performed by recrystallization afforded compound **6c** (70 mg, 25 %) as a white solid.

^{1}H-NMR (DMSO-d_6): δ 11.13 (1H, broad s, OH), 10.06 (1H, s, NH), 9.35 (1H, broad s, NH-OH), 7.77 (1H, d, J=7.9 Hz, Ar), 7.5 (1H, d, J= 8.0 Hz, Ar), 7.36 (1H, d, J=7.9 Hz, Ar), 7.28 – 7.21 (2H, m, Ar and CH=CH), 6.84 (1H, d, J=15.2 Hz, CH=CH)

^{13}C-NMR (DMSO-d_6): δ 166.1 (C=O), 163.1 (C=O), 134.9 (Ar, quaternary C), 132.2 (C=C), 130.0 (C=C), 127.9 (Ar), 127.3 (quaternary C, Cl-C), 127.3 (Ar), 126.9 (Ar)

Melting Point – 202 °C

FT-IR (ATR): 3255 (O-H), 1638 (C=O), 1618 (C=O) **(ν_{max}/cm^{-1})**

Experiment 19: Synthesis of ethyl (2E)-3-[(2-bromo-4-fluorophenyl)carbamoyl]prop-2-enoate (7a)

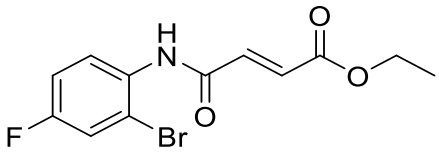

The procedure in experiment A was applied to mono-ethyl fumarate (0.8 g, 5.55 mmol). 2-Bromo-4-fluoroaniline (8.3 mmol) was used in this experiment. Purification of the reaction crude performed by recrystallization afforded compound **7a** (1g, 38 %) as a white solid.

^{1}H-NMR ($CDCl_3$): δ 8.44 – 8.41 (1H, m, Ar), 7.77 (1H, broad s, NH), 7.35 – 7.32 (1H, m, Ar), 7.12–7.05 (2H, m, Ar and CH=CH), 6.95 (1H, d, J= 15.3 Hz, CH=CH), 4.30 (2H, q, J=7.2 Hz, OCH_2CH_3), 1.35 (3H, t, J= 7.2 Hz, OCH_2CH_3)

^{13}C-NMR ($CDCl_3$): δ 165.2 (C=O), 160.2 (C=O), 151.4 (F-C, quaternary C), 135.9 (C=C), 132.2 (C=C), 131.6 (Ar, quaternary C), 123.1 (Ar), 120.5 (Br-C, quaternary C), 119.5 (Ar), 115.4 (Ar), 61.5 (CH_2CH_3), 14.2 (CH_2CH_3)

Melting Point – 130 °C

FT-IR (ATR): 3265 (N-H), 1714 (C=O), 1669 (C=O) **(ν_{max}/cm^{-1})**

<u>Experiment 20:</u> Synthesis of (2E)-3-[(2-bromo-4-fluorophenyl)carbamoyl]prop-2-enoic acid (7b)

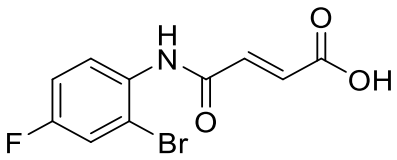

The procedure in experiment B was applied to compound **7a** (0.3 g, 0.95 mmol). Purification of the reaction crude performed by recrystallization afforded compound **7b** (243 mg, 89%) as a white solid.

^{1}H-NMR (DMSO-d_6): δ 13.05 (1H, broad s, OH), 10.13 (1H, s, NH), 7.70 – 7.63 (2H, m, Ar), 7.34 – 7.28 (1H, m, Ar), 7.25 (1H, d, J=15.4 Hz, C<u>H</u>=CH), 6.68 (1H, d, J=15.3 Hz, CH=C<u>H</u>)

^{13}C-NMR (DMSO-d_6): δ 166.7 (C=O), 162.8 (C=O), 161.2 (quaternary C, F-<u>C</u>), 136.8 (<u>C</u>=C), 132.8 (Ar, quaternary C), 131.9 (C=<u>C</u>), 129.4 (Ar), 120.1 (Ar), 119.5 (quaternary C, Br-<u>C</u>), 115.5 (Ar)

Melting Point – 230 °C

FT-IR (ATR): 3258 (O-H), 1698 (C=O), 1660 (C=O) **(ν_{max}/cm^{-1})**

<u>Experiment 21:</u> Synthesis of (2E)-N'-(2-bromo-4-fluorophenyl)-N-hydroxybut-2-enediamide (7c)

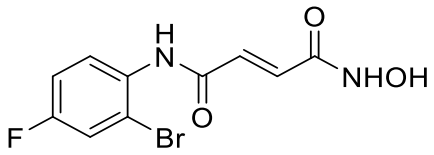

The procedure in experiment C was applied to compound **7a** (0.3 g, 1.1 mmol). Purification of the reaction crude performed by recrystallization afforded compound **7c** (79 mg, 27 %) as a white solid.

^{1}H-NMR (DMSO-d_6): δ 11.10 (1H, broad s, OH), 10.05 (1H, s, NH), 9.33 (1H, broad s, N<u>H</u>-OH), 7.69 – 7.62 (2H, m, Ar), 7.30 (1H, t, J= 8.2 Hz, Ar), 7.20 (1H, d, J= 15.2 Hz, C<u>H</u>=CH), 6.83 (1H, d, J= 15.2 Hz, CH=C<u>H</u>)

^{13}C-NMR (DMSO-d_6): δ 166.7 (C=O), 161.6 (C=O), 160.7 (quaternary C, F-<u>C</u>), 134.5 (<u>C</u>=C), 131.6 (Ar, quaternary C), 130.8 (C=<u>C</u>), 125.4 (Ar), 124.2 (quaternary C, Br-<u>C</u>), 120.9 (Ar), 114.7 (Ar)

Melting Point – 203 °C

FT-IR (ATR): 3259 (O-H), 1638 (C=O), 1614 (C=O) **(ν_{max}/cm^{-1})**

Experiment 22: Synthesis of ethyl (2E)-3-{[4-(trifluoromethyl)phenyl]carbamoyl}prop-2-enoate (8a)

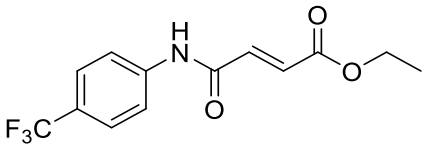

The procedure in experiment A was applied to mono-ethyl fumarate (0.8 g, 5.55 mmol. 4-(Trifluoromethyl)aniline (8.3 mmol) was used in this experiment. Purification of the reaction crude performed by recrystallization afforded compound **8a** (1.136 g, 71 %) as a white solid.

^{1}H-NMR ($CDCl_3$): δ 8.00 (1H, broad s, NH), 7.75 (1H, d, J= 8.3 Hz, Ar), 7.61 (1H, d, J= 8.4 Hz, Ar), 7.11 (1H, d, J= 15.3 Hz, C<u>H</u>=CH), 6.98 (1H, d, J= 15.4 Hz, CH=C<u>H</u>), 4.29 (2H, q, J=7.2 Hz, O<u>C</u>$H_2$$CH_3$), 1.34 (3H, t, J= 7.1 Hz, OCH_2<u>C</u>H_3)

^{13}C-NMR ($CDCl_3$): δ 166.7 (C=O), 162.5 (C=O), 140.9 (Ar, quaternary C), 135.7 (<u>C</u>=C), 133.1 (C=<u>C</u>), 132.1 (<u>C</u>-CF_3, quaternary C), 125.3 (Ar), 124.1 (C-<u>C</u>F_3, quaternary C), 121.9 (Ar), 61.4 (<u>C</u>H_2CH_3), 14.2 (CH_2<u>C</u>H_3)

Melting Point – 180 °C

FT-IR (ATR): 3350 (N-H), 1702 (C=O), 1682 (C=O) **(ν_{max}/cm^{-1})**

Experiment 23: Synthesis of (2E)-3-{[4-(trifluoromethyl)phenyl]carbamoyl}prop-2-enoic acid (8b)

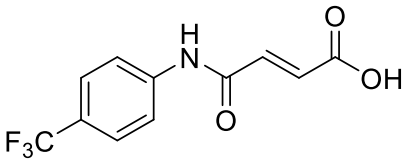

The procedure in experiment B was applied to compound **8a** (0.3 g, 1.2 mmol). Purification of the reaction crude performed by recrystallization afforded compound **8b** (211 mg, 70%) as a white solid.

^{1}H-NMR (DMSO-d_6): δ 13.08 (1H, broad s, OH), 10.84 (1H, s, NH), 7.88 (2H, d, J=8.4 Hz, Ar), 7.73 (2H, d, J= 8.4 Hz, Ar), 7.15 (1H, d, J= 15.4 Hz, C<u>H</u>=CH), 6.70 (1H, d, J= 15.4 Hz, C<u>H</u>=CH)

^{13}C-NMR (DMSO-d_6): δ 166.6 (C=O), 162.6 (C=O), 142.7 (Ar, quaternary C), 137.0 (<u>C</u>=C), 131.9 (C=<u>C</u>), 126.6 (Ar), 126.1 (<u>C</u>-CF_3, quaternary C), 124.4 (C-<u>C</u>F_3, quaternary C), 119.9 (Ar)

Melting Point – >250 °C

FT-IR (ATR): 3304 (O-H), 1695 (C=O), 1662 (C=O) **(ν_{max}/cm^{-1})**

<u>Experiment 24:</u> Synthesis of (2E)-N-hydroxy-N'-[4-trifluoromethyl)phenyl]but-2-enediamide (8c)

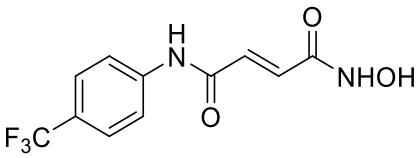

The procedure in experiment C was applied to compound **8a** (0.35 g, 1.2 mmol). Purification of the reaction crude performed by recrystallization afforded compound **8c** (326 mg, 97 %) as a yellow solid.

^{1}H-NMR (DMSO-d_6): δ 11.10 (1H, broad s, OH), 10.59 (1H, s, NH), 9.50 (1H, broad s, N<u>H</u>-OH), 7.89 (2H, d, J= 8.3 Hz, Ar), 7.66 (2H, d, J= 8.4 Hz, Ar), 6.81–6.73 (2H, m, C<u>H</u>=CH and CH=C<u>H</u>)

^{13}C-NMR (DMSO-d_6): δ 165.1 (C=O), 163.6 (C=O), 143.8 (Ar, quaternary C), 138.9 (<u>C</u>=C), 132.3 (C=<u>C</u>), 126.5 (Ar), 126.4 (<u>C</u>-CF_3, quaternary C), 123.6 (C-<u>C</u>F_3, quaternary C), 119.4 (Ar)

Melting Point – 213 °C

FT-IR (ATR): 3301 (O-H), 1636 (C=O), 1603 (C=O) **(ν_{max}/cm^{-1})**

<u>Experiment 25:</u> Synthesis of ethyl (2E)-3-[(3-methoxyphenyl)carbamoyl]prop-2-enoate (9a)

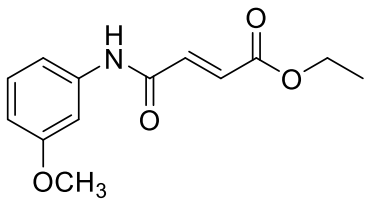

The procedure in experiment A was applied to mono-ethyl fumarate (0.8 g, 5.55 mmol). 3-Methoxyaniline (8.3 mmol) was used in this experiment. Purification of the reaction crude performed by recrystallization using afforded compound **9a** (0.971 g, 70.4 %) as a white solid.

^{1}H-NMR ($CDCl_3$): δ 7.72 (1H, broad s, NH), 7.24 (2H, t, J= 8.2 Hz, Ar), 7.11-7.05 (2H, m, Ar and C<u>H</u>=CH), 6.95 (1H, d, J= 15.2 Hz, CH=C<u>H</u>), 6.73-6.70 (1H, m, Ar), 4.28 (2H, q, J=7.2 Hz, O<u>C</u>$H_2$$CH_3$), 1.34 (3H, t, J= 7.1 Hz, OCH_2<u>C</u>H_3)

^{13}C-NMR ($CDCl_3$): δ 165.6 (C=O), 161.5 (C=O), 160.2 (<u>C</u>-OCH_3, quaternary), 136.7 (<u>C</u>=C), 132.1 (Ar, quaternary C), 131.5 (C=<u>C</u>), 129.8 (Ar), 112.1 (Ar), 110.9 (Ar), 105.8 (Ar), 61.4 (<u>C</u>$H_2$$CH_3$), 55.3 (C-O<u>C</u>$H_3$, quaternary C), 14.1 ($CH_2$<u>C</u>$H_3$)

Melting Point – 110 °C

FT-IR (ATR): 3354 (N-H), 1704 (C=O), 1681 (C=O) **(ν_{max}/cm^{-1})**

Experiment 26: Synthesis of (2E)-3-[(3-methoxyphenyl)carbamoyl]prop-2-enoic acid (9b)

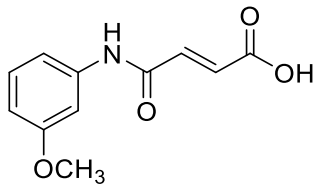

The procedure in experiment B was applied to compound **9a** (0.3 g, 1.2 mmol). Purification of the reaction crude performed by recrystallization afforded compound **9b** (237 mg, 89%) as a white solid.

^{1}H-NMR (DMSO-d_6): δ 13.02 (1H, broad s, OH), 10.49 (1H, s, NH), 7.25 (1H, t, J= 8.0 Hz, Ar), 7.19 (1H, d, J= 8.1 Hz, Ar), 7.13 (1H, d, J=15.4 Hz, CH=CH), 6.71 – 6.68 (1H, m, Ar), 6.66 (1H, d, J=15.4 Hz, CH=CH)

^{13}C-NMR (DMSO-d_6): δ 166.7 (C=O), 162.1 (C=O), 159.9 (C-OCH_3, quaternary), 140.2 (Ar, quaternary C), 137.6 (C=C), 131.2 (C=C), 130.1 (Ar), 112.2 (Ar), 109.9 (Ar), 105.7 (Ar), 55.5 (C-OCH_3, quaternary C)

Melting Point – 195 °C

FT-IR (ATR): 3292 (O-H), 1697 (C=O), 1658 (C=O) **(ν_{max}/cm^{-1})**

Experiment 27: Synthesis of (2E)-N-hydroxy-N'-(3-methoxyphenyl)but-2-enediamide (9c)

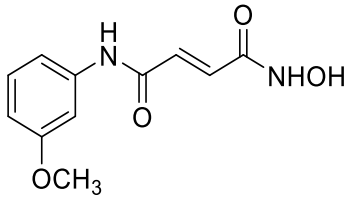

The procedure in experiment C was applied to compound **9a** (0.35 g, 1.4 mmol). Purification of the reaction crude performed by recrystallization afforded compound **9c** (30 mg, 15 %) as a yellow solid.

^{1}H-NMR (DMSO-d_6): δ 11.12 (1H, broad s, OH), 10.42 (1H, s, NH), 9.34 (1H, broad s, NH-OH), 7.27 – 7.18 (2H, m, Ar), 7.08 (1H, d, J= 15.1 Hz, CH=CH), 6.81 (1H, d, J= 15.1 Hz, CH=CH), 6.70 – 6.66 (1H, m, Ar)

^{13}C-NMR (DMSO-d_6): δ 166.6 (C=O), 162.6 (C=O),159.9 (C-OCH_3, quaternary), 140.4 (Ar, quaternary C), 132.9 (C=C), 131.7 (C=C), 130.1 (Ar), 112.1 (Ar), 109.7 (Ar), 105.7 (Ar), 55.5 (C-OCH_3, quaternary C)

Melting Point – 212 °C

FT-IR (ATR): 3209 (O-H), 1649 (C=O), 1618 (C=O) **(v_{max}/cm^{-1})**

Experiment 28: Synthesis of ethyl (2E)-3-[(2-iodophenyl)carbamoyl]prop-2-enoate (10a)

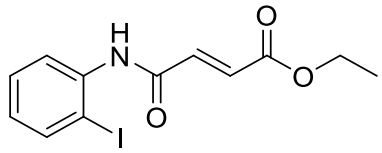

The procedure in experiment A was applied to mono-ethyl fumarate (0.6 g, 4.2 mmol). 2-iodoaniline (6.2 mmol) was used in this experiment. Purification of the reaction crude performed by recrystallization afforded compound **10a** (0.696 g, 48 %) as a white solid.

^{1}H-NMR ($CDCl_3$): δ 8.34 (1H, d, J= 7.9 Hz, Ar), 7.81 (1H, d, J= 7.9 Hz, Ar), 7.72 (1H, broad s, NH), 7.38 (1H, t, J= 8.1 Hz, Ar). 7.09 (1H, t, J= 15.2 Hz, C<u>H</u>=CH), 6.96 (1H, d, J= 15.2 Hz, CH=C<u>H</u>), 6.90 (1H, t, J= 7.9, Ar), 4.29 (2H, q, J=7.1 Hz, O<u>C</u>H_2CH_3), 1.35 (3H, t, J= 7.1 Hz, OCH_2<u>C</u>H_3)

^{13}C-NMR ($CDCl_3$): δ 165.2 (C=O), 161.7 (C=O), 138.9 (<u>C</u>=C), 137.6 (Ar, quaternary C), 136.2 (C=<u>C</u>), 132.0 (Ar), 129.4 (Ar), 126.7 (Ar), 122.0 (Ar), 95.2 (C-I, quaternary C), 61.5 (<u>C</u>H_2CH_3), 14.2 (CH_2<u>C</u>H_3)

Melting Point – 128 °C

FT-IR (ATR): 3273 (N-H), 1709 (C=O), 1667 (C=O) **(v_{max}/cm^{-1})**

Experiment 29: Synthesis of (2E)-3-[(2-iodophenyl)carbamoyl]prop-2-enoic acid (10b)

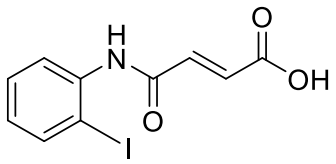

The procedure in experiment B was applied to compound **10a** (0.25 g, 0.7 mmol). Purification of the reaction crude performed by recrystallization afforded compound **10b** (222 mg, 97 %) as a white solid.

^{1}H-NMR (DMSO-d_6): δ 13.03 (1H, broad s, OH), 10.06 (1H, s, NH), 7.92 (1H, t, J= 7.9 Hz, Ar), 7.49 – 7.40 (2H, m, Ar), 7.24 (1H, d, J=15.4 Hz, C<u>H</u>=CH), 7.04 (1H, t, J=7.9 Hz, Ar), 6.67 (1H, d, J=15.5 Hz, CH=C<u>H</u>)

^{13}C-NMR (DMSO-d_6): δ 166.8 (C=O), 162.5 (C=O), 139.5 (<u>C</u>=C), 139.4 (Ar, quaternary C), 137.1 (C=<u>C</u>), 131.7 (Ar),129.2 (Ar), 128.7 (Ar), 127.9 (Ar), 96.9 (C-I, quaternary C)

Melting Point – 235 °C

FT-IR (ATR): 3262 (O-H), 1698 (C=O), 1662 (C=O) **(v_{max}/cm^{-1})**

Experiment 30: Synthesis of (2E)-N-hydroxy-N'-(2-iodophenyl)but-2-enediamide (10c)

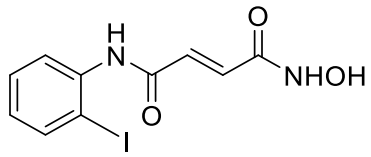

The procedure in experiment C was applied to compound **10a** (0.35 g, 1 mmol). Purification of the reaction crude performed by recrystallization afforded compound **10c** (141 mg, 42 %) as a yellow solid.

^{1}H-NMR (DMSO-d_6): δ 11.09 (1H, broad s, OH), 9.97 (1H, s, NH), 9.33 (1H, broad s, NH-OH), 7.91 (1H, d, J=7.8 Hz, Ar), 7.48–7.39 (2H, m, Ar), 7.18 (1H, d, J= 15.1 Hz, CH=CH), 7.03 (1H, t, J= 7.9 Hz, Ar), 6.83 (1H, d, J= 15.1 Hz, CH=CH),

^{13}C-NMR (DMSO-d_6): δ 166.7 (C=O), 161.6 (C=O), 139.6 (Ar, quaternary C), 139.5 (C=C), 132.1 (C=C), 129.1 (Ar), 128.6 (Ar), 127.9 (Ar), 97.0 (C-I, quaternary C)

Melting Point – 210 °C

FT-IR (ATR): 3249 (O-H), 1637 (C=O), 1615 (C=O) **(v_{max}/cm^{-1})**

Experiment 31: Synthesis of ethyl (2E)-3-[(4-iodophenyl)carbamoyl]prop-2-enoate (11a)

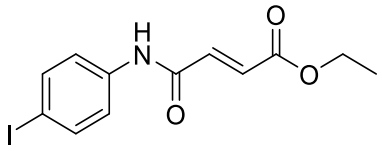

The procedure in experiment A was applied to mono-ethyl fumarate (0.6 g, 4.2 mmol). 4-iodoaniline (6.2 mmol) was used in this experiment. Purification of the reaction crude performed by recrystallization afforded compound **11a** (1.128 g, 81 %) as a purple solid.

^{1}H-NMR ($CDCl_3$): δ 7.77 (1H, broad s, NH), 7.65 (2H, d, J= 8.7 Hz, Ar), 7.39 (2H, d, J=8.7 Hz, Ar), 7.07 (1H, t, J= 15.4 Hz, CH=CH), 6.95 (1H, d, J= 15.4 Hz, CH=CH), 4.28 (2H, q, J=7.3 Hz, OCH_2CH_3), 1.34 (3H, t, J= 7.4 Hz, OCH_2CH_3)

^{13}C-NMR ($CDCl_3$): δ 165.6 (C=O), 161.5 (C=O), 138.1 (C=C), 137.1 (Ar, quaternary C), 136.2 (C=C), 131.9 (Ar), 121.8 (Ar), 88.6 (C-I, quaternary C), 61.5 (CH_2CH_3), 14.1 (CH_2CH_3)

Melting Point – 157 °C

FT-IR (ATR): 3338 (N-H), 1704 (C=O), 1668 (C=O) **(v_{max}/cm^{-1})**

Experiment 32: Synthesis of (2E)-3-[(4-iodophenyl)carbamoyl]prop-2-enoic acid (11b)

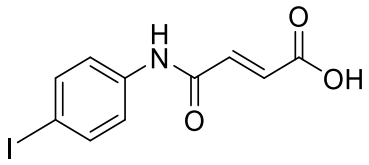

The procedure in experiment B was applied to compound **11a** (0.3 g, 0.9 mmol). Purification of the reaction crude performed by recrystallization afforded compound **11b** (243 mg, 88 %) as a gray solid.

^{1}H-NMR (DMSO-d_6): δ 13.03 (1H, broad s, OH), 10.60 (1H, s, NH), 7.69 (2H, d, J= 8.7 Hz, Ar), 7.51 (2H, d, J=8.7 Hz, Ar), 7.12 (1H, d, J=15.5 Hz, CH=CH), 6.66 (1H, d, J=15.6 Hz, CH=CH)

^{13}C-NMR (DMSO-d_6): δ 166.7 (C=O), 162.2 (C=O), 138.9 (Ar, quaternary C), 138.0 (Ar), 137.3 (C=C), 131.5 (C=C), 121.1 (Ar), 88.3 (C-I, quaternary C)

Melting Point – >250 °C

FT-IR (ATR): 3291 (O-H), 1695 (C=O), 1655 (C=O) **(v_{max}/cm^{-1})**

Experiment 33: Synthesis of (2E)-N-hydroxy-N'-(4-iodophenyl)but-2-enediamide (11c)

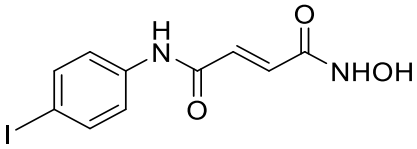

The procedure in experiment C was applied to compound **11a** (0.35 g, 1 mmol). Purification of the reaction crude performed by recrystallization afforded compound **11c** (103 mg, 31 %) as a white solid.

^{1}H-NMR (DMSO-d_6): δ 11.11 (1H, broad s, OH), 10.53 (1H, s, NH), 9.32 (1H, s, NH-OH), 7.68 (2H, d, J=8.6 Hz, Ar), 7.51 (2H, t, J=8.5 Hz, Ar), 7.08 (1H, d, J= 15.2 Hz, CH=CH), 6.82 (1H, d, J= 15.2 Hz, CH=CH)

^{13}C-NMR (DMSO-d_6): δ 166.7 (C=O), 161.6 (C=O), 138.5 (Ar, quaternary C), 137.8 (Ar), 137.3 (C=C), 131.5 (C=C), 121.1 (Ar), 86.1 (C-I, quaternary C)

Melting Point – 250 °C

FT-IR (ATR): 3264 (O-H), 1671 (C=O), 1621 (C=O) **(v_{max}/cm^{-1})**

Experiment 34: Synthesis of 5-(phenylcarbamoyl)pentanoate (12a)

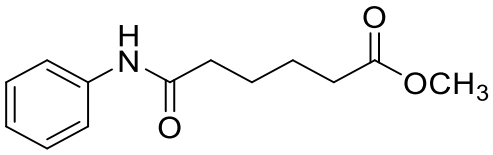

The procedure in experiment A was applied to adipic acid monomethyl ester (0.3 g,1.9 mmol). Previously distilled aniline (2.8 mmol) was used in this experiment. Purification of the reaction mixture by flash-column chromatography (7:3 hexane-ethyl acetate) afforded compound **12a** (412 mg, 94 %) as a white solid.

^{1}H-NMR ($CDCl_3$): δ 7.53 (2H, d, J=7.9 Hz, Ar), 7.36 (1H, s, NH), 7.32 (2H, t, J=7.8 Hz, Ar), 7.10 (1H, t, J=7.3 Hz, Ar), 3.68 (3H, s, O-$\underline{CH_3}$), 2.39 – 2.37 (4H, m, CH_2), 1.79 – 1.71 (4H, m, CH_2)

^{13}C-NMR ($CDCl_3$): δ 174.1 (C=O), 170.8 (C=O), 137.9 (Ar, quaternary C), 128.9 (Ar), 124.2 (Ar), 119.8 (Ar), 51.6 (O-$\underline{C}H_3$), 37.2 (CH_2), 33.6 (CH_2), 24.9 (CH_2), 24.2 (CH_2)

Melting Point – 50 °C

FT-IR (ATR): 3348 (N-H), 1703 (C=O), 1677 (C=O) **(ν_{max}/cm^{-1})**

Experiment 35: Synthesis of N-hydroxy-N'-phenylhexanediamide (12c)

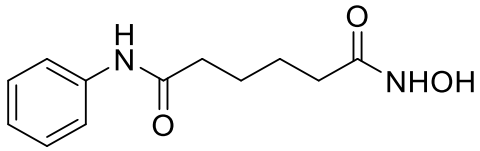

The procedure in experiment C was applied to compound **12a** (0.2 g, 0.85 mmol). Purification of the reaction crude performed by recrystallization afforded compound **12c** (72mg, 36 %) as a white solid.

^{1}H-NMR (DMSO-d_6): δ 11.35 (1H, broad s, OH), 9.85 (1H, s, NH), 8.67 (1H, s, N$\underline{H}$-OH), 7.58 (2H, d, J=8.2 Hz, Ar), 7.28 (2H, t, J=8.2 Hz, Ar), 7.02 (1H, t, J=7.4 Hz, Ar), 2.34 – 2.28 (2H, m, CH_2), 1.98 (2H, t, J=7.01 Hz, CH_2), 1.55 – 1.54 (4H, m, CH_2)

^{13}C-NMR (DMSO-d_6): δ 171.5 (C=O), 169.4 (C=O), 139.7 (Ar, quaternary C), 129.1 (Ar), 123.4 (Ar), 119.5 (Ar), 36.7 (CH_2), 32.6 (CH_2), 25.3 (CH_2), 25.2 (CH_2)

Melting Point – 193 °C

FT-IR (ATR): 3177 (O-H), 1655 (C=O), 1630 (C=O) **(ν_{max}/cm^{-1})**

Experiment 36: Synthesis of [(2-iodophenyl)carbamoyl]pentanoate (13a)

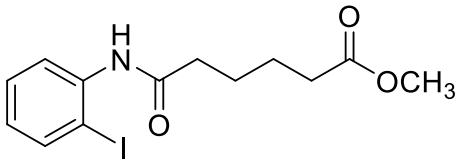

The procedure in experiment A was applied to adipic acid monomethyl ester (0.2 g, 1.2 mmol). 2-iodoaniline (1.9 mmol) was used in this experiment. Purification of the reaction mixture by silica flash-column chromatography (7:3 hexane-ethyl acetate) afforded compound **13a** (412 mg, 94 %) as a white solid.

^{1}H-NMR ($CDCl_3$): δ 8.20 (1H, d, J=7.9 Hz, Ar), 7.77 (1H, d, J=8.0 Hz, Ar), 7.43 (1H, s, NH), 7.34 (1H, t, J=8.1 Hz, Ar), 6.84 (1H, t, J=7.4 Hz, Ar), 3.68 (3H, s, O-$\underline{C}H_3$), 2.45 (2H, t, J=6.6 Hz, CH_2), 2.39 (2H, t, J=6.7 Hz, CH_2), 1.84 – 1.72 (4H, m, CH_2)

^{13}C-NMR ($CDCl_3$): δ 173.8 (C=O), 171.0 (C=O), 138.7 (Ar), 138.1 (Ar, quaternary C), 129.3 (Ar), 125.9 (Ar), 122.1 (Ar), 89.2 (I-$\underline{C}$, quaternary C), 51.6 (O-$\underline{C}H_3$), 37.5 (CH_2), 33.7 (CH_2), 24.9 (CH_2), 24.4 (CH_2)

Melting Point – 64 °C

FT-IR (ATR): 3260 (N-H), 1728 (C=O), 1655 (C=O) **(ν_{max}/cm^{-1})**

Experiment 37: Synthesis of N-hydroxy-N'-(2-iodophenyl)hexanediamide (13c)

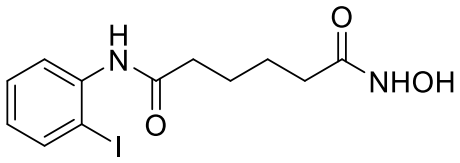

The procedure in experiment C was applied to compound **13a** (0.15 g, 0.4 mmol). Purification of the reaction crude performed by recrystallization afforded compound **13c** (97 mg, 65 %) as a white solid.

^{1}H-NMR (DMSO-d_6): δ 10.36 (1H, broad s, OH), 9.37 (1H, s, NH), 8.69 (1H, s, N$\underline{H}$-OH), 7.87 (2H, d, J=7.9 Hz, Ar), 7.45 – 7.35 (2H, m, Ar), 6.98 (2H, t, J=8.1 Hz, Ar), 2.51 – 2.50 (2H, m, CH_2), 1.99 – 1.98(2H, m, CH_2), 1.59 – 1.57 (4H, m, CH_2)

^{13}C-NMR (DMSO-d_6): δ 171.6 (C=O), 169.4 (C=O), 140.1 (Ar, quaternary C), 137.8 (Ar), 129.1 (Ar), 128.1 (Ar), 121.7 (Ar), 97.3 (I-$\underline{C}$, quaternary C), 36.7 (CH_2), 32.6 (CH_2), 25.3 (CH_2), 25.2 (CH_2)

Melting Point – 112 °C

FT-IR (ATR): 3237 (O-H), 1648 (C=O), 1625 (C=O) **(ν_{max}/cm^{-1})**

<u>Experiment 38:</u> Synthesis of [(4-iodophenyl)carbamoyl]pentanoate (14a)

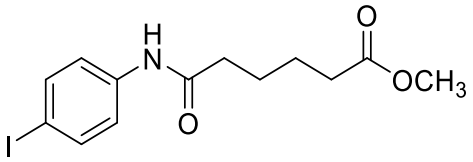

The procedure in experiment A was applied to adipic acid monomethyl ester (0.3 g, 1.9 mmol). 4-iodoaniline (2.8 mmol) was used in this experiment. Purification of the reaction crude performed by recrystallization afforded compound **14a** (647 mg, 96 %) as a white solid.

^{1}H-NMR ($CDCl_3$): δ 7.61 (2H, d, J=8.8 Hz, Ar), 7.41 (1H, broad s, NH), 7.33 (2H, d, J=8.7 Hz, Ar), 3.69 (3H, s, O-<u>C</u>H_3), 2.38 (4H, t, J=6.9 Hz, CH_2), 1.79 – 1.67 (4H, m, CH_2)

^{13}C-NMR ($CDCl_3$): δ 179.8 (C=O), 173.1 (C=O), 137.8 (Ar), 137.4 (Ar, quaternary C), 121.0 (Ar), 86.1 (I-<u>C</u>, quaternary C), 51.9 (O-<u>C</u>H_3), 37.5 (CH_2), 32.9 (CH_2), 27.0 (CH_2), 24.4 (CH_2)

Melting Point – 130 °C

FT-IR (ATR): 3358 (N-H), 1720 (C=O), 1692 (C=O) **(ν_{max}/cm^{-1})**

<u>Experiment 39:</u> Synthesis of 5-[(4-iodophenyl)carbamoyl]pentanoic acid (14b)

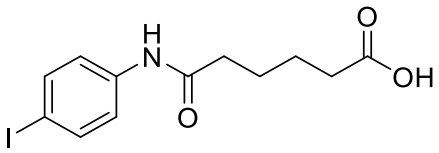

The procedure in experiment B was applied to compound **14a** (50 mg, 0.1 mmol). Purification of the reaction crude performed by recrystallization afforded compound **14b** (42 mg, 88 %) as a white solid.

^{1}H-NMR (DMSO-d_6): δ 11.8 (1H, broad s, OH), 9.99 (1H, s, NH), 7.61 (2H, d, J=8.7 Hz, Ar), 7.43 (2H, t, J=8.7 Hz, Ar), 2.30 (2H, t, J=7.2 Hz CH_2), 2.23 (2H, t, J=7.3 Hz, CH_2), 1.63 – 1.49 (4H, m, CH_2)

^{13}C-NMR (DMSO-d_6): δ 174.9 (C=O), 171.8 (C=O), 139.6 (Ar, quaternary C), 137.8 (Ar), 121.8 (Ar), 86.8 (I-<u>C,</u> quaternary C), 36.6 (CH_2), 33.9(CH_2), 25.0 (CH_2), 24.6 (CH_2)

Melting Point – 194 °C

FT-IR (ATR): 3291 (O-H), 1687 (C=O), 1655 (C=O) **(v_{max}/cm^{-1})**

<u>Experiment 40:</u> Synthesis of N-hydroxy-N'-(4-iodophenyl)hexanediamide (14c)

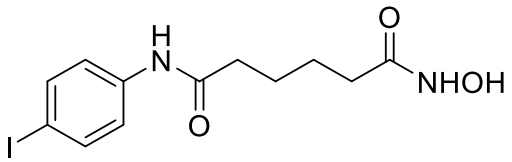

The procedure in experiment C was applied to compound **14a** (0.25 g, 0.7 mmol). Purification of the reaction crude performed by recrystallization afforded compound **14c** (38 mg, 15.2 %) as a white solid.

^{1}H-NMR (DMSO-d_6): δ 10.36 (1H, broad s, OH), 9.98 (1H, s, NH), 8.68 (1H, s, N<u>H</u>-OH), 7.61 (2H, d, J=8.8 Hz, Ar), 7.43 (2H, t, J=8.7 Hz, Ar), 2.35 – 2.27 (2H, m, CH_2), 1.99 – 1.95 (2H, m, CH_2), 1.56 – 1.50 (4H, m, CH_2)

^{13}C-NMR (DMSO-d_6): δ 171.8 (C=O), 169.4 (C=O), 139.6 (Ar, quaternary C), 137.8 (Ar), 121.7 (Ar), 86.8 (I-<u>C,</u> quaternary C), 36.5 (CH_2), 32.6 (CH_2), 25.3 (CH_2), 25.1 (CH_2)

Melting Point – 170 °C

FT-IR (ATR): 3209 (O-H), 1655 (C=O), 1625 (C=O) **(v_{max}/cm^{-1})**

<u>Experiment 41:</u> Synthesis of [(2-iodophenyl)carbamoyl]heptanoate (15a)

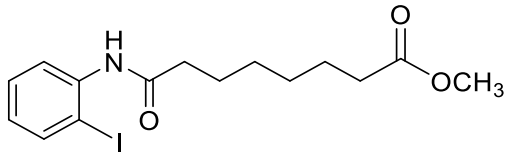

The procedure in experiment A was applied to suberic acid monomethyl ester (0.15 g, 0.8 mmol). 2-iodoaniline (1.2 mmol) was used in this experiment. Purification of the reaction mixture by flash column chromatography (7:3 hexane-ethyl acetate) afforded compound **15a** (84 mg, 27 %) as a white solid.

^{1}H-NMR ($CDCl_3$): δ 8.20 (1H, d, J=7.8 Hz, Ar), 7.76 (1H, d, J=7.9 Hz, Ar), 7.45 (1H, broad s, NH), 7.33 (1H, t, J= 7.8 Hz, Ar), 6.83 (1H, t, J= 7.8 Hz, Ar), 3.66 (3H, s, O-<u>CH_3</u>), 2.42 (2H, t, J=7.3 Hz, CH_2), 2.32 (2H, t, J=7.4 Hz, CH_2), 1.81 – 1.73 (2H, m, CH_2), 1.69 – 1.61 (2H, m, CH_2), 1.45 – 1.35 (4H, m, CH_2)

^{13}C-NMR ($CDCl_3$): δ 174.1 (C=O), 171.2 (C=O), 138.8 (Ar), 138.2 (Ar, quaternary C), 129.3 (Ar), 125.9 (Ar), 123.9 (Ar), 122.1 (Ar), 90.1 (I-C, quaternary C), 51.5 (O-CH_3), 37.5 (CH_2), 33.8 (CH_2), 24.9 (CH_2), 24.4 (CH_2)

Experiment 42: Synthesis of N-hydroxy-N'-(2-iodophenyl)octanediamide (15c)

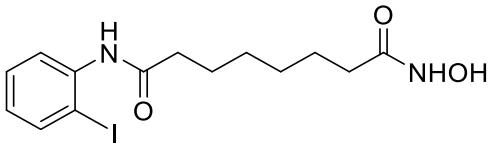

The procedure in experiment C was applied to compound **15a** (70 mg, 0.2 mmol). Purification of the reaction crude performed by recrystallization afforded compound **15c** (47 mg, 67 %) as a white solid.

^{1}H-NMR ($DMSO-d_6$): δ 10.35 (1H, broad s, OH), 9.36 (1H, s, NH), 8.70 (1H, s, NH-OH), 7.87 (1H, d, J=7.8 Hz, Ar), 7.40 – 7.35 (2H, m, Ar), 7.01 – 6.96 (1H, m, Ar), 2.32 (2H, t, J= 7.1 Hz, CH_2), 1.95 (2H, t, J= 7.2 Hz, CH_2), 1.63 – 1.57 (2H, m, CH_2), 1.54 – 1.47 (2H, m, CH_2), 1.34 – 1.24 (4H, m, CH_2)

^{13}C-NMR ($DMSO-d_6$): δ 179.8 (C=O), 169.9 (C=O),140.6 (Ar, quaternary C), 137.8 (Ar), 127.8 (Ar), 125.9 (Ar), 123.2 (Ar), 89.2 (I-C, quaternary C), 38.3 (CH_2), 32.5 (CH_2), 27.9 (CH_2), 25.6 (CH_2)

Melting Point – 128 °C

FT-IR (ATR): 3275 (O-H), 1659 (C=O), 1620 (C=O) **(ν_{max}/cm^{-1})**

Experiment 43: Synthesis of [(4-iodophenyl)carbamoyl]heptanoate (16a)

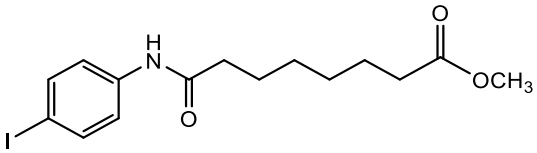

The procedure in experiment A was applied to suberic acid monomethyl ester (0.15 g, 0.8 mmol). 4-iodoaniline (1.2 mmol) was used in this experiment. Purification of the reaction crude performed by recrystallization afforded compound **16a** (211 mg, 68 %) as a purple solid.

^{1}H-NMR ($CDCl_3$): δ 7.61 (2H, d, J=8.8 Hz, Ar), 7.31 (2H, d, J=8.7 Hz, Ar), 7.21 (1H, broad s, NH),3.67 (3H, s, O-CH_3), 2.36 – 2.30 (4H, m, CH_2), 1.76 – 1.69 (2H, m, CH_2), 1.66 – 1.62 (2H, m, CH_2), 1.39 – 1.35 (4H, m, CH_2)

^{13}C-NMR ($CDCl_3$): δ 179.8 (C=O), 173.1 (C=O), 137.8 (Ar), 137.4 (Ar, quaternary C), 121.0 (Ar), 86.1 (I-C, quaternary C), 51.9 (O-CH_3), 38.3 (CH_2), 33.6 (CH_2), 28.3 (CH_2), 25.0 (CH_2)

Melting Point – 107 °C

FT-IR (ATR): 3365 (N-H), 1713 (C=O), 1682 (C=O) **(ν_{max}/cm^{-1})**

Experiment 44: Synthesis of N-hydroxy-N'-(4-iodophenyl)octanediamide (16c)

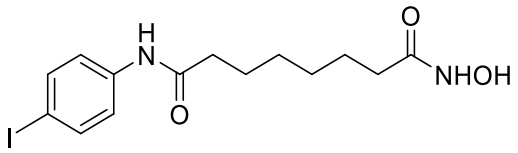

The procedure in experiment C was applied to compound **16a** (0.15 g, 0.4 mmol). Purification of the reaction crude performed by recrystallization afforded compound **16c** (31 mg, 21 %) as a purple solid.

^{1}H-NMR (DMSO-d_6): δ 10.33 (1H, broad s, OH), 9.96 (1H, s, NH), 8.66 (1H, s, NH-OH), 7.61 (2H, d, J=8.6 Hz, Ar), 7.43 (2H, d, J=8.6 Hz, Ar), 2.28 (2H, t, J= 7.4 Hz, CH_2), 1.94 (2H, t, J= 7.4 Hz, CH_2), 1.58 – 1.47 (4H, m, CH_2), 1.27 – 1.23 (4H, m, CH_2)

^{13}C-NMR (DMSO-d_6): δ 171.9 (C=O), 169.6 (C=O), 139.6 (Ar, quaternary C), 137.8 (Ar), 121.7 (Ar), 86.7 (I-C, quaternary C), 36.8 (CH_2), 32.7 (CH_2), 28.8 (CH_2), 25.4 (CH_2)

Melting Point – 153 °C

FT-IR (ATR): 3253 (N-H), 1700 (C=O), 1655 (C=O) **(ν_{max}/cm^{-1})**

Experiment 45: Synthesis of [(2-iodophenyl)carbamoyl]octanoate (17a)

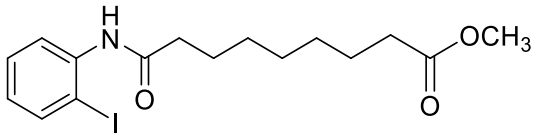

The procedure in experiment A was applied to azelaic acid monomethyl ester (0.25 g, 1.2 mmol). 2-iodoaniline (1.9 mmol) was used in this experiment. Purification of the reaction crude performed by recrystallization afforded compound **17a** (94 mg, 19 %) as a white solid.

^{1}H-NMR ($CDCl_3$): δ 8.21 (1H, d, J=7.8 Hz, Ar), 7.77 (1H, d, J=7.9 Hz, Ar), 7.45 (1H, broad s, NH), 7.33 (1H, t, J=8.0 Hz, Ar), 6.84 (1H, t, J=7.9 Hz, Ar), 3.66 (3H, s, O-CH_3), 2.42 (1H, t, J=7.4 Hz, CH_2), 2.31 (1H, t, J=7.5 Hz, CH_2), 1.79 – 1.72 (2H, m, CH_2), 1.67 – 1.59 (2H, m, CH_2), 1.42 – 1.32 (6H, m, CH_2)

^{13}C-NMR ($CDCl_3$): δ 174.2 (C=O), 171.3 (C=O), 138.8 (Ar), 138.2 (Ar, quaternary C), 129.2 (Ar), 125.9 (Ar), 122.1 (Ar), 90.0 (I-C, quaternary C), 51.5 (O-CH_3), 37.9 (Ar), 34.0 (CH_2), 28.9 (CH_2), 25.4 (CH_2), 24.9 (CH_2)

Melting Point – 75 °C

FT-IR (ATR): 3276 (N-H), 1697 (C=O), 1659 (C=O) **(ν_{max}/cm^{-1})**

Experiment 46: Synthesis of N-hydroxy-N'-(2-iodophenyl)nonanediamide (17c)

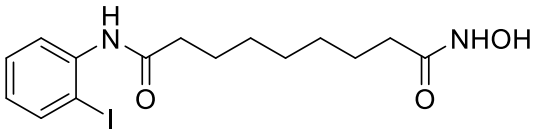

The procedure in experiment C was applied to compound **17a** (70 mg, 0.2 mmol). Purification of the reaction crude performed by recrystallization afforded compound **17c** (37 mg, 53 %) as a white solid.

^{1}H-NMR (DMSO-d_6): δ 10.33 (1H, broad s, OH), 9.35 (1H, s, NH), 8.66 (1H, s, NH-OH), 7.87 (1H, d, J=7.8 Hz, Ar), 7.41 – 7.35 (2H, m, Ar), 6.98 (1H, t, J=8.1 Hz, Ar), 2.32 (2H, t, J= 7.2 Hz, CH_2), 2.19 (2H, t, J= 7.3 Hz, CH_2), 1.63 – 1.60 (2H, m, CH_2), 1.54 – 1.49 (2H, m, CH_2), 1.35 – 1.26 (6H, m, CH_2)

^{13}C-NMR (DMSO-d_6): δ 175.0 (C=O), 171.8 (C=O), 140.1 (Ar, quaternary C), 139.3 (Ar), 129.0 (Ar), 128.0 (Ar), 97.2 (I-C, quaternary C), 36.2 (CH_2), 34.2 (CH_2), 32.7 (CH_2), 28.9 (CH_2), 25.6 (CH_2), 24.9 (CH_2)

Experiment 47: Synthesis of [(4-iodophenyl)carbamoyl]octanoate (18a)

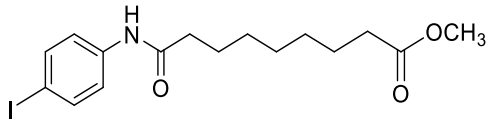

The procedure in experiment A was applied to azelaic acid monomethyl ester (0.3 g, 1.5 mmol). 4-iodoaniline (1.9 mmol) was used in this experiment. Purification of the reaction crude performed by recrystallization afforded compound **18a** (412 mg, 74 %) as a gray solid.

^{1}H-NMR ($CDCl_3$): δ 7.61 (2H, d, J=8.6 Hz, Ar), 7.31 (2H, d, J=8.6 Hz, Ar), 7.18 (1H, broad s, NH), 3.67 (3H, s, O-CH_3), 2.35 – 2.29 (4H, m, CH_2), 1. 72– 1.60 (4H, m, CH_2), 1.39 – 1.32 (6H, m, CH_2)

^{13}C-NMR ($CDCl_3$): δ 179.8 (C=O), 173.1 (C=O), 137.8 (Ar), 137.4 (Ar, quaternary C), 121.0 (Ar), 86.1 (I-C, quaternary C), 51.9 (O-CH_3), 38.3 (Ar), 33.6 (CH_2), 29.0 (CH_2), 28.6 (CH_2), 25.0 (CH_2)

Melting Point – 87 °C

FT-IR (ATR): 3309 (N-H), 1724 (C=O), 1690 (C=O) **(ν_{max}/cm^{-1})**

Experiment 48: Synthesis of N-hydroxy-N'-(4-iodophenyl)nonanediamide (18c)

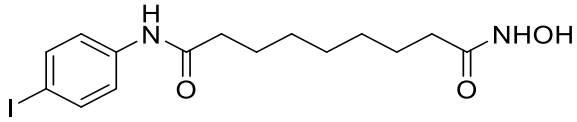

The procedure in experiment C was applied to compound **18a** (0.25 mg, 0.6 mmol). Purification of the reaction crude performed by recrystallization afforded compound **18c** (112 mg, 45 %) as a white solid.

^{1}H-NMR (DMSO-d_6): δ 10.32 (1H, broad s, OH), 9.95 (1H, s, NH), 8.66 (1H, s, NH-OH), 7.43 (2H, d, J=8.6 Hz, Ar), 7.21 (2H, d, J=8.7 Hz, Ar), 2.29 (2H, t, J=7.4 Hz, CH_2), 2.19 (2H, t, J= 7.5 Hz, CH_2), 1.58 – 1.47 (4H, m, CH_2), 1.30 – 1.25 (6H, m, CH_2)

^{13}C-NMR (DMSO-d_6): δ 174.9 (C=O), 171.9 (C=O), 130.6 (Ar, quaternary C), 137.7 (Ar), 121.7 (Ar), 86.7 (I-C, quaternary C), 36.8 (CH_2), 34.1 (CH_2), 28.9 (CH_2), 25.4 (CH_2), 24.9 (CH_2)

Melting Point – 130 °C

FT-IR (ATR): 3292 (O-H), 1687 (C=O), 1655 (C=O) **(ν_{max}/cm^{-1})**

Experiment 49: Attempted synthesis of ethyl (2E)-3-[(2-nitrophenyl)carbamoyl]prop-2-enoate

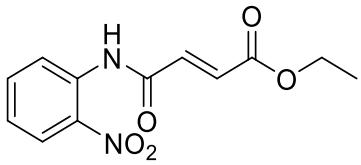

The procedure in experiment A was applied to the starting material mono-ethyl fumarate (0.8 g, 5.5 mmol). 2-nitroaniline (8.3 mmol) was used in this experiment. Purification of the reaction crude was performed by recrystallization using hexane and ethyl acetate but the ^{1}H-NMR spectra of the reaction product showed only the 2-nitroaniline structure to be present. Therefore, the reaction did not occur as expected.

<u>Experiment 50:</u> Attempted synthesis of 8-(phenylcarbamoyl)octanoate

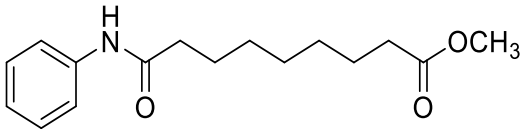

The procedure in experiment A was applied to the azelaic acid monomethyl ester (0.3 g, 1.5 mmol). Previously distilled aniline (2.2 mmol) was used in this experiment. Purification of the reaction crude was performed by recrystallization using hexane and ethyl acetate but ^{1}H-NMR spectra did not show the expected structure. Therefore, this reaction did not occur as expected.

II.2 Evaluation as anticancer agents

II.2.1 Cancer Cell lines and cell culture:

The MCF-7 Breast Cancer cell line (ATCC) was cultured in DMEM (Dulbecco's Modified Eagle Medium) from Invitrogen, supplemented with Fetal Bovine Serum (FBS) (10%), Glutamax (2%), Sodium Pyruvate (1%) and Pen Strep (1%).

The NCI-H460 Lung Cancer Cell line was cultured in RPMI 1640 medium (Invitrogen) supplemented with FBS (10%), Pen Strep (1%) and Puromycin (0.1%), a selection antibiotic.

Human Dermal Fibroblasts (HDF) (Innoprot) cells were cultured in IMDM (Iscove's Modified Dulbecco's Medium) supplemented with FBS (10%) and Pen Strep (1%).

MCF-7 and H460 cells were sub-cultured twice a week at $1.5x10^4/cm^2$. HDF cells were sub-cultured once a week at $4x10^3/cm^2$. Cells were cultured at 37ºC and 5% CO_2 in t-flasks. For sub-culture, cells were washed with phosphate-buffered saline (PBS) and then trypsinized using 0.05% trypsin-EDTA (Invitrogen), for 5 minutes. Viable cell concentration was assessed using trypan blue exclusion test. (Section II.2.2). Phase-contrast microscopy of H460, MCF-7 and HDF cells was performed using a Leica DMI6000.

II.2.2 Trypan blue exclusion method

Viable cells were counted using the trypan blue exclusion method. After incubation with a solution 0.1 % of trypan blue dye (Invitrogen), viable cells were counted in a Fuchs–Rosenthal hemocytometer chamber under the microscope. Trypan blue is a cell-impermeable dye, so viable cells appear colorless while non-viable cells that are membrane damaged are stained by trypan blue dye, appearing blue.

II.2.3 Optimization/implementation of PrestoBlue Cell Viability Assay

PrestoBlue Cell Viability Reagent (Invitrogen) consists of a resazurin-based solution that works as a cell viability indicator. Viable cells are known to maintain a reducing environment in their cytoplasm. PrestoBlue reagent contains a blue and nonfluorescent compound that when in contact with viable cells is reduced, becoming red and fluorescent. This can be measured by fluorescence measurements at 560/590 nm.

Optimal concentrations for each cell line were assessed by plating cells in 1:2 serial dilutions, ranging from $5x10^3$ to 19.50 cells/well for H460 and $1.5x10^4$ to 58 cells/well for MCF-7 and HDF. Cells were plated in 96 well plates according to the scheme in figure II.8 and cultured for 72h. The PrestoBlue viability assay was used as endpoint: cells were incubated for 40 minutes with 10 µl of PrestoBlue reagent at 37ºC. After this, 100 µl were collected to a black fluorescence reading plate and fluorescence reading was performed in an Infinite 200 PRO NanoQuant plate

reader (TECAN) at 560/590 nm. The assay blank consisted of culture medium without cells. Calibration Curves were constructed using Graph Pad Prism 6 software.

	1	2	3	4	5	6	7	8	9	10	11	12
A												
B		$1.5x10^4$	$7.5x10^3$	$3.75x10^3$	$1.88x10^3$	$9.38x10^2$	$4.69x10^2$	$2.34x10^2$	$1.17x10^2$	$5.86x10^1$	Blank	
C		$1.5x10^4$	$7.5x10^3$	$3.75x10^3$	$1.88x10^3$	$9.38x10^2$	$4.69x10^2$	$2.34x10^2$	$1.17x10^2$	$5.86x10^1$	Blank	
D		$1.5x10^4$	$7.5x10^3$	$3.75x10^3$	$1.88x10^3$	$9.38x10^2$	$4.69x10^2$	$2.34x10^2$	$1.17x10^2$	$5.86x10^1$	Blank	
E		$1.5x10^4$	$7.5x10^3$	$3.75x10^3$	$1.88x10^3$	$9.38x10^2$	$4.69x10^2$	$2.34x10^2$	$1.17x10^2$	$5.86x10^1$	Blank	
F		$1.5x10^4$	$7.5x10^3$	$3.75x10^3$	$1.88x10^3$	$9.38x10^2$	$4.69x10^2$	$2.34x10^2$	$1.17x10^2$	$5.86x10^1$	Blank	
G		$1.5x10^4$	$7.5x10^3$	$3.75x10^3$	$1.88x10^3$	$9.38x10^2$	$4.69x10^2$	$2.34x10^2$	$1.17x10^2$	$5.86x10^1$	Blank	
H												

	1	2	3	4	5	6	7	8	9	10	11	12
A												
B		$5x10^3$	$2.5x10^3$	$1.25x10^3$	$6.25x10^2$	$3.13x10^2$	$1.56x10^2$	$7.81x10^1$	$3.91x10^1$	$1.95x10^1$	Blank	
C		$5x10^3$	$2.5x10^3$	$1.25x10^3$	$6.25x10^2$	$3.13x10^2$	$1.56x10^2$	$7.81x10^1$	$3.91x10^1$	$1.95x10^1$	Blank	
D		$5x10^3$	$2.5x10^3$	$1.25x10^3$	$6.25x10^2$	$3.13x10^2$	$1.56x10^2$	$7.81x10^1$	$3.91x10^1$	$1.95x10^1$	Blank	
E		$5x10^3$	$2.5x10^3$	$1.25x10^3$	$6.25x10^2$	$3.13x10^2$	$1.56x10^2$	$7.81x10^1$	$3.91x10^1$	$1.95x10^1$	Blank	
F		$5x10^3$	$2.5x10^3$	$1.25x10^3$	$6.25x10^2$	$3.13x10^2$	$1.56x10^2$	$7.81x10^1$	$3.91x10^1$	$1.95x10^1$	Blank	
G		$5x10^3$	$2.5x10^3$	$1.25x10^3$	$6.25x10^2$	$3.13x10^2$	$1.56x10^2$	$7.81x10^1$	$3.91x10^1$	$1.95x10^1$	Blank	
H												

Figure II.8 – Plate schemes for implementation/optimization of PrestoBlue cell viability assay.

The optimal concentrations chosen for each cell type were: For MCF-7 cell line, $4x10^3$ cells/well or $1.25x10^4$ cells/cm^2, for H460 cell line $2.5x10^3$ cells/ well or $7.8x10^3$ cells/cm^2 and for HDF $2.5x10^3$ cells/well or $7.8x10^3$ cells/cm^2 (See Appendix). These concentrations were used in all experiments.

II.2.4 Determination of DMSO toxicity

Cancer cell lines were treated with a range of DMSO concentrations in order to assess DMSO toxicity for each of the cell lines and determine the maximum percentage of DMSO that could be used without being harmful to the cells.

Cells were plated at $7.8x10^3$ cells/cm^2 (H460) and $1.25x10^4$ cells/cm^2 (MCF-7) in 96 well plates and cultured for 24h for cells to adhere to the plate. After that, DMSO was added to the cultures and incubated for 48h, at 37ºC. DMSO percentages ranging from 4% to 0.016% were tested in a 1:2 serial dilution series, according to the scheme in figure II.9. The assay control was performed with cells in culture medium, without addition of DMSO. PrestoBlue viability assay was performed as described in section II.2.3. Values were normalized to the assay control. Dose-response curves were constructed using Graph Pad Prism 6 software.

	1	2	3	4	5	6	7	8	9	10	11	12
A												
B		4%	2%	1%	0.5%	0.25%	0.125%	0.063%	0.030%	0.016%	CTRL	
C		4%	2%	1%	0.5%	0.25%	0.125%	0.063%	0.030%	0.016%	CTRL	
D		4%	2%	1%	0.5%	0.25%	0.125%	0.063%	0.030%	0.016%	CTRL	
E		4%	2%	1%	0.5%	0.25%	0.125%	0.063%	0.030%	0.016%	CTRL	
F		4%	2%	1%	0.5%	0.25%	0.125%	0.063%	0.030%	0.016%	CTRL	
G		4%	2%	1%	0.5%	0.25%	0.125%	0.063%	0.030%	0.016%	CTRL	
H												

Figure II.9 – Plate scheme for determination of DMSO toxicity with % of DMSO tested. Control without DMSO (CTRL)

II.2.5 Dose-response curves of SAHA

SAHA (Sigma-Aldrich, Ref SMC0061) was dissolved in DMSO at a concentration of 50 mM and aliquots were stored at -20ºC. The compound was added to the cancer cell lines at different concentrations in order to study its effect on cell viability, generate dose response curves and calculate the IC50 (half maximal inhibitory concentration). IC50 is a key concept in pharmacology and is commonly referred to as the half-maximal inhibitory concentration. It works as a measure of the effectiveness of a compound in inhibiting a biological or biochemical function. This quantitative measure indicates how much of a particular drug is needed to inhibit a given biological process by half.

Cells were plated at $7.8x10^3$ cells/cm^2 (H460) and $1.25x10^4$ cells/cm^2 (MCF-7) in 96 well plates and cultured for 24h in 100 µl of culture medium. SAHA concentrations tested ranged from 0.5 mM to 5pM, in a media matrix with 0.9% DMSO, according to the scheme in figure II.10. To prepare this, SAHA compound was diluted in culture medium at a concentration of 1 mM and 1:10 serial dilutions were performed in culture medium with 1.8% DMSO. 100µl of each SAHA dilution was then added to each well of the culture plate. Cells were exposed to SAHA for 48h at 37ºC, after which Presto Blue viability assay was performed as described in section II.2.3. Dose-response curves were constructed using Graph Pad Prism 6 software.

	1	2	3	4	5	6	7	8	9	10	11	12
A												
B		0.5 mM	50 µM	5 µM	0.5 µM	50 nM	5 nM	0.5 nM	50 pM	5 pM	CTRL	
C		0.5 mM	50 µM	5 µM	0.5 µM	50 nM	5 nM	0.5 nM	50 pM	5 pM	CTRL	
D		0.5 mM	50 µM	5 µM	0.5 µM	50 nM	5 nM	0.5 nM	50 pM	5 pM	CTRL	
E		0.5 mM	50 µM	5 µM	0.5 µM	50 nM	5 nM	0.5 nM	50 pM	5 pM	CTRL	
F		0.5 mM	50 µM	5 µM	0.5 µM	50 nM	5 nM	0.5 nM	50 pM	5 pM	CTRL	
G		0.5 mM	50 µM	5 µM	0.5 µM	50 nM	5 nM	0.5 nM	50 pM	5 pM	CTRL	
H												

Figure II.10 – Plate scheme for dose-response curve of SAHA with concentrations of SAHA tested.

II.2.6 Drug Testing

Drug testing was performed using cell viability as endpoint measured by Presto Blue viability assay. Lung (H460) and breast (MCF-7) cancer cell lines were exposed to the newly synthesized compounds (Table III.3.B) and SAHA was used as a reference compound. Also, human dermal fibroblasts (HDF) were exposed to SAHA and synthesized compounds 15c and 16c, in order to test the effect of these molecules in normal/non-transformed cells. Cells were plated at $1.25x10^4$ cells/cm^2 for MCF-7 and $7.81x10^3$ cells/cm^2 for H460 and HDF 24h prior to the assay, in order for cells to adhere. Compounds were added to the plates in three different concentrations (500, 50 and 5µM), according to the scheme in figure II.11 and incubated for 48h at 37ºC. Presto Blue viability assay was performed as described in section II.2.3.

All compound concentrations were assayed in a matrix of culture medium with 0.9% DMSO (in cells) and DMSO controls used in all experiments. Values were normalized to DMSO controls. Data Graphs were constructed using Graph Pad Prism 6 software.

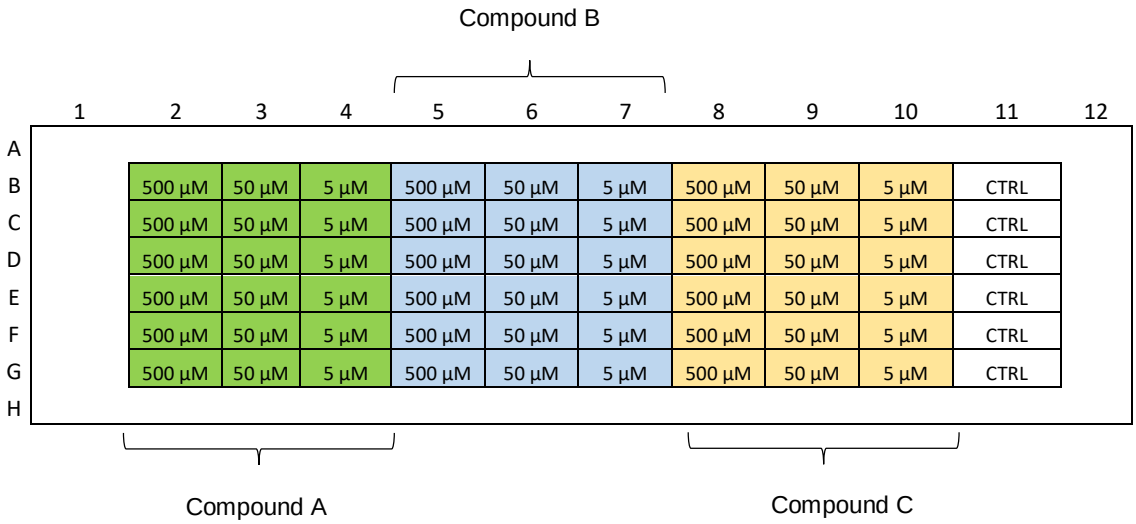

Figure II.11 - Plate scheme for drug testing of all compounds with concentrations tested.

II.2.7 Apoptosis Assay using NucView

In order to assess if SAHA and Compound 16c were able to induce apoptosis in MCF-7 breast cancer cell line, levels of apoptotic cells were determined using fluorescence labelling with a caspase probe (NucView) followed by flow cytometry. Caspase-3 activation is an early event and initiates apoptotic damage. Therefore, early stage apoptosis in cells can be accessed measuring levels of caspase-3. The Apoptosis Assay Kit NucView™ 488 (Biotium) consists of a DNA dye and a substrate moiety specific for caspase-3. Initially, the substrate is nonfunctional as a DNA dye and not fluorescent. The substrate crosses the cell membrane and in cytoplasm is

cleaved by caspase-3 forming a high-affinity DNA dye. After migration to the cell nucleus, the DNA dye is able to stain the nucleus with bright green fluorescence[35].

Cells were plated at 1.25x10^4 cells/cm^2 in 6 well plates and cultured for 24h. SAHA and Compound 16c were added to the cells at 50 µM and incubated for 48h at 37ºC. DMSO control was obtained by adding the same percentage of DMSO present in drug incubations to cells from an independent well. After the incubation time, cells were trypsinized (0.05% trypsin-EDTA) and collected. Cells (0.2-0.5x10^6) were centrifuged for 5 minutes at 300x *g*, at room temperature. After removal of the supernatant, the cell pellet was resuspended in 200µl of medium containing 1µl of NucView reagent and incubated for 1 hour at 37ºC. Cells were centrifuged at 300x *g* for 5 minutes and resuspended in 500µl of PBS for analysis by flow cytometry (CyFlow Space, Partec, Germany). Flow cytometry results were analysed using FlowJo software.

II.2.8 Cell Cycle analysis

In order to access if SAHA and Compound 16c were able to induce cell cycle arrest in MCF-7 breast cancer cell line, cell cycle analysis was performed using fluorescence labelling and flow cytometry. The cell cycle is characterized by consecutive events that take place in a cell leading to its division and duplication with the final goal of producing two daughter cells. It is possible to distinguish cells in different phases of the cell cycle by the amount of DNA present in the cell because during cell cycle DNA replication occurs. By labelling the cell DNA with a DNA intercalating probe such as propidium iodide (PI), correlation between fluorescence intensity and the amount of DNA present in the cell can be made. So, cells in phase G2/M which contain two copies of DNA will have the twice the fluorescence intensity when compared with cells in G1 phase that only have one copy of DNA. Cells in phase S will show an intermediate fluorescence[36].

This protocol for cell cycle analysis is based on findings published by Vindelov in 1977[37]. In his work, he was able to optimize the nuclei staining solution and their components. Up to date, the solution used for nuclei staining is called Vindelov´s solution and is composed of 1 g/L trisodic citrate, pH 7.6 (Sigma); 50 mg/L propidium iodide (Sigma); 0.1% NP 40 (Roche); 0.700 U/mL Ribonuclease A (Sigma) and 0.01 M NaCl (Merck). There are other different protocols for cell cycle analysis but this one was already optimized in the laboratory by previous colleagues and therefore was used in this experiment.

Cells were plated at 1.25x10^4 cells/cm^2 in 6 well plates and cultured for 24h. SAHA and Compound 16c were added to the cells at 50 µM and cells incubated for 48h at 37ºC. After incubation time, cells were trypsinized (0.05% trypsin-EDTA) and collected. Cells (1×10^6cells) were centrifuged for 5 min at 500x *g* at room temperature and washed by resuspension in PBS. After another centrifugation step, cells were resuspendend in 1ml of Vindelov´s solution and

incubated at room temperature for 2 hours. Next, cells were incubated overnight at 4ºC, and analysed by flow cytometry (CyFlow Space, Partec, Germany).

DMSO control was obtained by adding the same percentage of DMSO present in drug incubations to cells from an independent well. Data results were analysed using FlowJo software.

III. RESULTS AND DISCUSSION

III.1 Synthesis of new HDACi

Overall, 48 compounds were successfully synthesized (Table III.3) and 30 of them were used for further analysis in cancer cell lines (Table III.3-B).

In a first round of synthesis the linker 4 carbons long and a *trans* double bond was preserved (linker more similar to Belinostat). To this end, mono-ethyl fumarate was used as starting reagent in the first step of synthesis. Different aniline derivatives were used in order to obtain diverse capping groups for these compounds, where the aromatic ring has different atoms attached at different positions.

After the testing of these compounds (See section III.2.4.1) analysis of the results led to a second round of synthesis were the changes in capping group that led to a higher effect were kept, and compounds with other linkers (different carbon lengths) were synthesized. To achieve this, adipic acid monomethyl ester, suberic acid monomethyl ester and azelaic acid monomethyl ester were used as starting materials for the amide formation reaction. That enabled the synthesis of compounds with 6, 8 and 9 carbon chains in their linker, respectively. (The 8 carbon chain linker is equal to that found in SAHA structure).

Table III.3 - Structures of all synthesized compounds with respective numerations.

Table III.3.A - Ester intermediates obtained from 1st step of synthesis.

COMPOUND	STRUCTURE	COMPOUND	STRUCTURE
1a	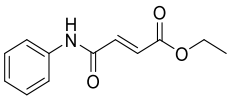	**10a**	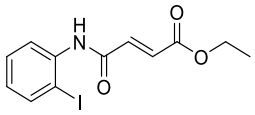
2a	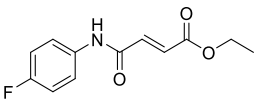	**11a**	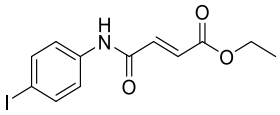
3a	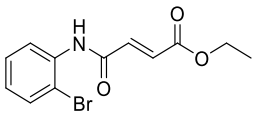	**12a**	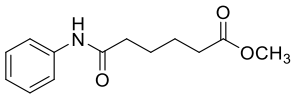
4a	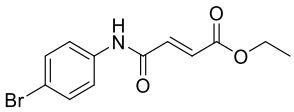	**13a**	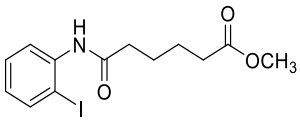
5a	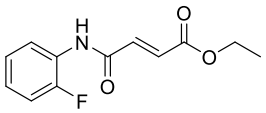	**14a**	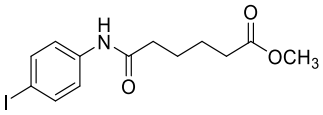
6a	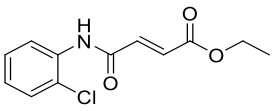	**15a**	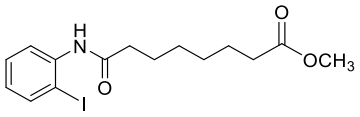
7a	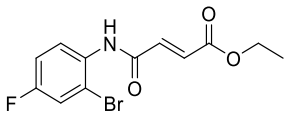	**16a**	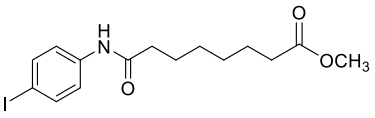
8a	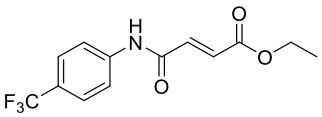	**17a**	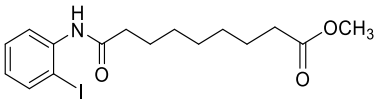
9a	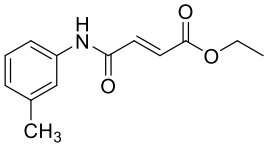	**18a**	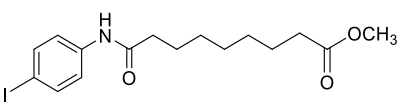

Table III.3.B - Carboxylic and hydroxamic derivatives synthesized - Compounds tested in cancer cell lines.

COMPOUND	STRUCTURE	COMPOUND	STRUCTURE
1b	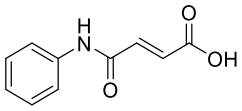	**5b**	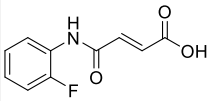
1c	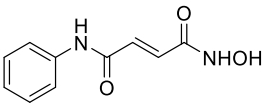	**5c**	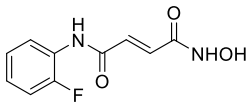
2b	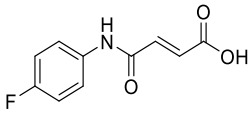	**6b**	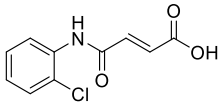
2c	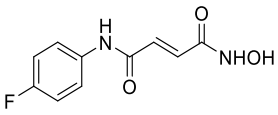	**6c**	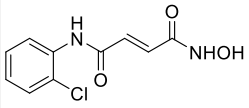
3b	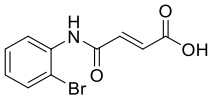	**7b**	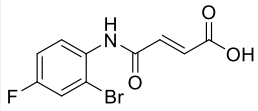
3c	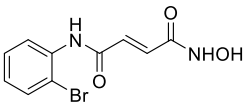	**7c**	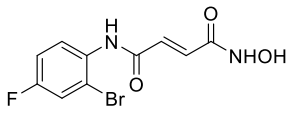
4b	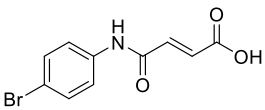	**8b**	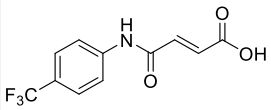
4c	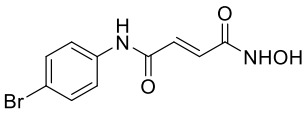	**8c**	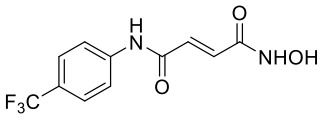

COMPOUND	STRUCTURE	COMPOUND	STRUCTURE
9b	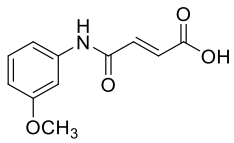	**13c**	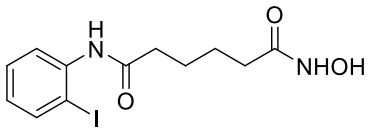
9c	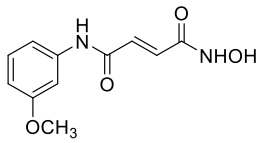	**14b**	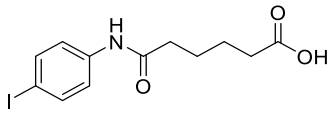
10b	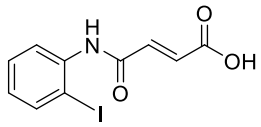	**14c**	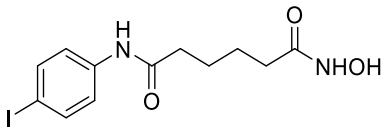
10c	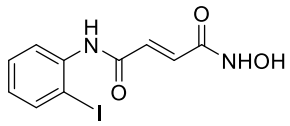	**15c**	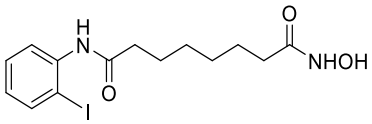
11b	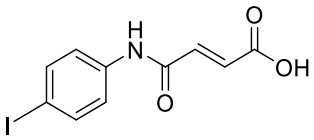	**16c**	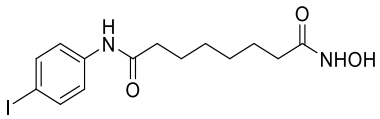
11c	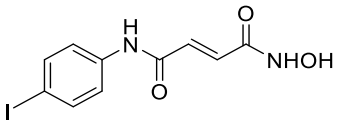	**17c**	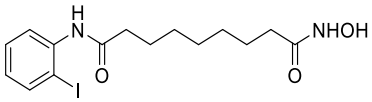
12c	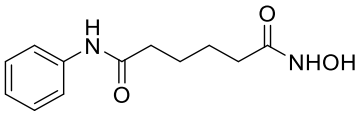	**18c**	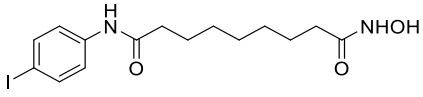

III.1.2 Results from the 1st round of synthesis

Table III.4 – 1st step of the synthesis using mono-ethyl fumarate as starting material and several anilines. The table describes the compounds obtained (respective numbering) and corresponding yields.

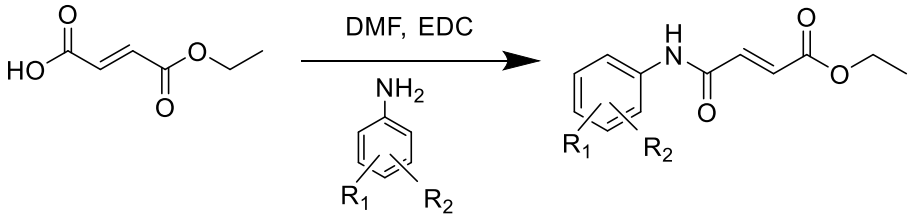

R1	R2	Position	Aniline used	Compound	Yield (%)
-	-	-	Aniline (Merck)	1a	73
F	-	*ortho*	2-Fluoroaniline (Aldrich)	5a	52
	-	*para*	4-Fluoroaniline (Fluka)	2a	74
	Br	Br-*ortho* F-*para*	2-Bromo-4-fluoroaniline (Aldrich)	7a	38
Br	-	*ortho*	2-Bromoaniline (Aldrich)	3a	41
	-	*para*	4-Bromoaniline (Aldrich)	4a	90
Cl	-	*ortho*	2-chloroaniline (Aldrich)	6a	54
F_3C	-	*para*	4-(Trifluoromethyl)aniline (Aldrich)	8a	71
OCH_3	-	*meta*	3-Methoxyaniline (Aldrich)	9a	70
I	-	*Ortho*	2-iodoaniline (TCI)	10a	48
	-	*Para*	4-iodoaniline (Alfa Aesar)	11a	80

Table III.5 – Synthesis of carboxylic acid derivatives from compounds present in table III.4. The table describes the compounds obtained (respective numbering) and corresponding yields.

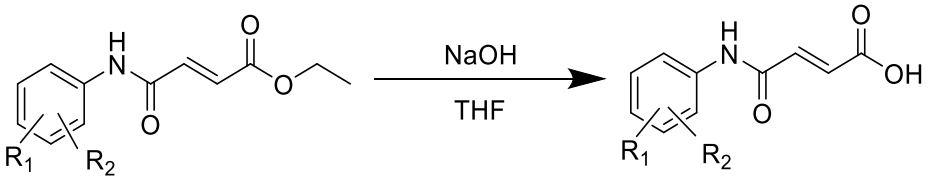

R1	R2	Position	Compound	Yield (%)
-	-	-	1b	26
F	-	*ortho*	5b	74
	-	*para*	2b	27
	Br	Br-*ortho* F-*para*	7b	89
Br	-	*ortho*	3b	49
	-	*para*	4b	74
Cl	-	*ortho*	6b	88
F_3C	-	*para*	8b	70
OCH_3	-	*meta*	9b	89
I	-	*ortho*	10b	97
	-	*para*	11b	88

Table III.6 - Synthesis of hydroxamic acid derivatives from compounds present in table III.4. The table describes the compounds obtained (respective numbering) and related yields.

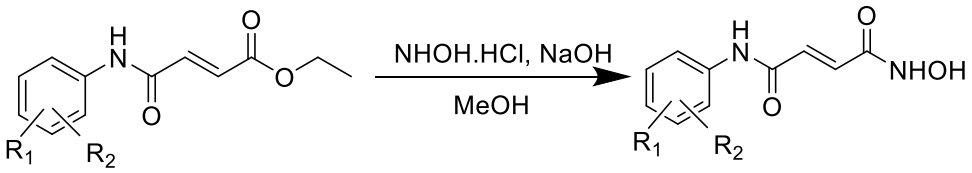

R1	R2	Position	Compound	Yield (%)
-	-	-	1c	43
F	-	*ortho*	5c	37
	-	*para*	2c	39
	Br	Br-*ortho* F-*para*	7c	27
Br	-	*ortho*	3c	51
	-	*para*	4c	29
Cl	-	*ortho*	6c	25
F_3C	-	*para*	8c	98
OCH_3	-	*meta*	9c	15
I	-	*ortho*	10c	42
	-	*para*	11c	31

III.1.3 Results from the 2nd round of synthesis

Table III.7 - 1st Step of the synthesis using adipic acid monomethyl ester as starting material and several anilines. The table describes compounds obtained (respective numbering) and corresponding yields.

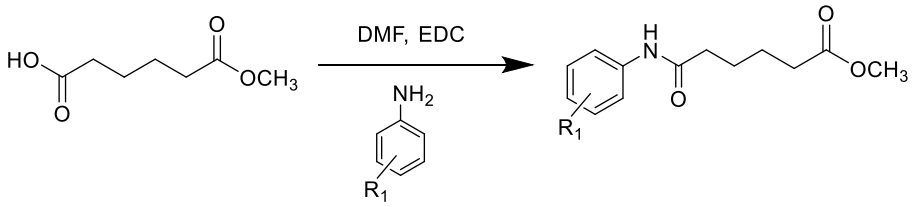

R1	Position	Aniline used	Compound	Yield (%)
-	-	Aniline	12a	94
I	*ortho*	2-iodoaniline (TCI)	13a	82
	para	4-iodoaniline (Alfa Aesar)	14a	96

Table III.8 - Synthesis of carboxylic acid derivative 14b.

14a **14b**

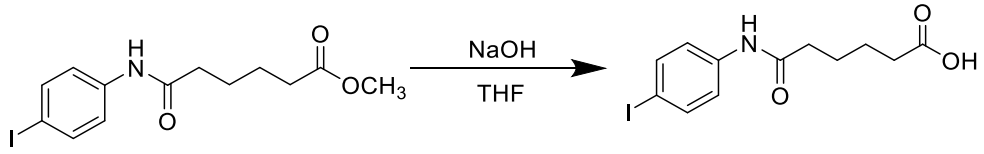

Compound	Yield (%)
14b	88

Table III.9 - Synthesis of hydroxamic acid derivatives from compounds present in table III.7. The table describes the compounds obtained (respective numbering) and corresponding yields.

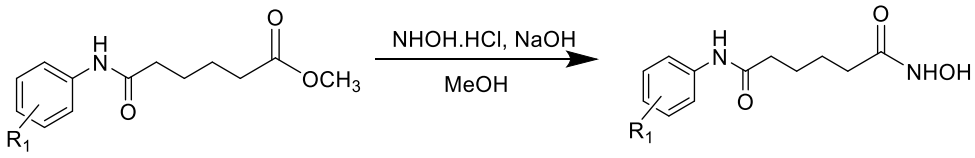

R1	Position	Compound	Yield (%)
-	-	12c	36
I	*ortho*	13c	65
	para	14c	15

Table III.10 - 1st Step of the synthesis using suberic acid monomethyl ester as starting material and several anilines. The table describes the compounds obtained (respective numbering) and corresponding yields.

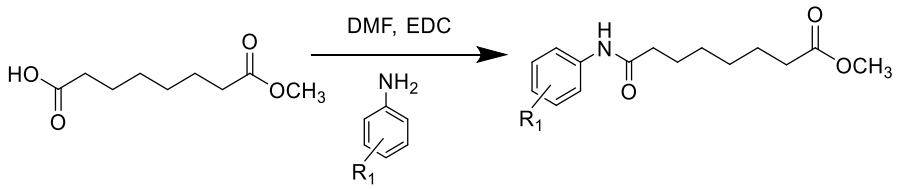

R1	Position	Aniline used	Compound	Yield (%)
I	*ortho*	2-iodoaniline (TCI)	15a	27
	para	4-iodoaniline (Alfa Aesar)	16a	68

Table III.11 - Synthesis of hydroxamic acid derivatives from compounds present in table III.10. The table describes the compounds obtained (respective numbering) and corresponding yields.

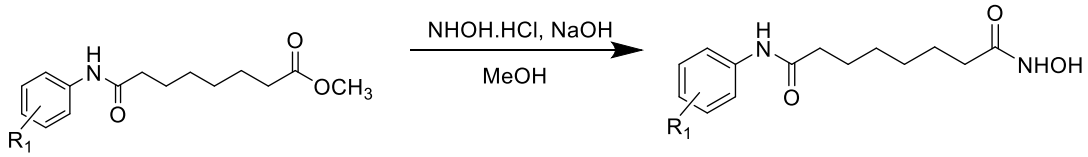

R1	Position	Compound	Yield (%)
I	*ortho*	15c	67
	para	16c	21

Table III.12 - 1st Step of the synthesis using azelaic acid monomethyl ester as starting material and several anilines. The table describes compounds obtained (respective numbering) and corresponding yields.

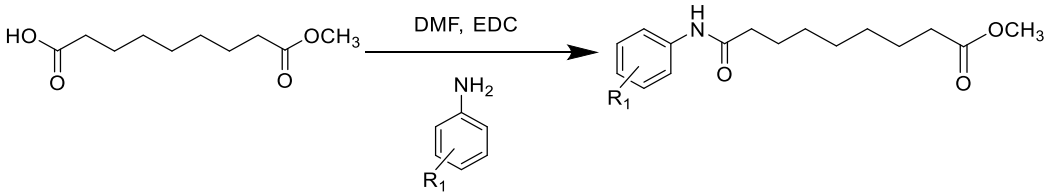

R1	Position	Aniline used	Compound	Yield (%)
I	*ortho*	2-iodoaniline (TCI)	17a	19
	para	4-iodoaniline (Alfa Aesar)	18a	74

Table III.13 - Synthesis of hydroxamic derivatives from compounds present in table III.12. The table describes the compounds obtained (respective numbering) and corresponding yields.

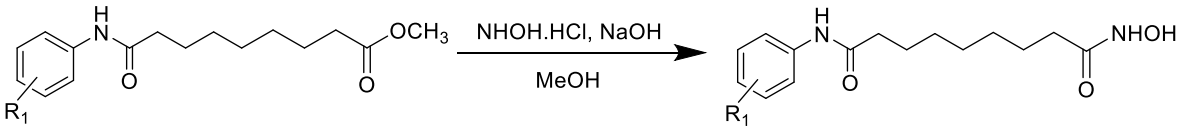

R1	Position	Compound	Yield (%)
I	*ortho*	17c	53
	para	18c	45

III.1.4 Discussion

Analyzing the yields of the compounds from the amide formation (1st step reaction), the amides were obtained in 19-96% yields. Carboxylic acid derivatives were obtained with 26-97% yields and hydroxamic acids were obtained with 15-98% yields.

In the reaction where carboxylic acids are formed, optimizations were introduced during the work up: addition of one more step of washing the ethyl ether phase with water and an acidification to a more acidic pH (closer to 3). These changes led to higher yields in comparison with first reactions where these changes were not implemented. (See table III.5 – section III.1.2)

Hydroxamic acids are normally obtained with a lower yield compared with the other steps. This is because under the reaction conditions used, NaOH is present and can hydrolyse the ester group to a carboxylic acid group. This by-product can be removed by washing the reaction mixture with sodium bicarbonate, but its formation lowers the yield of the desired hydroxamic acid product. In the literature, similar reactions showed 10-90% yield[32]. Optimizations were performed in order to achieve higher yields with an addition of a higher quantity of $NH_2OH.HCl$ to the mixture but the yields were not improved. Compound 9c (See figure III.12), was firstly obtained as a mixture with the corresponding carboxylic acid (9b), as can be seen in the top proton NMR spectrum. After washing with sodium bicarbonate the carboxylic acid was removed as its sodium salt, leaving the hydroxamic acid 9c pure (middle proton NMR spectrum).

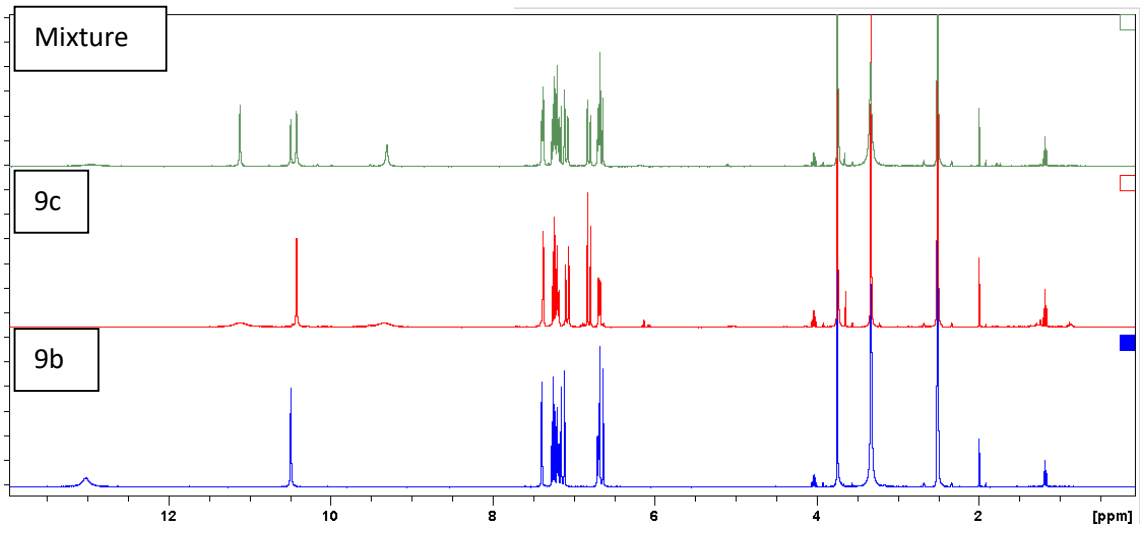

Figure III.12 – ^1H NMR spectra of compound 9c before (above) and after (below) the sodium bicarbonate ($NaHCO_3$) washing step and of compound 9b.

In the second round of synthesis, the use of different starting materials with longer carbon chain lengths led to methyl ester products that were not solid after work-up. Therefore, some compounds (12a, 13a and 15a) were purified using silica flash chromatography instead of recrystallization. Nevertheless, all synthesized compounds were solid after purification.

As mentioned before (section I.4.4), other compounds can be used as carboxyl-activating agents in coupling reactions such as N,N'-dicyclohexylcarbodiimide (DCC) and N,N'-diisopropylcarbodiimide (DIC). A small scale synthesis using DIC and DCC was performed in order to assess which is the better coupling agent and which leads to better yields. Reaction using DCC led to addition of more steps in work-up (filtration using celite), a lower yield comparing to when EDC is used, and impurities present in NMR spectra. Also, DCC can cause allergies therefore extra care is needed in handling this reagent. Reaction using DIC also led to a lower yield compared to when EDC is used. For these reasons, EDC was chosen as the best reagent to act as reaction activator and was used in all syntheses.

It is quite difficult to distinguish between carboxylic and hydroxamic acids where the rest of the structure is identical, even using NMR spectroscopy. Analysis of ^{1}H-NMR spectra comparing carboxylic acid and hydroxamic acid derivatives presented a shift of the peaks related to protons closer to the carbonyl groups. (See figure III.13).

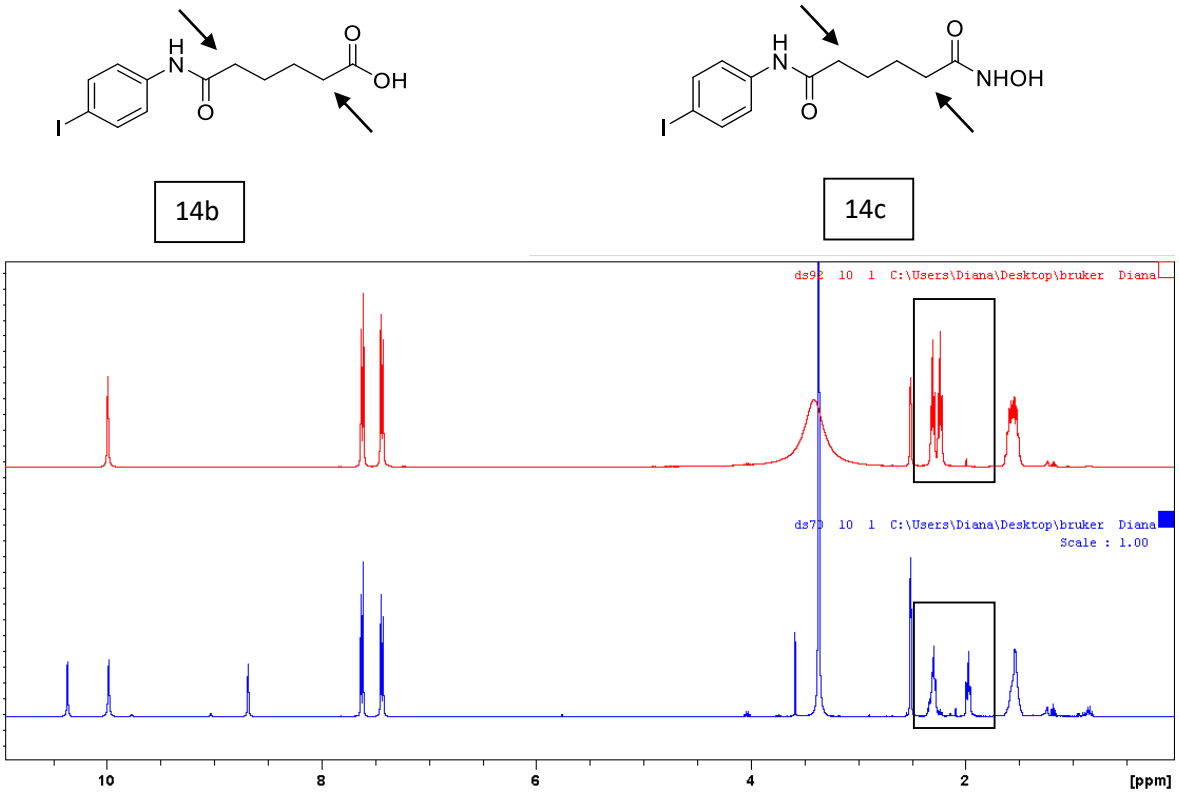

Figure III.13 - ^{1}H NMR spectra of compounds 14b (above) and 14c (below). In both spectra, the area important to distinguish between both derivatives is highlighted. At the top are the structures of compounds 14b and 14c, respectively.

The peaks highlighted in both spectra are related to the protons closer to the carbonyl groups (indicated by arrows in both structures). Comparing the two structures, in the carboxylic acid these peaks are closer together than in the hydroxamic acids. During the analysis of several spectra it was possible to see that this feature (more separated peaks) is preserved even in hydroxamic acids with different substituents in the benzenic ring.

It was possible to see differences between ^{1}H-NMR spectra of carboxylic and hydroxamic acids also in the compounds obtained in the first round of synthesis, in peaks related to protons present in the double bond. (See figure III.14)

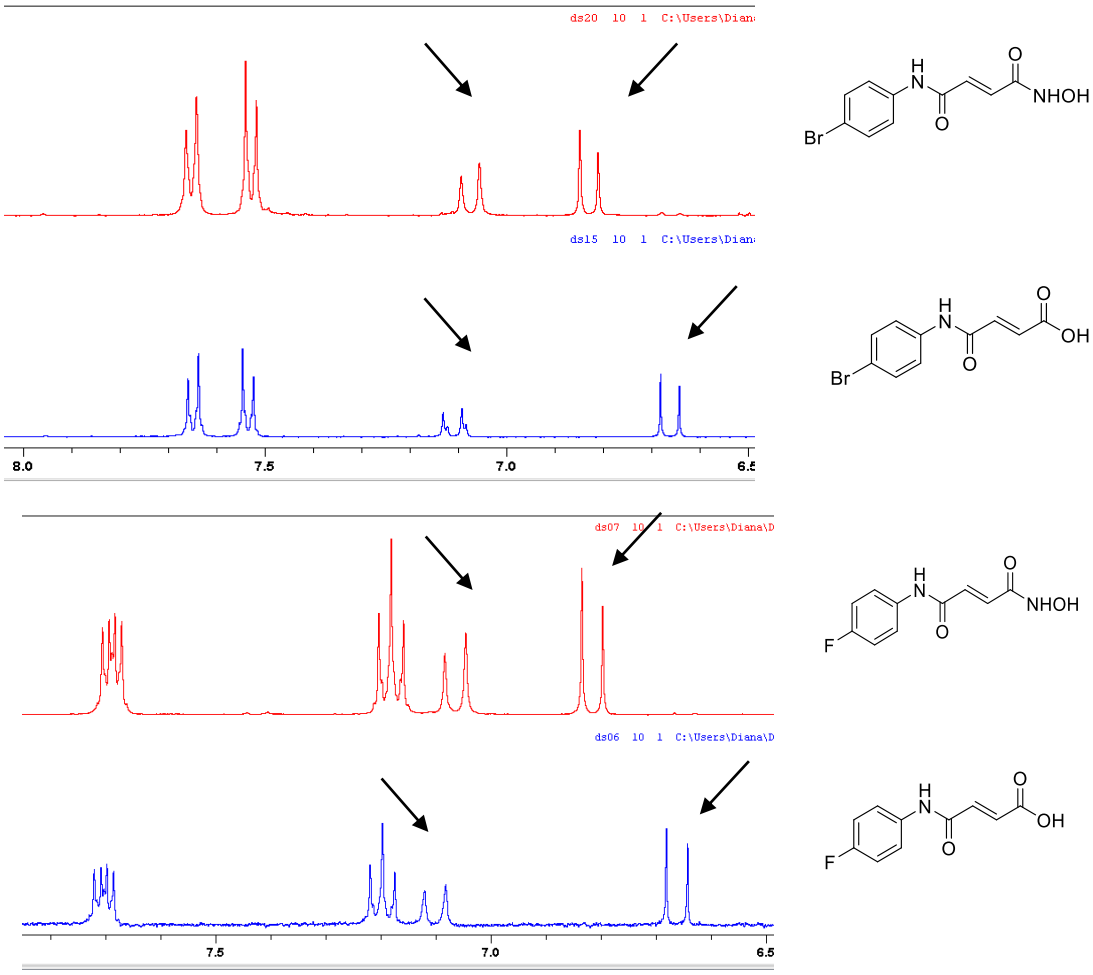

Figure III.14 - ^{1}H NMR spectra of compounds 4c, 4b, 2c and 2b, respectively. Structures of the compounds at the right of each spectrum.

Comparing the 1H-NMR spectra, a shift of the peaks related to the protons of the double bond can be observed (see figure III.14). In similar way as described before, these peaks (see arrows in the figure) are much closer together in hydroxamic acids and farther apart in carboxylic

acids. This was observed in several compounds, even with different atoms at different positions in the aromatic ring (examples in figure III.14).

Compound structures were confirmed by NMR spectroscopy before performing biological assays. All ester compounds obtained from the 1st step of synthesis were dissolved in $CDCl_3$ for NMR spectroscopy while carboxylic and hydroxamic acids were dissolved in DMSO-d_6.

All tested compounds (table III.3.B) and also SAHA were dissolved in DMSO at a concentration of 50 mM taking into account the SAHA solubility in DMSO (≥15 mg/mL).

III.2 New HDACi evaluation as anticancer agents

For the evaluation of the newly synthesized compounds as anticancer agents, two different cancer cell lines were used: MCF-7, a breast cancer cell line and H460, a lung cancer cell line. (See figure III.15).

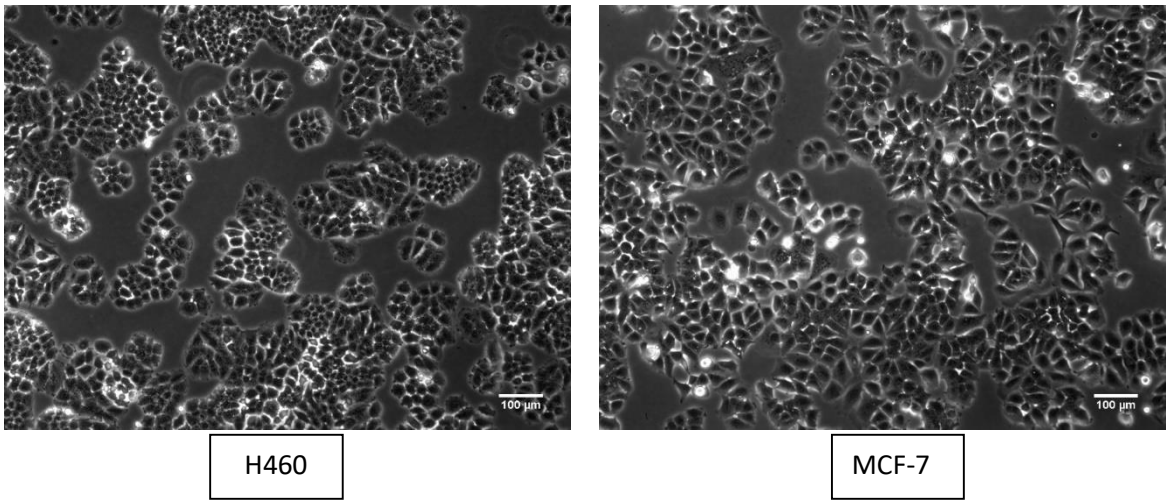

Figure III.15 - Phase-contrast microscopy of H460 cells (left) and MCF-7 cells (right). Scale bars represents 100 µm.

Also, HDF (Human Dermal Fibroblasts) were used as a normal cell model for testing the effect of SAHA, compound 15c and compound 16c in cell viability of non-malignant cells (See figure III.16).

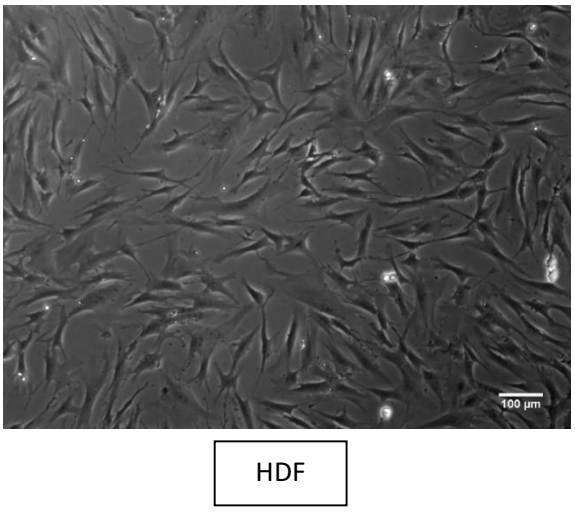

Figure III.16 - Phase-contrast microscopy of Human Dermal Fibroblasts. Scale bar represents 100 µm.

III.2.1 Determination of DMSO toxicity

All compounds, including the positive control SAHA, were dissolved in DMSO. DMSO has been shown to be toxic to mammalian cells, even at low concentrations [38]. DMSO toxicity for each of the cell lines used in this study was assessed by treating MCF-7 and H460 cells with a range of DMSO concentrations (0.016 to 4%).

The dose-response curves obtained are presented in Figure III.17.

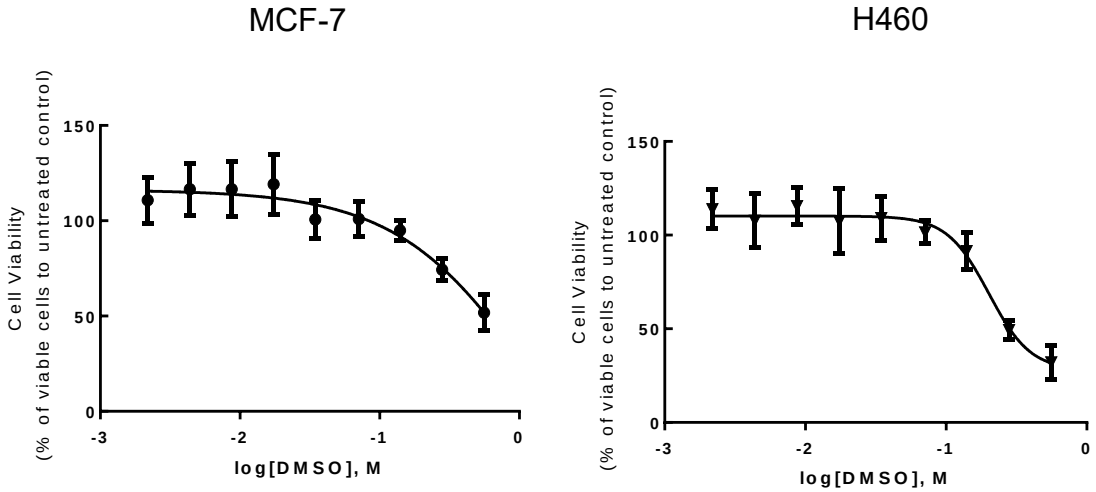

Figure III.17 – Dose-response curves for DMSO for each cancer cell line (MCF-7 and H460). Dose-response curves were generated using Graph Pad Prism 6 software.

DMSO percentages of 4% and 2% had a clearly effect on cell viability of both cancer cell lines, causing a decrease in the percentage of live cells, higher than 25% for MCF-7 cells and 50% for H460 cells. The H460 cell line seems to be more sensitive to DMSO than MCF-7, as it presented a higher toxicity (lower percentages of live cells comparing to MCF-7) at 4% and 2%. For DMSO percentages below 1%, cell viability was not affected, with cell viabilities of approximately 100%. Therefore, 1% DMSO was chosen as the maximum of DMSO to be used in further assays.

III.2.2 Drug Testing

III.2.2.1 1ST round Compounds Testing

All compounds obtained in the first round of synthesis were tested on cancer cell lines (MCF-7 and H460) using cell viability as end-point. SAHA was used as positive control in the drug testing assays because it is an HDACi already approved as anticancer drug and the new synthesized compounds are structurally similar. To assess SAHA anticancer affect in the implemented assay set-up, the compound was added to each of the cancer cell lines at three different concentrations: 500 µM, 50 µM and 5 µM, and was incubated for 48h, after which cell viability was measured using the PrestoBlue Assay (See figure III.18).

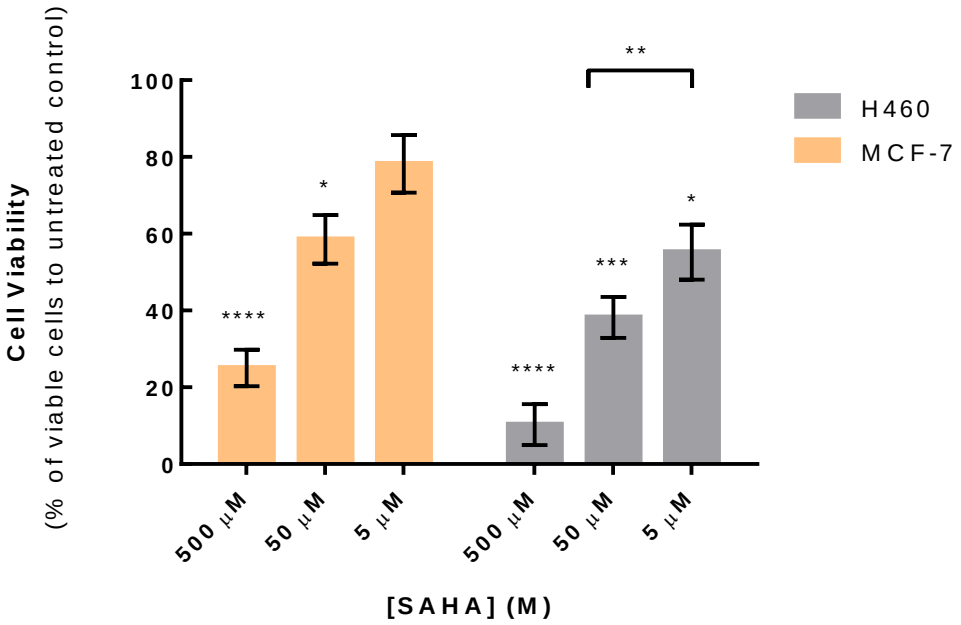

Figure III.18 - Effect of SAHA on MCF-7 and H460 cell viability, determined by PrestoBlue assay. Both cancer cells lines were treated with three different concentrations of SAHA: 500 50 and 5 µM, for 48h. Data are mean ± SD of three independent experiments; asterisks indicate significant difference to negative control (*p≤0.05, **p≤0.01, ***p≤0.001 and ****p≤0.0001) by one-way ANOVA analysis with Kruskal-Wallis comparison test. Graph constructed using Graph Pad Prism 6 software.

Analyzing the results, a negative effect of SAHA on cell viability in both cancer cell lines is observed. Addition of SAHA to the cultures led to a decrease in cell viability in all three concentrations tested, in a dose-dependent manner.

For H460 cells, 5 µM of SAHA led to a significant reduction in cell viability to 50 ±7.5%, which is in line with the IC50 of 2.3 µM previously reported for this cell line[25]. On the other hand, 5 µM of SAHA only led to a reduction in MCF-7 cell viability to 80 ±7.2%, despite the previous report of an IC50 of 0.75 µM for this cell line[39]. *P. Munster et al* calculated an IC50 of 0.75 µM after 120h of continuous exposure to SAHA and in this experiment MCF-7 cells were treated with SAHA for 48h which can explain the differences in IC50. Alternatively, this result can be due to differences between lots of MCF-7 cells. It has been reported in some studies that MCF-7 cells,

even from the same frozen batch, can present genetic variations and this heterogeneity can have serious consequences for the reproducibility of experiments[40].

SAHA and similar HDACi have an antiproliferative effect in malignant cells[19]. The results obtained suggest that the H460 cell line presents higher sensitivity to SAHA action, and the fact that this cell line is more proliferative than MCF-7 could explain this result.

The newly synthesized compounds (see section III.1.2) were also tested in both cancer cell lines, using the same assay set-up. As described in section III.1, in the first generation of hydroxamic acid compounds, the linker was kept constant and the capping group was altered, with the addition of different atoms or groups to the benzenic ring in different positions. The atoms/groups added were: -F, -Br, -I, $-F_3C$, $-OCH_3$, and Cl. Synthesis of a compound without any atom addition to benzenic ring (1c) and a compound with addition of both fluorine and bromine atoms was also performed successfully (7c). (See table 3.B for the compounds structure.)

The drug assays of all hydroxamic acid compounds synthesized are presented in figure III.19.

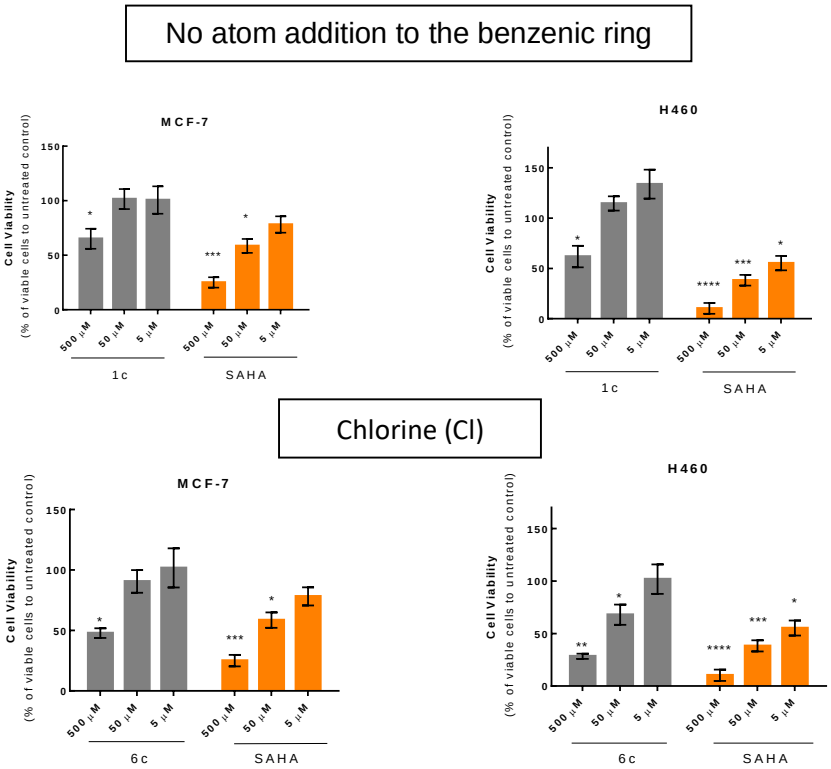

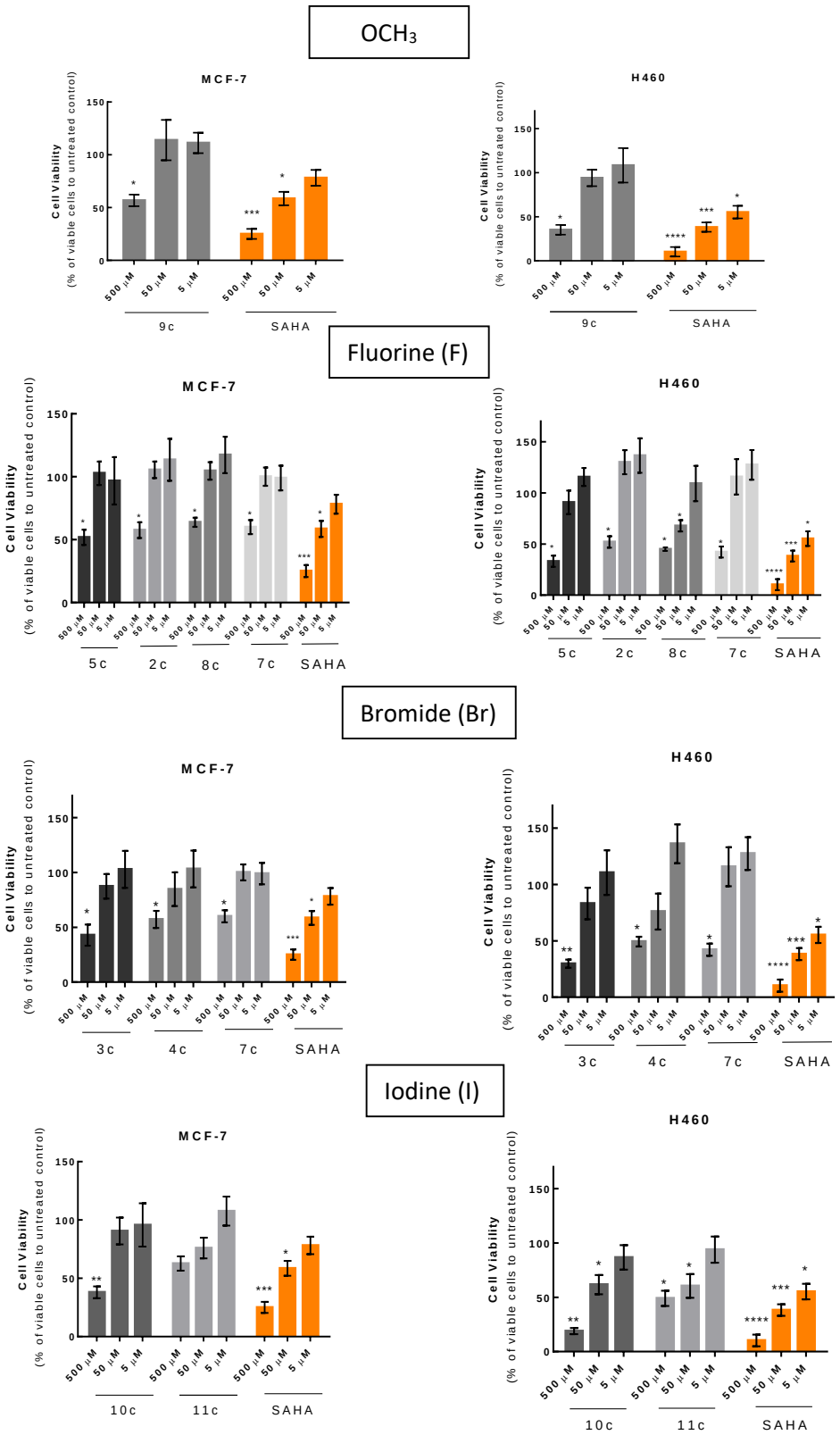

Figure III.19 - Effect of SAHA and the hydroxamic compounds synthesized in the 1st round of synthesis on MCF-7 and H460 cell viability, determined by PrestoBlue assay. Both cancer cells lines were treated with three different concentrations of SAHA: 500, 50 and 5 µM, for 48h. Data are mean ± SD of two independent experiments; asterisks indicate significant difference to negative control (*p≤0.05, **p≤0.01, ***p≤0.001 and ****p≤0.0001) by one-way ANOVA analysis with Kruskal-Wallis comparison test. Graph constructed using Graph Pad Prism 6 software.

All tested hydroxamic acid compounds had a negative effect on cell viability in both breast and lung cancer cells, mainly at 500 µM. In H460 cell line, compounds 10c, 11c, and 8c showed a significant reduction in cell viability even at 50 µM. However, none of the new compounds tested had an effect comparable to SAHA.

The changes in capping group made in the analogues produced did not improve the toxic effect in MCF-7 and H460 cells. In general, the first generation hydroxamic compounds showed a higher effect in H460 cells than in MCF-7 cells, similarly to what was observed for SAHA.

Interestingly compound 1c (Figure III.21), that only differs from SAHA in terms of the length of the linker (see SAHA structure in section I.4.2), presented a weaker effect when compared to SAHA in both cancer cells lines (65.2 ± 9 % vs 25 ± 5 % of cell viability for 500 µM concentration in MCF-7 and 61.2 ± 10 % vs 10.3 ± 5 % of cell viability for 500 µM concentration in H460). This result suggested that linker size present in SAHA could be critical to the effect of this type of compounds in cancer cell lines and led to the hypothesis that spacers with longer carbon lengths (more similar to SAHA) could lead to more effective compounds.

Taking into account the results for all the atomic substitutions, the *ortho* position (compounds 5c, 3c and 10c), seems to favor a higher effect in cell viability, compared with additions of the same atom in another positions.

As for the atom itself, compounds with iodine resulted in the higher decrement in cell concentration. Compound 10c, with iodine in *ortho* position, was the best candidate from the first generation compounds, presenting an effect closer to SAHA at 500 µM. (19 ± 3% vs 10 ± 5%, respectively).

The results concerning the effect of the synthesized carboxylic acids are presented in Figure III.20.

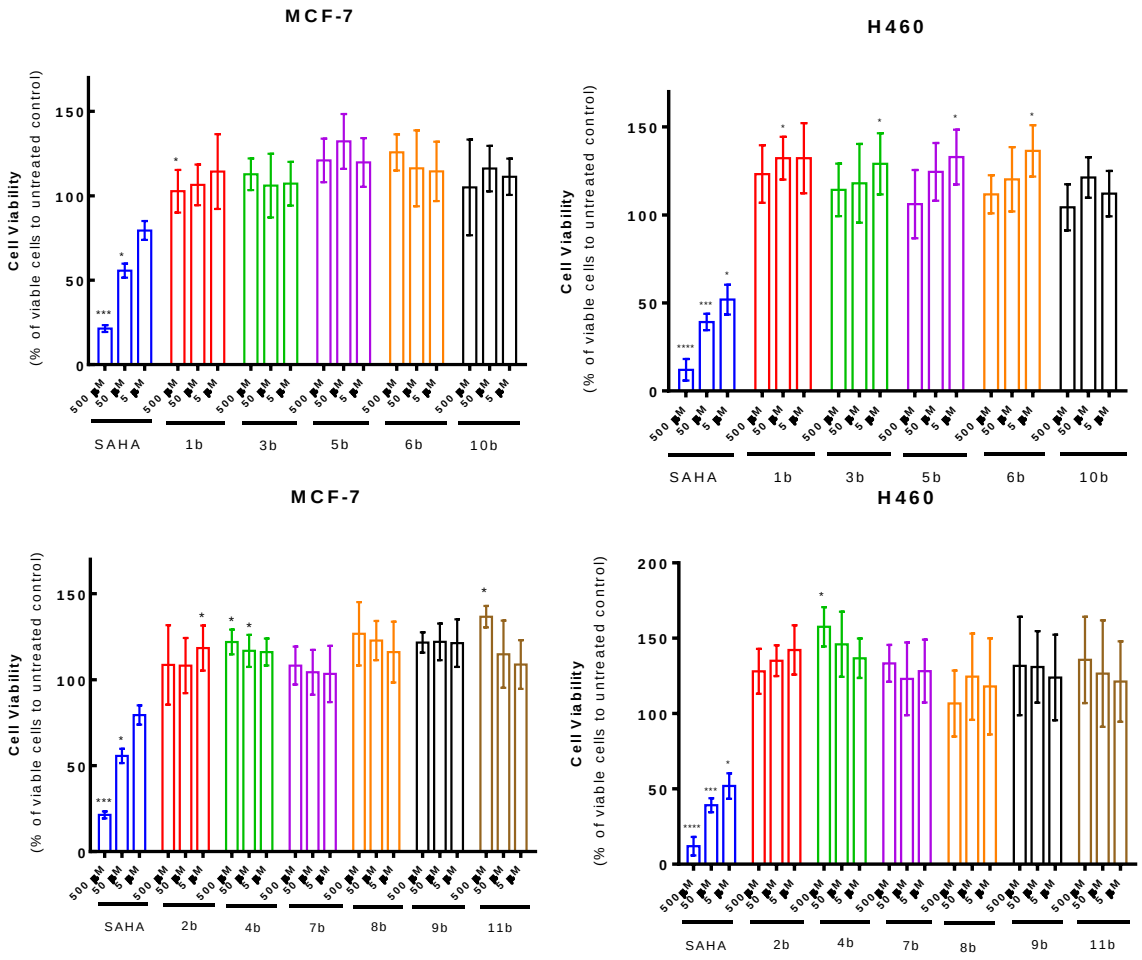

Figure III.20 – Effect of SAHA and the carboxylic compounds synthesized in the 1st round of synthesis on MCF-7 and H460 cell viability, determined by PrestoBlue assay. Both cancer cells lines were treated with three different concentrations of SAHA: 500, 50 and 5 μM, for 48h. Data are mean ± SD of two independent experiments; asterisks indicate significant difference to negative control (*p≤0.05, **p≤0.01, ***p≤0.001 and ****p≤0.0001) by one-way ANOVA analysis with Kruskal-Wallis comparison test. Graph constructed using Graph Pad Prism 6 software.

None of the compounds showed a negative effect in cell viability, at any of the concentrations tested. So, the results suggest that the hydroxamic acid moiety is essential for the action of these compounds as anticancer drugs. Indeed, the hydroxamic acid moiety has been proposed to be critical for the HDAC inhibitory activity, working as a metal chelator that interacts with the zinc present in the active pocket of HDAC enzymes[34]. Although carboxylic acids are also metal chelators, they are not as strong as hydroxamic, which may explain the lack of activity of compounds with carboxylic moieties.

In summary, the hydroxamic acids synthesized had a negative impact on cell viability of the cancer cell lines tested, contrary to the carboxylic acids, that showed no effect in both breast and lung cancer cells. None of the tested compounds showed an effect comparable to SAHA,

indicating that the structure modifications did not lead to a more potent compound. The results suggested that the linker length is probably very important for the anticancer effect and that the substitution in the benzene ring in an *ortho* position, especially with iodine, can potentially generate compounds with improved potency.

Taking into account these observations, a new series of analogues was planned, including hydroxamic acid derivatives with longer carbon chains as linkers - 6, 8 and 9 carbon long chains; with iodine atoms added to the benzenic ring in not only in the *ortho* but also in the *para* position.

A carboxylic acid compound (14b) and a compound without any addition to benzene (12c) were also synthesized with a longer carbon chain in order to evaluate if the previous results are maintained when the linker is altered.

III.2.2.2 2ND round Compounds Testing

After successful synthesis of the new compounds (See section III.1.3), these molecules were tested in MCF-7 and H460 cells, and cell viability was assessed (Figure III.21).

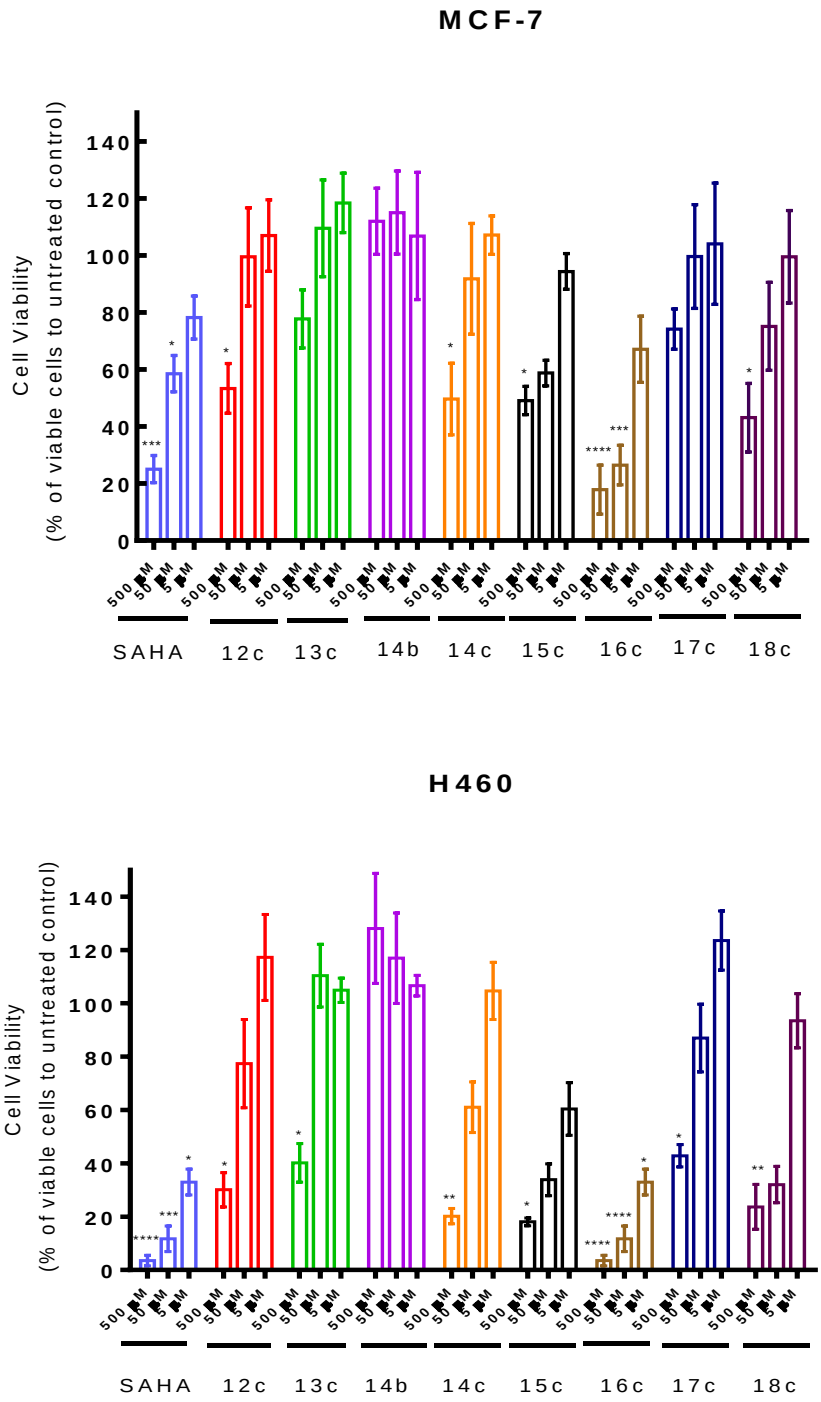

Figure III.21 – Effect of SAHA and all compounds synthesized in the 2nd round of synthesis on MCF-7 and H460 cell viability, determined by PrestoBlue assay. Both cancer cells lines were treated with three different concentrations of SAHA: 500, 50 and 5 µM, for 48h. Data are mean ± SD of two independent experiments; asterisks indicate significant difference to negative control (*p≤0.05, **p≤0.01, ***p≤0.001 and ****p≤0.0001) by one-way ANOVA analysis with Kruskal-Wallis comparison test. Graph constructed using Graph Pad Prism 6 software.

Compound 16c showed a significant reduction in cell viability of both MCF-7 and H460 cells, higher than SAHA especially at 50 µM. (26.5 ± 6 % vs 58.4 ± 6 %, for MCF-7, respectively and 11.7 ± 5% vs 38.2 ± 5 % for H460, respectively).

In H460 cells, 16c showed a significant reduction in cell viability also at 5 µM, and this effect is higher than in cells treated with SAHA. (32.9 ± 5% vs 55.2 ± 7%, respectively).

Compound 15c also showed a significant effect, especially on the H460 cell line at 50 µM (33.8 ± 6 %).

Compound 14b was the only compound tested that had no effect on cell viability, in any of the concentration tested, similarly to the carboxylic acids previously tested.

In general, all compounds tested showed stronger effect on H460 cells than on MCF-7 and this can be due to the fact that MCF-7 cell line is not so proliferative as H460.

Both 15c, 16c and SAHA have an 8 carbon chain length as linker, suggesting that the linker has the optimal size. Moreover, compound 16c has a structure similar to SAHA, with an 8 carbon chain as a linker and a hydroxamic acid moiety, but differs only in the presence of an iodide atom in the *para* position of the benzenic ring, suggesting that this substitution can also increase the compound activity.

This result suggests compound 16c as a putative new HDACi with anticancer effects. To further evaluate the potential of the compound, further studies are required to address compound toxicity in normal cells, o define its mechanisms of action and compare it to already FDA approved drugs, like SAHA.

III.2.3 Evaluation of Compound 16c

II.2.3.1 Normal Cell resistance

As mentioned before in section I.4.3, HDACi are normally associated with normal cell resistance and FDA-approved compounds show antitumor action in cancerous cells at concentrations to which normal cells show little toxicity[27]. HDF were used for testing normal cell toxicity of compound 16c, the best candidate from the previous screening. SAHA and compound 15c were used as controls. Effect on HDF viability was measured using PrestoBlue cell viability assay, as before (figure III.22).

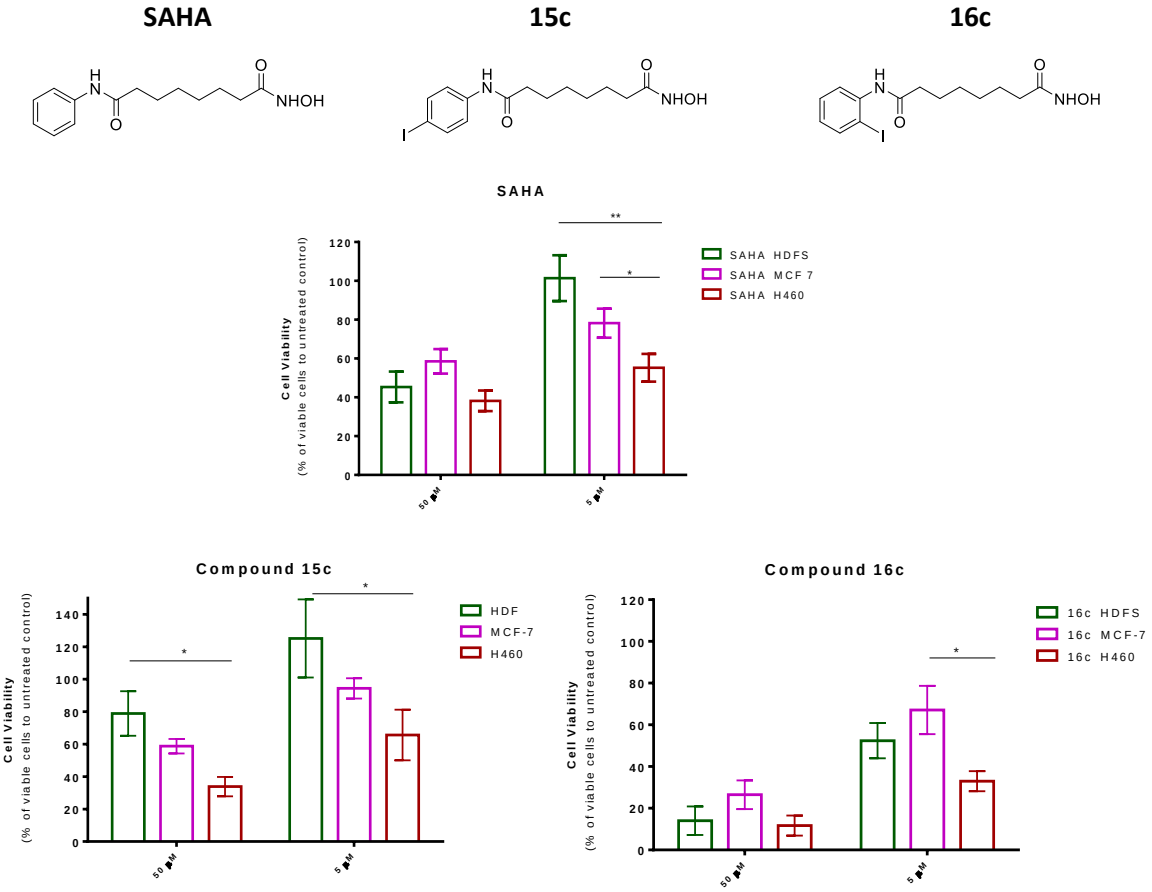

Figure III.22- Effect of SAHA and compound 16c in MCF-7, H460 and HDF cell viability, determined by PrestoBlue assay. All cell lines were treated with two different concentrations of SAHA and 16c: 50 and 5 µM, for 48h. Data are mean ± SD of two independent experiments; asterisks indicate significant difference (*p≤0.05 and **p≤0.01) by one-way ANOVA analysis with Kruskal-Wallis comparison test. Graph constructed using Graph Pad Prism 6 software.

Incubation with compound 16c caused a reduction on HDF viability in all concentrations tested. At the lower concentration tested (5 µM), 16c caused a reduction in HDF viability to 52 ± 8% whereas SAHA and compound 15c had no effect on cell viability.

These results are consistent with reported findings that normal cells are relatively resistant to SAHA-induced cell death. *J. Lee at al.* reported that after 72 h of culture with 5 µM SAHA, there was >80% loss of cell viability of LNCaP (prostate cancer cells) and 30% of A549 (human lung adenocarcinoma cells), but no detectable loss of cell viability of the normal cells, HFS[31].

Also, this result suggests that the presence of an iodine atom in the capping group apparently increases the cytotoxic effect of hydroxamic acids in cancer cells (section III.2.4.2), when compared to SAHA, but also its cytotoxic effect in normal cells.

For the lower concentration tested (5 µM), compound 16c had a cytotoxic effect in cancer cells approximately twofold higher that SAHA, so it is possible that in a lower concentration range, this compound presents the normal cell resistance described for this class of molecules. In the future, generation of dose-response curves of compound 16c will be required, to evaluate the potency of the compound in cancer cells and normal cell resistance and evaluate if these cells present different sensitivities to compound toxicity at lower concentrations.

III.2.3.2 Apoptosis Induction and Cell Cycle Arrest

As mentioned in section I.4.3, the action of SAHA and several HDACi as anti-cancer drugs involves their ability to induce/stimulate apoptosis and to induce cell cycle arrest in malignant cells[6]. Therefore, a preliminary evaluation of the capacity of compound 16c to induce apoptosis and cell cycle arrest in MCF-7 breast cancer cells was conducted. Apoptosis is triggered by caspase activation, and caspase-3 activation is an early event stage apoptosis. Therefore, early stage apoptosis can be accessed by measuring caspase-3 levels[35]. Compound 16c and SAHA were added to MCF-7 cells at 50 µM and apoptosis was assessed after 48h. (Figure III.23).

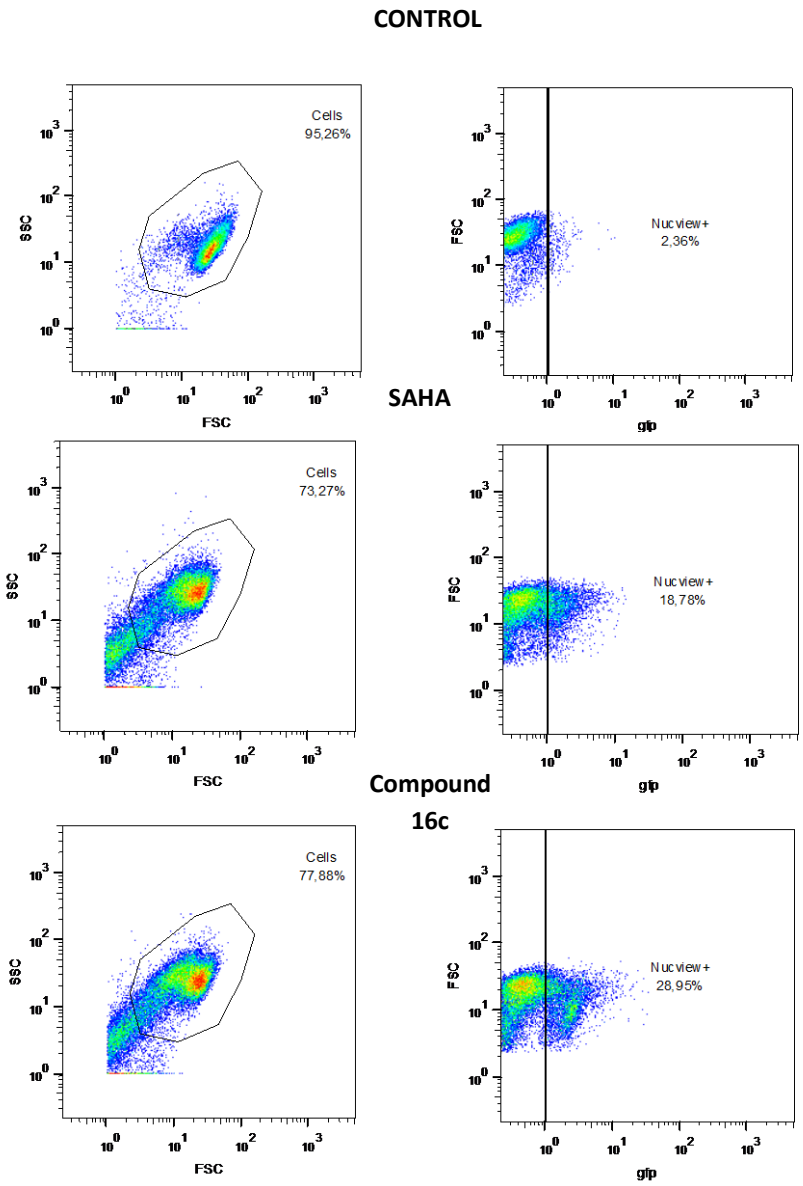

Figure III.23 – Induction of apoptosis by SAHA and Compound 16c. MCF-7 cells were cultured in the presence of compound 16c, SAHA or in culture medium with vehicle control (control) for 48h, collected and processed for apoptosis analysis using fluorescence labelling with a caspase probe (NucView) followed by flow cytometry.

Compound 16c and SAHA induced apoptosis (approximately 29 and 19%, respectively, compared with 2% in control). Compound 16c led to a higher induction of apoptosis than SAHA however, additional biological replicates are required to draw conclusions on the significance of these differences. Nonetheless, the results obtained suggest that compound 16c induces apoptosis in MCF-7 cells, as described for SAHA and other HDACi. *Hugh et al.* observed that 48h exposure to 4 µM of SAHA resulted in 20% apoptotic MCF-7 cells[41].

Further studies at additional compound concentrations and including other cancer and normal cells are required to corroborate these preliminary results.

In order to assess if compound 16c is able to induce cell cycle arrest in MCF-7 cells, cell cycle analysis was performed using flow cytometry and propidium iodide (PI) as intercalating dye. (Figure III.24).

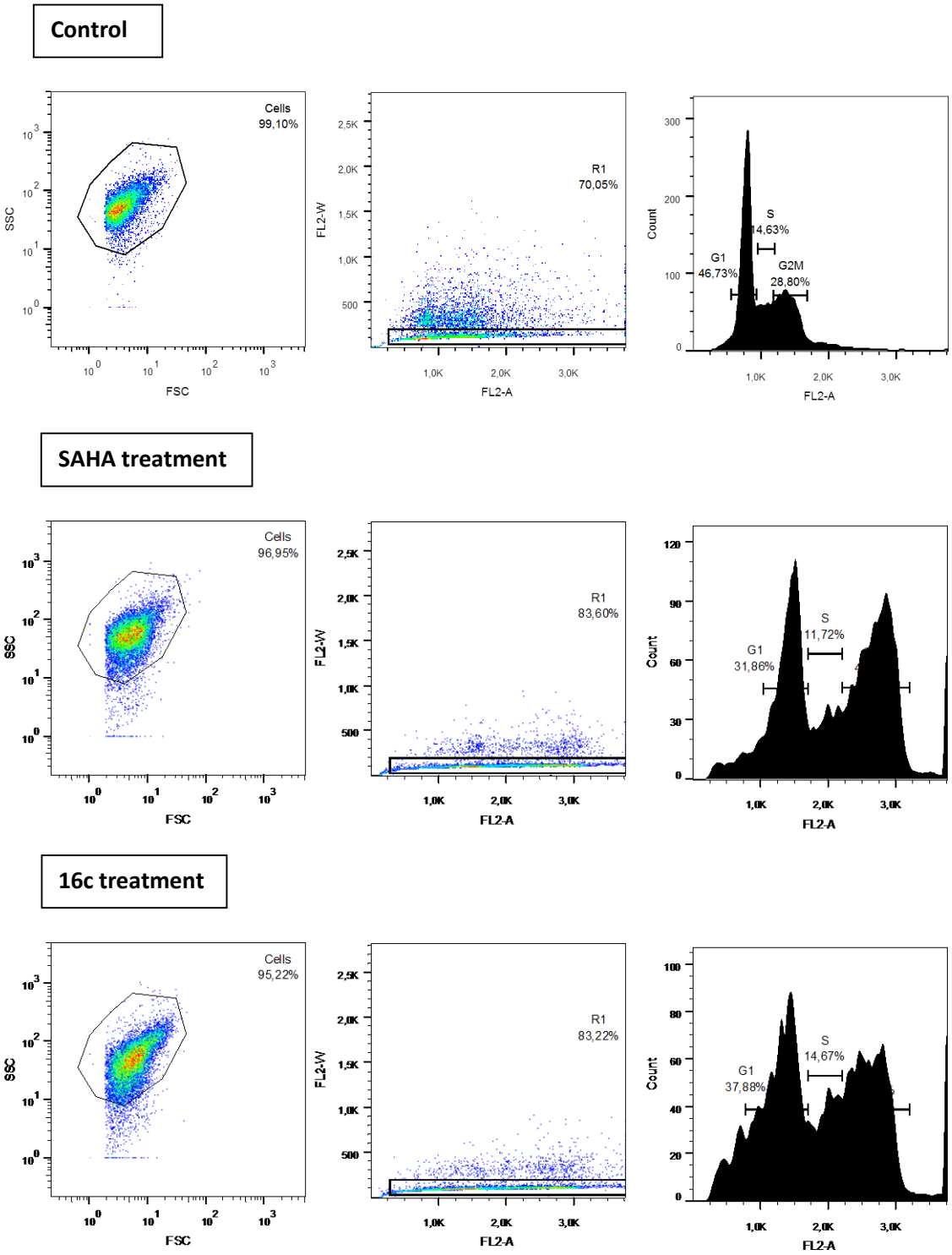

Figure III.24 – Cell cycle analysis of MCF-7 cells. MCF-7 cells were cultured in the presence of compound 16c, SAHA or in culture medium with vehicle control (control) for 48h, collected and processed for cell cycle analysis by flow cytometry. Gated region (left), doublet discrimination step (middle) and counted cells in each phase of the cell cycle (G1, S and G2/M).

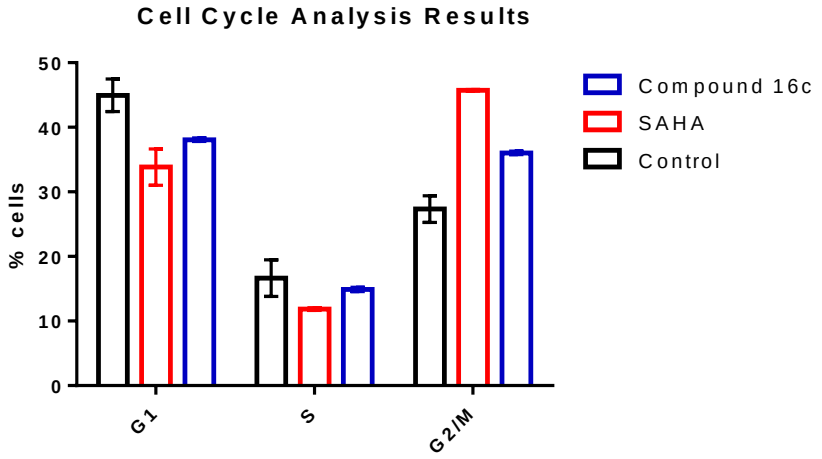

Figure III.25 – Cell cycle analysis of MCF-7 cells. MCF-7 cells were cultured in the presence of compound 16c, SAHA or in culture medium with vehicle control (control) for 48h, collected and processed for cell cycle analysis by flow cytometry.

As mentioned in section II.2.8, cells in phase G2/M which contain two copies of DNA will have the double of fluorescence intensity when compared with cells in G1 phase that only have one copy of DNA. Cells in phase S will show an intermediate fluorescence.

MCF-7 cells cultured in the presence of vehicle alone (control) showed higher percentage of cells in G1 phase of cell cycle (approximately 47%) than in S (approximately 15%) and G2/M phase (approximately 29%).

Histograms of MCF-7 cells treated with SAHA and compound 16c presented broader G1 peaks when compared with untreated cells. Apoptotic cells often have fractional DNA due to the fact that the fragmented (with low molecular weight) DNA undergoes extraction during the staining procedure and they are represented on the DNA content frequency histograms by “sub-G1” peaks[42]. A high amount of apoptotic cells and “sub-G1” peaks can lead to the appearance of broader G1 peaks similarly to the observed in this experiment.

Cells treated with SAHA presented an increased percentage of cells in G2/M phase, compared with cells treated with vehicle control (45% and 29% percent, respectively). These results are in agreement with previous literature reports. In published results, HDACi induced G2/M phase arrest, shown by an increase in the percentage of cells in G2/M phase for MCF-7 cells treated with 4 µM of SAHA after 24h and 48h [41].

In a similar way, cells treated with compound 16c presented an increased percentage of cells in G2/M phase, compared with cells treated with vehicle control (35 % and 29 % percent, respectively).

Therefore, both compounds are able to induce cell cycle arrest at the G2/M phase of cell cycle in the MCF-7 breast cancer cell line. This increase is higher for cells treated with SAHA than for cells treated with compound 16c, therefore SAHA seems to induce a more severe cell cycle arrest than compound 16c in MCF-7 cells.

Further studies at additional compound concentrations and including other cancer and normal cell lines are required to corroborate these preliminary results.

In summary, compound 16c has a structure similar to SAHA, with an 8 carbon chain as a linker and a hydroxamic moiety, but differs in the presence of an iodine atom in the *para* position of the benzenic ring. Results suggested that this substitution increased the compound activity towards cancer cell lines but 16c also revealed toxicity against HDF cells. Furthermore, preliminary results showed that 16c was able to induce apoptosis and cell cycle arrest at the G2/M phase of the cell cycle in the MCF-7 breast cancer cell line.

It is important to create new drugs, but with an acceptable therapeutic index and useful properties. High potency is in general associated with long-term binding of the drug to the receptor[43].

In an hydroxamic HDACi such as SAHA, the capping group is important for the interaction with the amino acid residues near the entrance of the active site. The results obtained suggest that the iodine atom in the benzene ring is interacting with those amino acids, enabling the access to the active site and increasing the binding, resulting in a more potent compound.

Moreover, taking into account the hypothesis proposed by *J.Lee et al.* that normal but not transformed cells repair DNA damage upon removal of HDACi, a long-term binding could increase the toxicity of the compound. That could explain the high toxicity showed by 16c towards HDF cells.

IV. CONCLUSIONS

In this work, 30 analogues of HDACi approved drugs (SAHA and Belinostat) were successfully synthesized and evaluated as anticancer agents in breast (MCF-7) and lung (H460) cancer cell lines.

None of the carboxylic acids tested showed a decrease in cell viability in any of the concentrations tested, in both MCF-7 and H460 cells.

Cells treated with the hydroxamic acids synthesized presented a decrease in cell viability and this effect was higher with substitution in the benzene ring in an *ortho* position, especially with iodine and with bigger linker sizes.

Synthesized compound hydroxy-N'-(4-iodophenyl)octanediamide (16c) had a cytotoxic effect in cancer cells approximately twofold higher that SAHA even at the lowest concentration tested (5 µM). Furthermore, preliminary results showed that 16c was able to induce apoptosis and cell cycle arrest at the G2/M phase of the cell cycle in the MCF-7 breast cancer cell line.

An important characteristic of HDACi is that they induce cancer cell death at concentrations to which normal cells are relatively resistant, making them well suited for cancer therapy. However, compound 16c showed an effect on cell viability also in HFS. In the future, generation of dose-response curves of compound 16c will be required, to evaluate the potency of the compound in cancer cells and normal cell resistance, and evaluate if these cells present different sensitivities to compound toxicity at lower concentrations.

HDACi action leads to differences in histone acetylation levels that can be measured by western blotting using antibodies for acetylated histones. In future work, it is important to use this technique in order to assess if compound 16c is able to increase histone acetylation levels.

V. REFERENCES

1. WHO-World Health Organization accessed in August, 2016. at <http://www.who.int/mediacentre/factsheets/fs297/en/>

2. Ropero, S. & Esteller, M. The role of histone deacetylases (HDACs) in human cancer. *Mol. Oncol.* **1,** 19–25 (2007).

3. You, J. S. & Jones, P. a. Cancer Genetics and Epigenetics: Two Sides of the Same Coin? *Cancer Cell* **22,** 9–20 (2012).

4. West, A. C. & Johnstone, R. W. New and emerging HDAC inhibitors for cancer treatment. *J Clin Invest.* **124,** 30–39 (2014).

5. Fraga, M. F. *et al.* Loss of acetylation at Lys16 and trimethylation at Lys20 of histone H4 is a common hallmark of human cancer. *Nat. Genet.* **37,** 391–400 (2005).

6. Kim, T. Y., Bang, Y. J. & Robertson, K. D. Histone deacetylase inhibitors for cancer therapy. *Epigenetics* **1,** 14–23 (2006).

7. Kouzarides, T. Chromatin Modifications and Their Function. *Cell* **128,** 693–705 (2007).

8. Katoch, O., Dwarakanath, B. & Agrawala, P. K. HDAC inhibitors: applications in oncology and beyond. *HOAJ Biol.* **2,** 8 (2013).

9. Kakutani, T. *et al.* Translating the Histone Code. *Science (80-.).* **293,** 1074–1081 (2001).

10. Ververis, K., Hiong, A., Karagiannis, T. C. & Licciardi, P. V. Histone deacetylase inhibitors (HDACIS): Multitargeted anticancer agents. *Biol. Targets Ther.* **7,** 47–60 (2013).

11. de Ruijter, A. J. M., van Gennip, A. H., Caron, H. N., Kemp, S. & van Kuilenburg, A. B. P. Histone deacetylases (HDACs): characterization of the classical HDAC family. *Biochem. J.* **370,** 737–49 (2003).

12. Marks, P. a. Histone deacetylase inhibitors: a chemical genetics approach to understanding cellular functions. *Biochim. Biophys. Acta* **1799,** 717–725 (2010).

13. Carafa, V., Nebbioso, A. & Altucci, L. Sirtuins and disease: The road ahead. *Front. Pharmacol.* **3 JAN,** 1–6 (2012).

14. Allen, M. J. *et al.* Identification of novel small molecule enhancers of protein production by cultured mammalian cells. *Biotechnol. Bioeng.* **100,** 1193–1204 (2008).

15. Chuang, D. M., Leng, Y., Marinova, Z., Kim, H. J. & Chiu, C. T. Multiple roles of HDAC inhibition in neurodegenerative conditions. *Trends Neurosci.* **32,** 591–601 (2009).

16. Falkenberg, K. J. & Johnstone, R. W. Histone deacetylases and their inhibitors in cancer, neurological diseases and immune disorders. *Nat. Rev. Drug Discov.* **13,** 673–91 (2014).

17. Dietz, K. C. & Casaccia, P. HDAC inhibitors and neurodegeneration: At the edge between protection and damage. *Pharmacol. Res.* **62,** 11–17 (2010).

18. Nakagawa, M. *et al.* Expression profile of class I histone deacetylases in human cancer tissues. *Oncol. Rep.* **18,** 769–74 (2007).

19. Mottamal, M., Zheng, S., Huang, T. L. & Wang, G. Histone deacetylase inhibitors in clinical studies as templates for new anticancer agents. *Molecules* **20,** 3898–3941 (2015).

20. Panobinostat - FDA approved drug accessed in August, 2016. at <http://www.fda.gov/drugs/informationondrugs/approveddrugs/ucm435339.htm>

21. Mann, B. S., Johnson, J. R., Cohen, M. H., Justice, R. & Pazdur, R. FDA approval

summary: vorinostat for treatment of advanced primary cutaneous T-cell lymphoma. *Oncologist* **12,** 1247–52 (2007).

22. Kelly, W. K. *et al.* Phase I study of an oral histone deacetylase inhibitor, suberoylanilide hydroxamic acid, in patients with advanced cancer. *J. Clin. Oncol.* **23,** 3923–3931 (2005).

23. Marks, P. a. Discovery and development of SAHA as an anticancer agent. *Oncogene* **26,** 1351–1356 (2007).

24. Marks, P. A., Richon, V. M. & Rifkind, R. A. Histone Deacetylase Inhibitors: Inducers of Differentiation or Apoptosis of Transformed Cells. *JNCI J. Natl. Cancer Inst.* **92,** 1210–1216 (2000).

25. Komatsu, N. *et al.* SAHA, a HDAC inhibitor, has profound anti-growth activity against non-small cell lung cancer cells. *Oncol. Rep.* **15,** 187–191 (2006).

26. Butler, L. M. *et al.* Suberoylanilide hydroxamic acid, an inhibitor of histone deacetylase, suppresses the growth of prostate cancer cells in vitro and in vivo. *Cancer Res* **60,** 5165–5170 (2000).

27. Ungerstedt, J. S. *et al.* Role of thioredoxin in the response of normal and transformed cells to histone deacetylase inhibitors. *Proc. Natl. Acad. Sci. U. S. A.* **102,** 673–8 (2005).

28. Khan, O. & La Thangue, N. B. HDAC inhibitors in cancer biology: emerging mechanisms and clinical applications. *Immunol. Cell Biol.* **90,** 85–94 (2012).

29. Bose, P., Dai, Y. & Grant, S. Histone deacetylase inhibitor (HDACI) mechanisms of action: Emerging insights. *Pharmacol. Ther.* **143,** 323–336 (2014).

30. Camphausen, K. *et al.* Enhancement of in vitro and in vivo tumor cell radiosensitivity by valproic acid. *Int. J. Cancer* **114,** 380–386 (2005).

31. Lee, J. H., Choy, M. L., Ngo, L., Foster, S. S. & Marks, P. A. Histone deacetylase inhibitor induces DNA damage, which normal but not transformed cells can repair. *Proc Natl Acad Sci U S A* **107,** 14639–14644 (2010).

32. Wang, H. *et al.* Discovery of (2E)-3-{2-butyl-1-[2-(diethylamino)ethyl]-1H-benzimidazol-5-yl}-N-hydroxyacrylamide (SB939), an orally active histone deacetylase inhibitor with a superior preclinical profile. *J. Med. Chem.* **54,** 4694–4720 (2011).

33. Gediya, L. K., Chopra, P., Purushottamachar, P., Maheshwari, N. & Njar, V. C. O. A New Simple and High-Yield Synthesis of Suberoylanilide Hydroxamic Acid and Its Inhibitory Effect Alone or in Combination with Retinoids on Proliferation of Human Prostate Cancer Cells. 5047–5051 (2005).

34. Salmi-Smail, C. *et al.* Modified cap group suberoylanilide hydroxamic acid histone deacetylase inhibitor derivatives reveal improved selective antileukemic activity. *J. Med. Chem.* **53,** 3038–3047 (2010).

35. Cen, H., Mao, F., Aronchik, I., Fuentes, R. J. & Firestone, G. L. DEVD-NucView488: a novel class of enzyme substrates for real-time detection of caspase-3 activity in live cells. *FASEB J.* **22,** 2243–2252 (2008).

36. Cecchini, M. J., Amiri, M. & Dick, F. A. Analysis of Cell Cycle Position in Mammalian Cells. *J. Vis. Exp.* **7,** 1–8 (2012).

37. Vindelov, L. L. Flow microfluorometric analysis of nuclear DNA in cells from solid tumors and cell suspensions. A new method for rapid isolation and straining of nuclei. *Virchows Arch. B, Cell Pathol.* **24,** 227–42 (1977).

38. Galvao, J. *et al.* Unexpected low-dose toxicity of the universal solvent DMSO. *FASEB J.* **28,** 1317–1330 (2014).

39. Munster, P. N. *et al.* The histone deacetylase inhibitor suberoylanilide hydroxamic acid induces differentiation of human breast cancer cells. *Cancer Res.* **61,** 8492–7 (2001).

40. Kleensang, A. *et al.* Genetic variability in a frozen batch of MCF-7 cells invisible in routine authentication affecting cell function. *Sci. Rep.* **6,** 28994 (2016).

41. Huang, L. & Pardee, A. B. Suberoylanilide hydroxamic acid as a potential therapeutic agent for human breast cancer treatment. *Mol. Med.* **6,** 849–66 (2000).

42. Pozarowski, P. & Darzynkiewicz, Z. in *Methods in Molecular Biology, vol. 281: Checkpoint Controls and Cancer, Volume 2: Activation and Regulation Protocols* (2004).

43. Marks, P. a & Breslow, R. Dimethyl sulfoxide to vorinostat: development of this histone deacetylase inhibitor as an anticancer drug. *Nat. Biotechnol.* **25,** 84–90 (2007).

44. Pons, D. *et al.* Epigenetic histone acetylation modifiers in vascular remodelling: New targets for therapy in cardiovascular disease. *Eur. Heart J.* **30,** 266–277 (2009).

45. Marks, P. A. *et al.* Histone Deacetylases and Cancer: Causes and Therapies. *Nat. Rev. Cancer* **1,** 194–202 (2001).

VI. APPENDIX

MCF-7

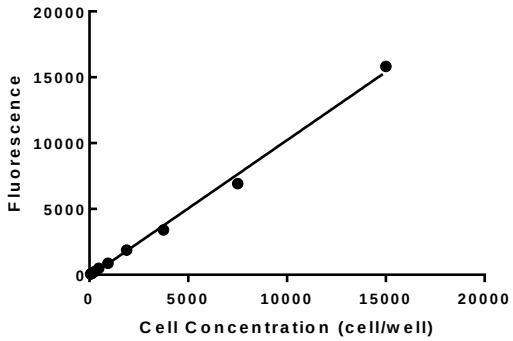

$Y=1,0362x – 139,44$

$R^2=0,9959$

H460

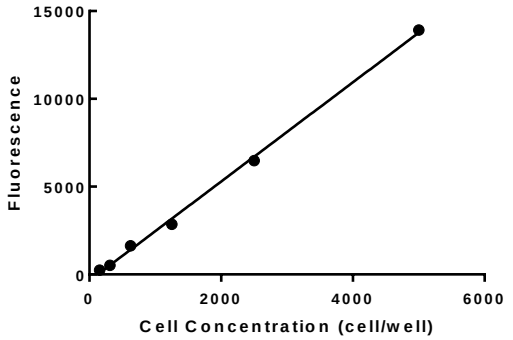

$Y=2,8248x – 359,35$

$R^2=0,9975$

HDF

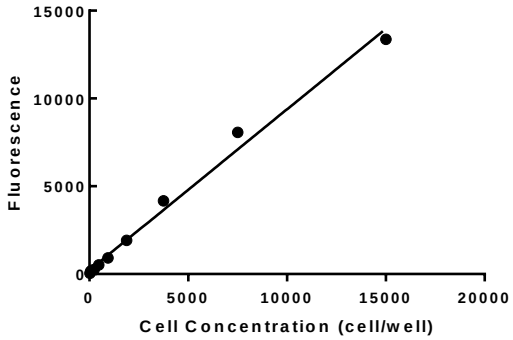

$Y = 0,9135x + 248,03$

$R^2 = 0,9901$

Figure III.26 - Standard curves obtained for each cells (MCF-7, H460 and HDF) for PrestoBlue Cell Viability Assay. See section II.2.3